IDENTIFICATION AND ELUCIDATION OF MIR-214 AND MIR-29A AS POTENT REGULATORS OF LIVER FIBROSIS

By

Matthew K. Knabel

A dissertation submitted to Johns Hopkins University in conformity with the requirements for the degree of Doctor of Philosophy

Baltimore, MD

October, 2013

Abstract

Liver fibrosis is the accumulation of extracellular matrix proteins in response to hepatocellular injury. Worldwide, liver fibrosis and cirrhosis accounts for nearly 160,000 deaths per year. It results from many different etiologies, including excessive alcohol consumption, viral infections and obesity. Our group has a vested interest in the molecular mechanisms that underlie this disease. Many patients on a solid organ transplant waiting list have excessive fibrosis, and those who receive a transplant often develop complications associated with recurrent fibrosis.

One of the main objectives of our lab is to identify novel biomarkers of liver fibrosis, which will open avenues to understand novel mechanisms. Using this approach, we also test and develop therapeutic options to ameliorate liver fibrosis. This thesis focuses on identifying and understanding microRNA (miRNA) changes during fibrotic conditions. miRNAs are small, single-stranded RNA molecules that negatively regulate protein translation. In the following studies, we systematically examine changes in miRNA expression during liver fibrosis and identify two novel mechanisms that have cell-specific expression and function in the liver during liver fibrosis.

In our first study, we describe a family of miRNAs that is upregulated during human and rodent liver fibrosis. This group of miRNAs, the miR-214/199 family, has five specific unique mature sequences that have been reported to regulate a variety of different targets. In the liver, expression of this family is focused predominantly in nonparenchymal cells. One member of this miRNA family, miR-214-5p, regulates expression of Twist1, a mesenchymal transcription factor that promotes expression of

this family. Using *in vitro* techniques, we characterize this novel negative feedback loop in activated hepatic stellate cells. Inhibition of Twist1 is associated with downregulation of alpha-SMA, Col1a1 and CTGF, and reduces activation and migration of stellate cells and expression of the miR-214/199 family. Inhibiting miR-214-5p is associated with increased alpha-SMA, Col1a1 and stellate cell migration. Taken together, these findings suggest a novel negative feedback loop that regulates accumulation of fibrosis in the liver.

In the next chapter, we report that miR-29a is downregulated significantly during liver fibrosis. miR-29a targets many extracellular matrix proteins, including collagen, elastin and fibrillin. Using an adeno-associated virus, we expressed miR-29a in hepatocytes of mice treated with carbon tetrachloride (CCl_4). We report a dramatic therapeutic benefit when maintaining miR-29a expression in hepatocytes. Using an *in vitro* approach, we show that miR-29a is packaged into exosomes, and miR-29a is transferred from hepatocytes to stellate cells to regulate collagen expression. Finally, we create an inducible miR-29a transgenic mouse, and future directions the lab will pursue to further characterize these therapeutically beneficial observations.

This work establishes roles of two different miRNA families that are dysregulated during liver fibrosis. Our efforts are great examples that point towards the need to consider miRNA expression on a cell-specific level. Characterizing other miRNAs would lead to identification of specific biomarkers, novel mechanisms and individual therapeutic options in nearly every pathogenic setting.

Advisor: Daniel S. Warren, Ph.D.

Reader: Zhaoli Sun, M.D., Ph.D.

Preface

There are many people who have helped me through my five years in the Human Genetics Program. While each one's contributions have varied, it has become increasingly evident that I would not complete this thesis without the support of the following people.

I would not be the scientist that I am today without the direction of my thesis advisor, Dan Warren. His critical observations of every piece of data that I present has taught me to analyze experimental results both in the settings of a given experiment as well as in the big picture of liver disease. I also give special thanks to Andrew Cameron, Robert Montgomery and Andrew Singer, who have provided educational and personal support over the past five years.

I thank many lab mates. In my earlier years, I was fortunate enough to work with a handful of great physician scientists. Bonnie Lonze, Sunil Karhadkar and Anthony Mark were a great team of clinicians who taught me many techniques that I still apply. I thank Kalyani Ramachandran and Tyler Creamer, who have provided not only support (both technically and emotionally) but have made the lab an enjoyable and fun work environment.

Our lab has greatly benefitted from the support of nearby labs in the Surgery Department. In particular, Zhaoli Sun and his group of energetic and extremely helpful lab members have been a wealth of information, especially in small animal model surgeries and husbandry. I also thank Dr. Sun for agreeing to carefully read through this thesis.

I thank Hal Dietz and Steve Leach for serving as the remaining members of my Thesis Committee Meeting. Their astute observations and generous recommendations helped forge this thesis into a coherent and consistent story. Steve deserves an additional token of gratitude. Along with Michael Parsons, Steve gave me my first job in science. Working for Steve and Mike helped foster a love and appreciation for science that resulted in enrollment in this program. I cannot thank them enough for taking a chance on me.

I was privileged to have three great rotations during my first year. I thank Ben Ho Park and Gregg Semenza for allowing me to rotate through their labs. I learned invaluable techniques and gained immeasurable experience. I utilize most techniques to this day.

The Human Genetics Ph.D. Program is a well-oiled machine only because of the strength in its administrative and professional leadership. I thank Dave Valle and Sandy Muscelli for their tireless and constant support during my graduate school experience.

One of the best assets in this program is the plethora of information passed down from more experienced students. One former student, Dave Gorkin, has been instrumental in preparation of this thesis. I thank him for fielding not only important questions but enthusiastically answering the most mundane requests. He has been a good source of information, and more importantly, a good friend over the past five years.

I would not be able to tolerate the dearth of results early in my career without the support of my classmates and friends. It was easier to stay on track with the example that they all portrayed. Specifically, Ben Leadem, Juan Calderon, Jen Poitras,

Mike Rodgers and John Gustin have provided love, support and (just as importantly) relief through happy hour beers and extended lunches.

It's hard for me to think about biology and not reminisce about my very early learning moments at Scranton Prep with Suzanne Fitzsimmons, my first biology teacher. Her unique and tireless approaches to teaching biology sparked my interest early and started me along this path.

Finally, I cannot give enough gratitude to my family. Being one of nine children, I often think of my parents, Joe and MaryLou Knabel, as my first teachers in genetics. Aside from fostering my intellectual goals, my parents have provided unconditional and constant love, support and interest in me and for my scientific endeavors. My siblings have become some of my best friends, and I love and thank each of them very dearly.

Most importantly, I thank my wife, Molly, and our baby girl, Charley. My relationship with Molly predates enrollment in this program. She has endured the stress that goes along with long nights of studying and the ups and downs associated with failures and successes in lab. I love you, honey. None of this would be possible without your love and motivation. This is for you and Charley.

Table of Contents

List of Tables

List of Figures

1. CHAPTER 1. INTRODUCTION

1.1 Liver fibrosis and public health

Liver fibrosis is a reversible phenotype that is associated with increased deposition of extracellular matrix proteins, upregulation of proinflammatory cytokines, oxidative stress, apoptosis and steatosis (Lee et al., 2011). Chronic viral infection, long-term excessive alcohol intake, exposure to toxins and obesity contribute to the etiology of liver fibrosis, which, if left untreated, can develop into chronic liver disease and cirrhosis. According to the CDC, chronic liver disease and cirrhosis contributed to over 33,000 deaths in the United States in 2011, making it one of the highest causes of preventable death (Hoyert et al., 2012).

Liver fibrosis often presents as the primary phenotype which leads to functional complications, including coagulation disorders, bacterial infections and portal hypertension. Because of the buildup of extracellular matrix proteins, liver architecture changes dramatically and hepatocyte function is compromised due to a disruption in cell-to-cell contact or through altered blood flow.

Chronic liver fibrosis is a progressive and long-developing disease. As a result, success in clinical trials for liver fibrosis treatment has been limited. Because no FDA-approved pharmacotherapeutic options currently are available, the standard of care for someone with end-stage liver disease as a result of progressive liver fibrosis is an organ transplant. However, considering the high cost to this procedure, the scarcity of donor grafts and increasing number of patients waiting for an organ (Figure 1-1A), this approach is limited. As important, of all organs transplanted, less than 65% survive to

five years (Figure 1-1B). Identifying the molecular mechanisms behind the progression of this disease would ameliorate these staggering numbers.

Several genetic diseases present with a fibrotic phenotype. Among them, the most prevalently diagnosed pediatric disorders and syndromes are congenital hepatic fibrosis, Wilson disease and alpha-1 antitrypsin deficiency (Taddei et al., 2008). Each inherited disorder is associated with different primary defects. In congenital hepatic fibrosis, bile ducts and blood vessels constrict and disallow bile, nutrients and other metabolites to be processed by the liver (Rawat et al., 2013). Copper transport is compromised in patients with Wilson disease, causing an accumulation of copper in the liver that contributes to fibrosis development (Roberts et al., 2008). Patients with alpha-1 antitrypsin deficiency present usually during the third to sixth decade of life due to a mutation that leads to a buildup of neutrophil elastase, which in excess will attack and injure normal liver cells (Topic et al., 2012). Although each presents with different initial symptoms, liver fibrosis develops in all three diseases.

Because fibrosis of the liver undergoes periods of accumulation and regression over many year, many times it occurs asymptomatically, especially in patients with nonalcoholic fatty liver disease (Milic et al., 2012). However, through meta-analysis and retrospective studies, it is becoming increasingly appreciated that liver fibrosis is a pre-cancerous stage. About 80% of patients who are diagnosed with hepatocellular carcinoma (HCC) present with liver cirrhosis (Llovet et al., 2003). Recent data suggest that the mortality rate from HCC is increasing in developed countries (Deuffic et al., 1998; El-Serag et al., 1999; La Vecchia et al., 2000). Identifying molecular markers and mechanisms underlying liver fibrosis would allow for the development of novel gene and

drug therapies, and such approaches have been successful (Prickett et al., 2012; Peng et al. 2012; Lorenzen et al., 2011).

1.2 The liver undergoes many cellular changes during fibrosis

During liver fibrosis, tissue morphology dramatically changes. Treatment of a hepatotoxin like carbon tetrachloride (CCl_4) or ingestion of alcohol, both of which have been utilized in animal models in work described in this thesis, causes cell apoptosis, release of reactive oxygen species and paracrine stimulation of endothelial and hepatic stellate cells (HSC) (Lee et al., 2011). Quiescent HSCs lose Vitamin A lipid droplets and transform into activated myofibroblasts that produce extracellular matrix proteins. As the injury worsens, the organ scars, and disrupts cell-cell interactions, angiogenesis and blood flow (Jiao et al., 2009).

Emerging mechanisms underlying stellate cell activation are being identified. While "classic" pathways like the PDGF and TGF-beta signaling pathways play a role both in activation of stellate cells and maintenance of activation, members in other pathways including the VEGF, NFkB and JAK/STAT signaling pathways have been implicated in regulation of HSC activation (Lee et al., 2011).

Interestingly, liver fibrosis is a reversible phenotype. Removal of the insult (i.e. CCl_4 or alcohol) often leads to regression of fibrosis. Lineage tracing studies have suggested that after removal of the insult, about half of myofibroblasts apoptose while the other half revert to an inactive phenotype that is similar to quiescent HSCs (Kisseleva et al., 2012). Therapeutic approaches have focused on inactivating ECM-producing myofibroblasts. However, due to other known functions, inhibitors of fibrogenic

cytokines have had varying success to alleviate deposition of extracellular matrix proteins and activation of stellate cells. Losartan, for example, has been limited as a therapeutic agent because it has both anti-fibrotic and anti-angiogenic effects (Parlakgumus et al., 2013). These nonspecific and unwanted effects call for a need to identify and develop more specific therapeutic options.

1.3 miRNAs biogenesis, processing and function

miRNAs have a unique processing mechanism that results in a 19-24 nucleotide molecule that negatively regulates translation. After transcription, usually by RNA Polymerase II, the long pri-miRNA sequence is cleaved at the base of the primary stem loop by Drosha RNase III endonuclease (Lee et al, 2003). The pre-miRNA hairpin is actively transported from the nucleus to the cytoplasm by Ran-GTP and the export receptor Exportin-5 (Yi et al., 2003; Lund et al., 2004). Dicer, another endonuclease, processes the hairpin in the cytoplasm, and one mature miRNA strand is incorporated into the RNA-induced silencing complex (RISC), where it regulates protein and mRNA expression (Bartel, 2004).

Understanding miRNA processing from Drosha through RISC has evolved over the past 15 years. Originally, evidence based on thermodynamic free energy of the miRNA 3' overhanging sequences suggested that one strand is preferentially processed while the other strand is degraded. Recent studies indicate that both strands of a microRNA hairpin can be processed (Kuchenbauer et al, 2011), and the second strand, sometimes called the miRNA* (star) strand, may even have regulatory roles (Yang et al, 2011). Described in detail in Chapter 2, miR-214 is a miRNA that has non-preferential

strand bias which allows a cell to transcribe one primary transcript that produces two regulatory genes with different sets of targets.

The human genome has over 1000 miRNAs, and each can regulate multiple genes, pathways and networks during normal and pathogenic physiology (Grimson et al., 2007; Lewis et al., 2005). miRNA dysregulation has been implicated as a factor associated with liver fibrosis (Roderburg et al., 2012; Li et al., 2012; Kwiecinski et al., 2012; Kogure et al., 2012). miRNAs have been overexpressed or repressed to understand their role in organ fibrosis (Lakner et al., 2012; Ogawa et al., 2012). Understanding the different molecular networks where a specific miRNA functions will be vital to understand its importance in the development of therapies. Studies described in Chapters 2 and 3 assess expression and determine function of miR-214 and miR-29a during liver fibrosis.

1.4 Therapeutic methods of gene delivery

Understanding genetic changes during a pathogenic state has led to the development of strategies to regulate expression using viral vectors, mimics or inhibitors. Gene therapy that regulates miRNA expression has had success recently in small animal models (van Rooij et al., 2008), including therapy that targets the liver (Kota et al., 2009; Jopling et al., 2005). The liver is an attractive organ for systemic therapeutic delivery of genetic material because it constantly encounters and interacts with circulating blood. Others have achieved cell-specific expression of viruses and nanoparticles, including successful delivery to hepatocytes (Sands, 2010; Wang et al., 2008; Hu et al., 2013).

Off-target effects present an issue when considering mode of delivery, and this becomes an important obstacle during preclinical and clinical testing. Adeno-associated viruses are non-integrating viruses that have organ- and cell-specific tropism (Zincarelli et al, 2008). Importantly, AAVs have been reported to have very little off-target effects, making them extremely enticing options for gene delivery. An AAV product for treatment of lipoprotein lipase deficiency has even been licensed in Europe (Pollack, 2012).

In Chapter 3, we utilize AAV serotype 8 to deliver miR-29a to hepatocytes. Mice treated with one systemic injection of AAV8 develop no clinical signs of toxicity. Therapeutically, we report that delivery of miR-29a AAV is strongly associated with protection from and, in one model, regression of liver fibrosis. This study serves as another example of successful systemic therapeutic delivery of genetic material to a specific cell type to treat a pathogenic state.

1.5 Figures: Chapter 1

Figure 1-1. UNOS data for solid organ transplants.

A

Patients on a Registered Waiting List for Any Organ	**127,508**
Patients on a Registered Waiting List for a Liver Transplant	**16,414**
Patients Added Each Year to a Liver Transplant Waiting List	**10,829**
Number of Liver Transplants Performed Each Year	**6,337**

B

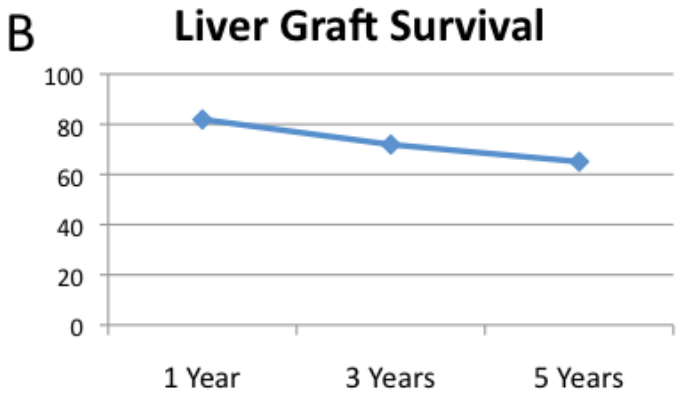

A) UNOS data as of September, 2013. B) Liver graft survival data for 1, 3 and 5 years after an organ transplant as of September, 2013.

2. CHAPTER 2. IDENTIFICATION OF A NOVEL NEGATIVE FEEDBACK LOOP INVOLVING MIR-214 AND TWIST1 IN LIVER FIBROSIS

2.1 Introduction

A growing number of publications have identified changes in microRNA (miRNA) expression that are associated with organ fibrosis. Recognizing dysregulation of miRNA and identifying miRNA targets can lead to understanding of molecular mechanisms in a pathogenic setting. We set out to examine miRNA dynamics during liver fibrosis using a published alcohol intake model (Lieber et al., 1982). We comprehensively surveyed expression of over 350 miRNAs in whole liver tissue during fibrosis. Our goal was to identify changes in whole tissue, determine cell-specific expression, and understand function of miRNAs during fibrosis. We hypothesized that this approach would lead to discovery of novel molecular markers and mechanisms and could even lead to development of individual treatment options for patients with organ fibrosis.

miRNAs have been reported to be co-expressed and function as genomic miRNA networks (Zhang et al., 2009; Guo et al., 2012; Mendell, 2008). One group, the miR-214/199 family, is transcribed from three different loci in the human genome, and some members of this group have been implicated in organ fibrosis (Murakami et al., 2011; Iizuka et al., 2012; Aurora et al., 2012). However, cell specific expression and function of this miRNA family during liver fibrosis are unknown. In this study, we identified that all unique sequences of the miR-214/199 family are upregulated in rodent liver fibrosis, and this family's expression in the liver is concentrated predominantly in

nonparenchymal cells. One member of the miR-214/199 family, miR-214-5p, specifically targets and negatively regulates its own transcription factor, Twist1, in stellate cells. Interestingly, miR-214-5p is sufficient to regulate hepatic stellate cell activation, migration and collagen production.

miR-214 and miR-199a are upregulated by Twist1, a mesenchymal cell transcription factor (Lee et al., 2009). Both gain of Twist1 and loss of members of the miR-214/199 family have been associated with increases in cancer metastasis (Yang et al., 2006; Li et al., 2012). During fibrosis, stellate cells lose lipid droplets, become activated and migrate to the site of hepatocellular injury. We investigated the role of Twist1 and miR-214 in a fibrotic setting. Interestingly, a knockout model of the entire hairpin of miR-214 is associated with increased cardiac fibrosis and decreased survival rate after induced myocardial infarction (Aurora et al., 2012), suggesting that miR-214 could have a protective role during fibrosis.

Here, we report that Twist1 is an important transcription factor that regulates expression of pro-fibrotic gene expression. Inhibition of Twist1 is associated with loss of expression of a cohort of pro-fibrotic genes. miR-214-5p directly targets and negatively regulates Twist1 in activated hepatic stellate cells, and loss of miR-214-5p upregulates Twist1 and downstream targets, including alpha-SMA and Col1a1. Taken together, these findings imply mir-214-5p and Twist1 as members of an important negative feedback loop contributing to the control of stellate cell activation, migration and collagen deposition.

2.2 Results

2.2.1 miR-214-3p and miR-199a-3p are upregulated in human and rodent liver fibrosis.

During liver fibrosis, activated stellate cells and collagen production increase. We treated male Lewis rats with a published model of alcohol intake to induce liver fibrosis (Lieber et al., 1982). After six weeks of alcohol consumption, only the group treated both with alcohol and carbon tetrachloride (CCl_4) (which we termed the 'combination group') develop histological evidence of fibrosis (Figure 2-1A). An increase in fibrosis is associated with an increase in alpha-smooth muscle actin-positive activated stellate cells in this cohort (Figure 2-1B).

Dysregulation of miRNAs has been implicated in liver fibrosis (He et al., 2012; Vettori et al., 2012; Hinz et al., 2012; Haybaeck et al., 2011), and others have reported that miRNAs dynamically change in alcohol-related liver fibrosis (Bala et al., 2012). We examined miRNA changes in all four groups, and compared those changes to our histological data. In a miRNA qPCR array that detects expression of over 350 miRNAs, miR-214-3p and miR-199a-3p are two of most upregulated miRNAs in the combination group (Table 2-1). Because different models of liver fibrosis have many commonalities both in histology and gene array expression, we cross-referenced our data from the alcohol-induced rat fibrosis model with a second rodent fibrosis model (described in Chapter 3). Both miR-214-3p and miR-199a-3p are among 18 miRNAs that are upregulated by more than 1.5-fold in the fibrotic groups of both models, suggesting that they could have an important function in liver fibrosis (Table 2-1).

Both miR-214-3p and miR-199a-3p are processed from DMN3os, a 6kb untranslated RNA that is transcribed from the opposite strand of an intron of DNM3 (Loebel et al., 2005; Watanabe et al., 2008). While DNM3os-specific miRNAs were upregulated, we do not detect a significant increase in DNM3 mRNA or protein in our model (unpublished data). Furthermore, while Twist1 has been reported to upregulate DNM3os (Lee et al, 2009), there is no Twist1 consensus binding-site 5' to the transcription start site of DNM3, implying that transcriptional upregulation of miR-214-5p and miR199a-3p is independent of DNM3 transcription.

To examine whether this group of miRNAs is upregulated during human liver fibrosis, we obtained samples that were scored by a pathologist as having portal fibrosis, bridging fibrosis or cirrhosis. miR-214-3p and miR-199a-3p are significantly upregulated in the bridging and cirrhotic groups, and miR-214-3p is also significantly upregulated in patients with portal fibrosis (Figure 2-2A). Interestingly, upregulation of miR-214-3p and miR-199a-3p has no significant correlation with hepatitis C infection (HCV), reported drug or alcohol use, or liver enzymes (Table 2-2), suggesting that upregulation of miR-214-3p and miR-199a-3p could be fibrosis-specific.

We also observe upregulation of miR-214-3p and miR-199a-3p from serial biopsies of an individual patient who developed recurrent HCV after a liver transplant (Figure 2-2B). miR-214-3p and mir-199a-3p expression in whole tissue steadily increases over a 15-month period as HCV recurred and fibrosis developed (Table 2-3).

2.2.2 Both strands of miR-214 are equally expressed, and all unique strands of the miR-214/199 cluster are upregulated in a rodent liver fibrosis model.

The miR-214/199 family has four different miRNAs expressed from three conserved loci (Figure 2-4A). The miR-214/199 family is transcribed from the opposite strand of introns of a family of genes called dynamins. This miRNA family has 5 unique miRNA strands. Recent studies indicate that both strands of a microRNA hairpin can be processed (Kuchenbauer et al., 2011), and the miRNA* (star) strand may even have regulatory roles (Yang et al., 2011). miRBase reports deep sequencing reads of each strand for many miRNAs, and deep sequencing reads can imply strand bias during processing. An *in silico* analysis of strand expression indicates that in about 11% of all miRNAs both strands are expressed in <1:2 ratio (3p:5p), suggesting that the miRNA* strand of these miRNAs may have a functional role. Included in this group is mir-214, whose strands are expressed in nearly equal levels (Figure 2-3A). Conversely, miR-199a had a biased ratio (>10:1). The ratios of miR-214 and miR-199a were confirmed in our model, as mir-214 has a nearly 1:1 ratio in each group in our rat liver fibrosis model (Figure 2-3B).

Given the evolutionary conservation of this miRNA family, we hypothesized that other unique strands in this family are upregulated. Indeed, miR-214-5p, miR-199a-5p and miR-199b are also significantly upregulated in the combination group of our rodent fibrosis model. Not only is DNM3 expression not significantly dysregulated during liver fibrosis, DNM1 and DNM2 message is unchanged (unpublished data). We also measured miRNA expression for all five unique strands in this family in a second rodent model of liver fibrosis (described in Chapter 3). All five strands after 8 weeks of CCl_4 treatment in BL/6 mice are significantly upregulated (Figure 2-4C), suggesting that the entire miR-214/199 family may have a functional role in organ fibrosis.

2.2.3 miR-214-5p has two mature transcripts.

Although we report that mmu-miR-214-5p is significantly upregulated in rat liver fibrosis, miRBase reports that miR-214 has a different 5p mature sequence (Figure 2-5A). Since rno-miR-214-5p has a limited number of reported deep sequencing reads, we examined expression of rno-miR-214-5p in our rodent models. Rno-miR-214-5p is significantly upregulated in both of our rodent models, including our mouse model, after induction of liver fibrosis (Figure 2-5B-C). We tested rno-miR-214-5p expression from human miR-214 by transfecting an adeno-associated viral vector containing the entire hairpin of human miR-214 into HeLa cells. Surprisingly, all three mature sequences of miR-214, including rno-miR-214-5p, are significantly upregulated after transfection with human miR-214 (Figure 2-5D), implying that at least three mature sequences are processed in human, mouse and rat miR-214.

2.2.4 miR-214 is expressed predominantly in non-parenchymal cells, including activated stellate cells, during liver fibrosis.

The liver is a heterogeneous organ consisting of many different cell types including hepatocytes, stellate cells, Kuppfer cells and endothelial cells. Expression profiles in different cell types have revealed that miRNAs have tissue- and cell-specific expression (Santoro et al., 2013; Sood et al., 2006), and others have even developed methods to predict cell-specific miRNA expression (Lee et al., 2012). We set out to examine the mir-214/199 family expression pattern during liver fibrosis in different cell populations. miR-214 is focused predominantly in the nonparenchymal regions of the

liver (Figure 2-6), and an increase in expression in nonparenchymal cells correlates with an increase deposition of extracellular matrix proteins. Additionally, this expression patterns overlaps a similar pattern of alpha-smooth muscle actin (α-SMA) expression (Figure 2-1B), suggesting that this family of miRNAs may be expressed in hepatic stellate cells. An *in silico* analysis of cell specific expression of miR-214-3p and miR-199a-5p indicates that, while both are expressed in the liver, uninjured hepatocytes do not express these miRNAs (Halushka, unpublished data). Instead, this family of miRNAs is expressed more highly in adipocytes, fibroblasts and smooth muscle cells, indicating that these miRNAs may be exclusive to stellate cells and other collagen-producing cells.

To determine cell-specific expression of the miR-214/199 family, we examined baseline expression in an activated stellate cell line (LX-2 cells), and compared it to three different hepatoctyte-derived lines, HuH7, HepG2 and primary human hepatocytes. LX-2 cells have increased expression of the miR-214/199 family compared to hepatocytes, pinpointing its expression to activated stellate cells (Figure 2-7A).

During fibrosis, the total number alpha-SMA-positive activated stellate cells is increased. Although the miR-214/199 family is upregulated in liver fibrosis, we cannot definitively rule out that the increase in the miR-214/199 family is merely the result of an increase in total stellate cell number. To examine if processing of the miR-214/199 family is increased in stellate cell, we treated LX-2 cells with a proinflammatory cytokine, TGF-beta. TGF-beta treatment is associated with a significant upregulation of alpha-SMA, Col1a1, CTGF, FN1 and PDGF-R-beta (Figure 2-7B), all reported to increase during liver fibrosis (Chakraborty et al., 2012). Twist1, miR-214-3p, miR-214-5p and miR-199a-3p are also significantly increased (Figure 2-7B-C), confirming that

there is an upregulation of Twist1 and the miR-214/199 family transcription or miRNA processing in stellate cells during fibrosis.

2.2.5 miR-214-5p targets Twist1, which is upregulated in liver fibrosis.

A consensus Twist1 binding-site has been reported upstream of DNM3os (Lee et al., 2009). This sequence (CATATGT) is 5' to the transcriptional start sites of miR-199a-1 and miR-199b, suggesting that Twist1 may transcriptionally upregulate the entire miR-214/199 family. Interestingly, the 3' UTR of Twist1 has a conserved miR-214-5p binding site. To test whether miR-214 interacts with its own transcription factor to regulate expression, we cloned the 3' UTR of Twist1 into a luciferase vector and co-transfected this vector with plasmids containing no miRNA, miR-214 or miR-199a into HeLa cells. While luciferase activity does not change in cells co-transfected with miR-199a, coexpression of miR-214 with the 3'UTR of Twist1 reduces luciferase expression by more than half (Figure 2-8A-B), indicating that miR-214 regulates expression of Twist1 protein expression.

Next, we were interested to determine Twist1 expression in liver fibrosis. Twist1 mRNA and protein are significantly upregulated in the combination group (Figure 2-9A-C). Consistent with upregulation of Twist1, Twist2, a conserved homolog of Twist1, is increased after 4 weeks of CCl_4 treatment (Figure 2-9D).

2.2.6 Inhibition of Twist1 in LX-2 cells downregulates the miR-214/199 family and pro-fibrotic markers

Twist1 is a mesenchymal transcription factor that promotes growth, proliferation and cell migration (Qin et al., 2011). miR-214 has been implicated as a factor controlling cancer cell migration (Li et al., 2012). In addition, other have shown that knockout of miR-214 is associated with increased fibrosis and decreased survival rate in animals after induced myocardial infarction (Aurora et al., 2012). Given that both Twist1 and the miR-214/199 family are upregulated during liver fibrosis, we hypothesized that miR-214-5p could negatively regulate enhanced expression of Twist1 in stellate cells, limiting activation and migration. We inhibited Twist1 expression and examined differential transcription of downstream targets, including pro-fibrotic genes. Inhibition of Twist1 in LX-2 cells leads to significant downregulation of all five miR-214/199 members (Figure 2-10B). Twist-1 inhibition is also associated with a significant decrease in expression of alpha-SMA, CTGF, FN1 and MMP2 (Figure 2-10A), suggesting that Twist1 is necessary for expression of pro-fibrotic genes in activated stellate cells. Phenotypically, cells treated with Twist1 siRNA have limited migration (Figure 2-10C-D), implying that Twist1 plays an important role in activation and migration of hepatic stellate cells.

2.2.7 Inhibition of miR-214-5p is associated with increased activation, collagen production and migration of hepatic stellate cells.

LX-2 cells are transformed hepatic stellate cells that express miR-214-3p and miR-214-5p equally. Since miR-214-5p targets Twist1, which is sufficient to regulate expression of alpha-SMA, CTGF and FN1, we hypothesized that expression of miR-214-5p could contribute to fibrosis progression in stellate cells. Consistent with inhibition of Twist1, inhibition of only miR-214-5p causes a significant increase in alpha-SMA and

Col1a1 (Figure 2-11). Interestingly, Twist1 message and protein are also significantly increased (Figure 2-12A-C).

Given the increase in Twist1 after inhibition of miR-214-5p, we were interested to examine the dynamics of reported downstream markers of Twist1. miR-214-3p and miR-199a-3p are significantly upregulated after inhibition of miR-214-5p. However, after miR-214-3p inhibition, expression of Twist1 and other DNM3os miRNAs remain unchanged (Figure 2-12C).

Since Twist1 is a mesenchymal-specific transcription factor, we examined expression of epithelial and mesenchymal markers after miR-214-5p inhibition. While there is a non-significant decrease in E-cadherin, an epithelial marker (unpublished data), Vimentin, Zeb1 and Zeb2 are significantly increased after inhibition of only miR-214-5p in LX-2 cells (Figure 2-12D). However, there was no significant upregulation of mesenchymal markers in cells treated with miR-214-3p.

To determine the functional effect of inhibiting miR-214-5p in LX-2 cells, we performed a scratch assay to evaluate cell migration (Liang et al., 2007). After 18 hours, cells transfected with miR-214-5p, but not miR-214-3p, migrate significantly further compared to those transfected with scrambled inhibitor (Figure 2-13A-B). A similar migration pattern is observed in cells overexpressed with Twist1, suggesting that miR-214-5p may control cell migration in a Twist1 dependent manner.

2.2.8 Inhibition of miR-214-5p exacerbates activation, migration and collagen production of stellate cells in a Twist1-dependent manner.

We have shown that regulating expression of Twist1 and miR-214-5p have nearly opposite effects – inhibiting Twist1 limits expression of pro-fibrotic genes and the miR-214/199 family while inhibiting miR-214-5p is associated with an increase in pro-fibrotic gene and other members of the miR-214/199 family. We hypothesized that miR-214-5p is regulating Twist1 expression in LX-2 cells. To test this, we cloned Twist1 (including its 3'UTR) into pcDNA3+. Transfecting this vector while inhibiting miR-214-5p causes a significant increase in Twist1 (Figure 2-14A-B). We also report a significant transcriptional upregulation of miR-214-3p, miR-199a-3p and miR-199b, as well as pro-fibrotic markers alpha-SMA, Col1a1, CTGF and PDGF-R-beta (Figure 2-14C-D).

Phenotypically, overexpression of Twist1 leads to migration of LX-2 cells. Interestingly, overexpressing Twist-1 while inhibiting miR-214-5p causes LX-2 cells to migrate significantly more quickly compared with overexpression of Twist1 transfected with scrambled inhibitor (Figure 2-15A-B), indicating that miR-214-5p and Twist1 are important in activation and migration of stellate cells.

2.3 Discussion

In this study, we examined expression of the miR-214/199 family, a group of miRNAs that are under transcriptional control of Twist1. We determined that upregulation of the miR-214/199 family was associated with an increase in human and rodent liver fibrosis. For the first time, we have shown that upregulation of miR-214-3p and miR-199a-3p can be followed in an individual patient during progression of fibrosis after organ transplant. Increased expression of miR-214-3p and miR-199a-3p even predates clinical observations of fibrosis in serial liver biopsies of our transplant patient.

These results indicate that the miR-214/199 family is a reliable biomarker of varying degrees of liver fibrosis both in a cohort of patients and even in an individual patient.

Though we examined homogenous whole liver tissue, it is important to understand miRNA expression in a cell-specific manner. Ascertaining cell-specific expression of a miRNA family would help identify mRNA targets and functional consequences of dynamic change during injury. As indicated by *in situ* hybridization, miR-214 is expressed predominately in non-parenchymal cells, including hepatic stellate cells, endothelial cells and Kuppfer cells, during liver fibrosis. Our *in vitro* data determined that expression of the miR-214/199 family was concentrated in stellate cells, and expression of miRNAs in this family was increased after TGF-beta-induced activation of stellate cells, suggesting that upregulation of the miR-214/199 family in whole tissue is due not only to an increase in myofibroblasts but also to an increase in individual cell expression of this family. Consistent with these observations, recent studies have reported that members of this family are upregulated in cells transitioning to a mesenchymal state in the other organs (Denby et al., 2011).

Original experimental evidence indicated that miRNAs preferentially express one strand and degrade the other strand. Using miR-214, we have demonstrated that both strands of a miRNA are equally expressed in the liver, which opens up the possibility of two different sets of miRNA targets. Here, miR-214-5p (the star strand) regulates Twist1 expression during stellate cell activation. According to miRBase data, equal expression of both strands represents 11% of all miRNA biology, which increases the total number of miRNA target sets by more than ten-fold.

After cleaving by Drosha, the average pri-miRNA hairpin length is 60 nucleotides (Starega-Roslin et al., 2011). However, the hairpin of miR-214 is 115 nucleotides, nearly twice the average size. miRBase reports that rno-miR-214-5p has a different mature sequence, which is proximal to the base of the hairpin. Although rno-miR-214-5p differs from the mouse and human sequence, all three species have identical rat- and human/mouse-specific mature miR-214-5p nucleotide sequences. To our surprise, all three mature miRNAs are significantly upregulated in humans, mice and rats. There is a one-nucleotide overlap between rno-miR-214-5p and mmu/hsa-miR-214-5p, implying that both mature sequences cannot be processed from the same hairpin. However, our observations indicate that miR-214 can process at least three mature sequences. Because of this, miR-214 might have three unique sets of targets. It would be interesting to understand if increased miRNA hairpin size correlates to more than two predicted mature miRNAs. Further studies to explore rno-miR-214 targets would elucidate this novel and unique phenomenon in miRNA biology, and indicate if this observation has a functional consequence.

Proliferating hepatic stellate cells are important producers of extracellular matrix proteins during liver injury. They migrate to the site of injury, producing ECM proteins to protect damaged hepatocytes. Recent studies on individual members of the miR-214/199 family have suggested that this family may act as negative regulators of proliferation (Zhang et al., 2012; Jia et al., 2012; Derfoul et al., 2011). Using data from these experiments, we propose a model of miR-214-5p's role in liver fibrosis (Figure 2-16). During alcohol-induced liver fibrosis, Twist1 mRNA and protein are upregulated. All three loci of the miR-214/199 family in the human genome have a Twist1 consensus

binding site, suggesting transcriptional regulation. miR-214 interacts with a conserved 7merM8-binding site in the 3'UTR of Twist1. When inhibiting expression of miR-214-5p, Twist1, mRNA of pro-fibrotic genes and mesenchymal transcription factors are significantly upregulated. miR-214-5p expression in LX-2 may regulates hepatic stellate cell activation, collagen production and mesenchymal gene expression through Twist1.

Others have shown that miR-214 increases upon activation of primary hepatic stellate cells (Maubach et al., 2011). However, the role of miR-214 in activated stellate cells was unknown. For the first time, we have provided functional evidence that this interaction controls a stellate cell phenotype. Overexpressing Twist1 in LX-2 cells leads to faster cell migration over 18 hours. In the same manner, inhibiting miR-214-5p in the same cell type not only upregulates pro-fibrotic and mesenchymal markers but also leads to a faster cell migration. Finally, we confirmed the functional interaction between Twist1 and miR-214-5p when we overexpressed Twist1 (including its 3'UTR) while inhibiting miR-214-5p. This cohort has increased expression of Twist1, the miR-214/199 family and pro-fibrotic markers. Taken together, our data suggest that miR-214-5p regulates activation and migration of stellate cells through Twist1.

Liver fibrosis and cirrhosis is the strongest predisposing factor of hepatocellular cancer. 80% of patients with hepatocellular carcinoma are reported to have cirrhotic livers (Llovet et al., 2003). Loss of expression of members in the miR-214/199a family has been associated with increased metastasis (Li et al., 2012), and others have shown that pharmaceutically inhibiting Twist1 inhibits migration of breast cancer cells (Pai et al., 2013). Similar to what is reported in cancer models, our data suggest that miR-214-

5p plays a prominent role in limiting stellate cell migration. By targeting Twist1, miR-214-5p might be suppressing initiation of tumor differentiation in the liver.

This study has, for the first time, identified a negative feedback loop involving Twist1 and miR-214-5p that contributes to activated hepatic stellate cells. Twist1 has not been studied as a regulator of liver fibrosis in this detail. Here, we show that it is sufficient to control expression of alpha-SMA and Col1a1, and induce migration of activated stellate cells. Importantly, expression of miR-214-5p limits increased expression of Twist1 and its downstream targets. These studies point out a unique paradox in miRNA biology: an increase in miR-214 during liver fibrosis may in fact be protective against cirrhosis by negatively regulating Twist1, a gene product that is also upregulated. One would predict that treating non-parenchymal liver cells *in vivo* with mimics or an overexpression vector would ameliorate liver fibrosis. Alternately, studying a genetic model knocking out miR-214 under fibrotic conditions would further elucidate miR-214's role during liver disease.

2.4 Materials and methods

2.4.1 Animal Models.

Animals were housed and experiments were performed with approval by the Johns Hopkins School of Medicine Animal Care and Use Committee. Seven- and eight-week old male Lewis rats were divided into four groups and received the following: an isocaloric control diet according to the Lieber–DeCarli Regimen (Lieber et al., 1982); a diet with 7% ethanol; an isocaloric diet with biweekly injections of 0.1 mL/kg carbon tetrachloride (CCl_4; Sigma-Aldrich, St. Louis, MO); or a combination treatment of EtOH

and CCl_4. Two- and three-month-old C57BL/6 female mice were given 1 mL/kg of CCl_4 intraperitoneally biweekly for zero, one, four or eight weeks. CCl_4 was diluted in corn oil. mT/mG mice (stock number 007576, The Jackson Laboratory (Jax), Bar Harbor, ME) were crossed to Twist2:cre (008712, Jax). The resulting offspring was treated with 1ml/kg CCl_4 for zero or four weeks. At the conclusion of the experiments, animal livers were perfused with cold PBS and harvested.

2.4.2 Human Samples.

RNA from 10-50 μm formalin-fixed, paraffin-embedded sections of livers with varying degrees of fibrosis was isolated using Trizol (Invitrogen, Carlsbad, CA), according to the manufacturer's protocol. Samples were used in accordance with the Johns Hopkins School of Medicine Institutional Review Board.

2.4.3 Histology.

Whole liver tissue was fixed in 10% formalin (Sigma-Aldrich) overnight. The tissues then were transferred to 70% ethanol and embedded in paraffin. 5μm sections of tissue were cut and stained with Masson's trichrome by the Johns Hopkins Reference Histology Lab (Baltimore, MD).

2.4.4 MicroRNA Array.

Total rat liver RNA was extracted using a mirVana miRNA Isolation Kit (Ambion, Inc, Austin, TX) according to the manufacturer's protocol. RNA was DNase treated (DNase I Amplification Grade; Invitrogen), and 500 ng of RNA was reverse

transcribed without pre-amplification using Megaplex RT Primers (Rodent Pool A v2.0; Applied Biosystems, Carlsbad, CA) and TaqMan MicroRNA Reverse Transcription Kit (ABI), according to the manufacturer's protocol. The microarray was run on the 7900HT Fast Real-Time PCR System with TaqMan Array Rodent MicroRNA A Cards v2.0 (ABI), according to the manufacturer's protocol. The geometric mean of each plate was used for normalization.

2.4.5 Immunostaining.

Formalin-fixed, paraffin-embedded tissues were sectioned. 5 μm sections were transferred to Superfrost/Plus Microscope Slides (Fisher Scientific, Pittsburgh, PA) and melted onto the slide for 30' at 60°C. The tissues were stained using monoclonal anti-α-smooth muscle actin conjugated to Cy3 (Sigma-Aldrich), diluted 1:100 in PBST. Tissues were counterstained with Hoechst 33258 (Molecular Probes, Eugene, OR), mounted using Prolong Gold Antifade Reagent (Invitrogen, Carlsbad, CA), and subsequently imaged under identical conditions.

2.4.6 In situ Hybridization.

6 μm sections were cut in RNase free conditions, and incubated with double (5' and 3')-DIG labeled probe for miR-214 (Exiqon, Woburn, MA), according to the manufacturer's protocol, and anti-DIG-AP (Roche, Branchburg, NJ) was used to detect miR-214.

2.4.7 Cell Culture.

LX-2 cells (generously provided by James Potter and Anirban Maitra), immortalized human hepatic stellate cells, were grown in DMEM supplemented with 10% fetal bovine serum (FBS), penicillin and streptomycin. Cells were transfected in triplicate with miRIDIAN Hairpin Inhibitors (Thermo Fisher Scientific, Waltham, MA) or siRNA (Santa Cruz Biotechnology, Inc., Dallas, TX) using Lipofectamine 2000 (Invitrogen) according to the manufacturer's protocol. Media was changed 8-12 hours after transfection and RNA and protein lysates were isolated 24 hours after transfection as previously described.

2.4.8 TGF-beta Treatment of LX-2 Cells.

LX-2 cells were grown to 90% confluence. They were washed, and normal growth media was changed with serum-starved media (DMEM supplemented with 0.2% fetal bovine serum (FBS), penicillin and streptomycin) for 24 hours, at which time a subset of cells was transfected with scrambled or Twist1 siRNA. Cells then were treated with 5ng/ml TGF-beta (Roche) in serum-starved media. RNA was isolated 24 hours later.

2.4.9 RNA Isolation and qPCR.

For animal and *in vitro* samples, total RNA was isolated from whole liver tissue using Trizol (Invitrogen) according to manufacturer's protocol. RNA was DNAse treated (Invitrogen), according to the manufacturer's protocol, and was reverse transcribed using TaqMan MicroRNA Reverse Transcription Kit (ABI) with miRNA specific primers (ABI) and High Capacity Reverse Transcription Kit (ABI) for 18s rRNA and all other

non-miRNAs, all according to the manufacturer's protocol. qPCR was performed using pre-designed TaqMan primers and probes (ABI), according to manufacturer's protocol. qPCR using primers for alpha-SMA, Col1a1, CTGF, FN1, PDGF-R-b, TGF-beta, MMP9, MMP2, TIMP-1, Twist1, E-cadherin, N-cadherin, Vimentin, Zeb1, Zeb2, DNM1 DNM2, and DMN3 was performed using Fast SYBR Green Master Mix (ABI). Genes amplified using SYBR Green were normalized to beta-Actin. The 2(-delta delta C(T)) Method was used to analyze PCR reactions.

2.4.10 Protein Isolation and Western Blot.

25 mg of homogenized tissue and LX-2 cells were suspended in RIPA buffer supplemented with Protein Inhibitor Cocktail (Sigma), according to manufacturer's protocol. Lysates were quantified using a BCA protein assay (Pierce, Rockford, IL). 10-50 µg was loaded in each lane, and after transfer, the membrane was probed for Twist1 (Abcam, Cambridge, MA), DNM3 (Abcam) or b-Actin (Sigma). Secondary antibodies (LI-COR, Lincoln, NE) were used to enhance detection of lysates, and signals were visualized using an Odyssey scanner (LI-COR).

2.4.11 Molecular Cloning.

Hsa-miR-214 and hsa-miR-199a were amplified and fragments were cloned into pAAV8 ef1a-eGFP at the FseI site and sequenced. The 3'UTR of Human Twist1 was cloned into the pGL3 vector at the XbaI site. Human Twist1_3'UTR was cloned into the EcoRI site of the pcDNA3+ vector. Clones positive by restriction digest were sequenced. One positive clone from each DNA sequence was used for subsequent studies.

2.4.12 In silico Strand Bias Analysis.

Deep sequencing reads from all miRNAs on TaqMan Array Rodent MicroRNA A Cards v2.0 (described above) were recorded from the miRBase website. Read ratios were divided into three categories based on 3p:5p expression: < 1:2, 1:2 – 1:5, and > 1:5. To examine miR-214 and miR-199a strand bias in each rat cohort, each 5p strand was normalized to the 3p strand and all groups were normalized to miR-214 in the diet control group.

2.4.13 Luciferase Reporter Assays.

2.5×10^5 HeLa cells were plated in triplicate wells of a 24-well plate and transfected 24 hours later with 500 ng of a pAAV8 plasmid (Control, miR-214 or miR-199a), 100 ng of the indicated pGL3 3' UTR reporter construct and 5 ng of phRL-SV40 (Promega, Madison, WI) using Lipofectamine 2000 (Invitrogen) according to the manufacturer's protocol. 24 hours after transfection, cells were lysed and assayed for firefly and renilla luciferase activity using the Dual-Luciferase Reporter Assay System (Promega). Firefly luciferase activity was normalized to renilla luciferase activity for each transfected well.

2.4.14 Cell Migration Assay.

6-well cell culture plates were coated with poly-L-lysine (Sigma), and cells were plated and a scratch was made as previously described [26]. Briefly, cells were transfected with gene plasmids (pcDNA3_Twist1_3'UTR), siRNA (Scrambled siRNA or Twist1; Santa Cruz Biotechnology, Inc.), or inhibitors (scrambled, miR-214-5p or miR-

214-3p; Thermo Scientific) using Lipofectamine 2000. After 24 hours, a scratch was made with a p200 tip, and cells were washed with PBS and examined at 12 or 18 hours after the scratch. At time = 0h, at least 10 images were taken, and at time = 12 hours or 18 hours, at least 20 images were taken. For each image, ImageJ was used to measure the area void of migrating cells.

2.4.15 Statistics.

A student two-tailed t-test was used to determine significance for all qPCR, Western blot and migration assays.

2.5 Tables: Chapter 2

Table 2-1. miRNAs upregulated by 1.5-fold in rodent models of liver fibrosis.

	RAT MODEL		MOUSE MODEL	
	FOLD CHANGE			
Assay	**Diet Control**	**Combination Treatment**	**Untreated**	**8 Weeks CCl_4**
mmu-miR-214	1.00	**21.03**	1.00	**1.88**
mmu-miR-434-3p	1.00	16.81	1.00	1.65
mmu-miR-199a-3p	1.00	**14.08**	1.00	**1.57**
mmu-miR-181c	1.00	14.04	1.00	2.78
mmu-miR-409-3p	1.00	5.91	1.00	10.42
mmu-miR-34a	1.00	5.58	1.00	3.11
mmu-miR-301a	1.00	5.43	1.00	1.50
rno-miR-351	1.00	5.12	1.00	1.77
mmu-miR-15b	1.00	4.74	1.00	2.44
mmu-miR-125a-5p	1.00	3.79	1.00	1.72
mmu-miR-142-3p	1.00	3.40	1.00	1.76
mmu-miR-99b	1.00	2.61	1.00	1.74
mmu-miR-25	1.00	2.50	1.00	1.64
mmu-miR-142-5p	1.00	2.11	1.00	1.94
mmu-miR-34b-3p	1.00	2.03	1.00	2.35
mmu-miR-342-3p	1.00	1.96	1.00	1.99
mmu-miR-497	1.00	1.79	1.00	2.47
mmu-miR-324-5p	1.00	1.58	1.00	1.69

Rat model = 6 weeks of EtOH/CCl_4 in male Lewis rats.

Mouse Model = 8 weeks of biweekly CCl_4 injections.

Fold Change: Relative to Diet Control or Untreated Group, respectively.

Table 2-2. Clinical observations of patients with liver fibrosis.

Cohort	HCV+	Drug Use*	EtOH Use*	Age at bx (years)	AST (U/L)	ALT (U/L)	Total Bilirubin (mg/dL)	Albumin (g/dL)
No Fibrosis	n=8	n=2	None (n=1)	40.50 +/- 5.50	49.38 +/- 18.30	65.50 +/- 47.54	0.61 +/- 0.27	3.96 +/- 0.36
(n=8)			Moderate (n=2)					
			Abuse (n=1)					
Portal Fibrosis	n=8	n=2	None (n=1)	46.88 +/- 6.27	74.86 +/- 78.60	66.00 +/- 41.03	0.85 +/- 0.67	4.21 +/- 0.38
(n=8)			Abuse (n=4)					
Bridging Fibrosis	n=6	n=0	None (n=4)	50.00 +/- 5.48	54.00 +/- 19.93	53.50 +/- 21.69	0.40 +/- 0.06	3.45 +/- 0.42
(n=7)			Moderate (n=1)					
			Abuse (n=1)					
Cirrhosis	n=2	n=0	None (n=1)	44.00 +/- 8.49	128.50 +/- 6.36	87.00 +/- 42.43	1.45 +/- 1.20	2.75 +/- 1.20
(n=3)			Moderate (n=1)					

*Self-reported

HCV+: Hepatitis-C positive

AST: Aspartate aminotransferase.

ALT: Alanine aminotransferase.

Table 2-3. Clinical observations of transplant patient with recurrent HCV.

Time Relative to Transplant	Explant	2 mos	3.5 mos	8 mos	15 mos
Pathological Findings	Cirrhotic	No Fibrosis; Spotty Necrosis	No Fibrosis; Spotty Necrosis	No Fibrosis; Inflammation	Moderate Portal Fibrosis; Early Bridging Fibrosis

2.6 Figures: Chapter 2

Figure 2-1. Combination treatment of ethanol and CCl_4 is associated with increases in fibrosis and activated stellate cells.

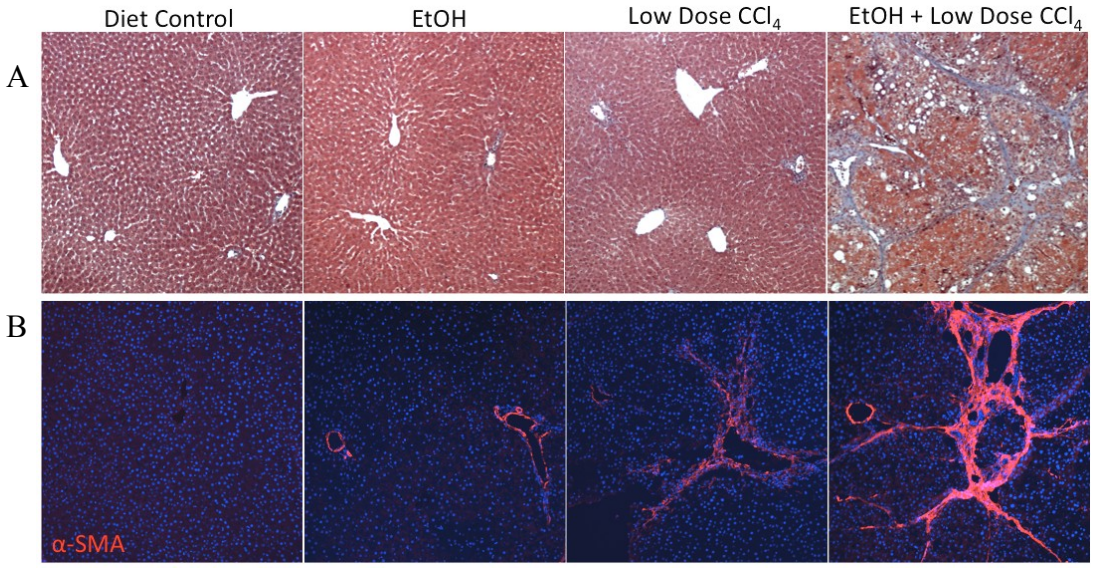

A) Representative 10x images of 5 µm liver sections with Maisson trichrome stain. B) Representative 10x images of 5 µm liver sections stained with alpha-SMA (red) and counterstained with DAPI (blue). All images were taken under identical conditions.

Figure 2-2. Upregulation of miR-214-3p and miR-199a-3p in human fibrosis.

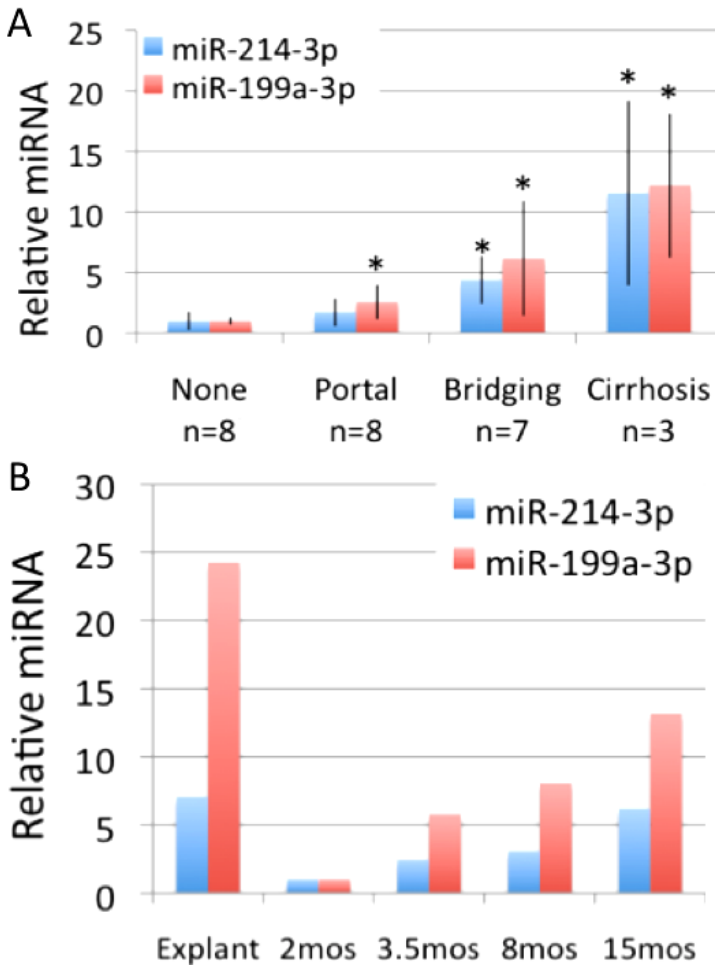

A) Expression of miR-214-3p and miR-199a-3p are significantly upregulated in patients with pathologist-scored fibrosis. All groups were compared to group with no fibrosis. B) Expression of miR-214-3p and miR-199a-3p in an individual liver transplant recipient as fibrosis and hepatitis C recurred. All samples are relative to the two-month biopsy. Relative expression was normalized to 18s rRNA (* = p-value < 0.05). Error bars represent one standard deviation of uncertainty.

Figure 2-3. miR-214 has no post-transcriptional processing bias.

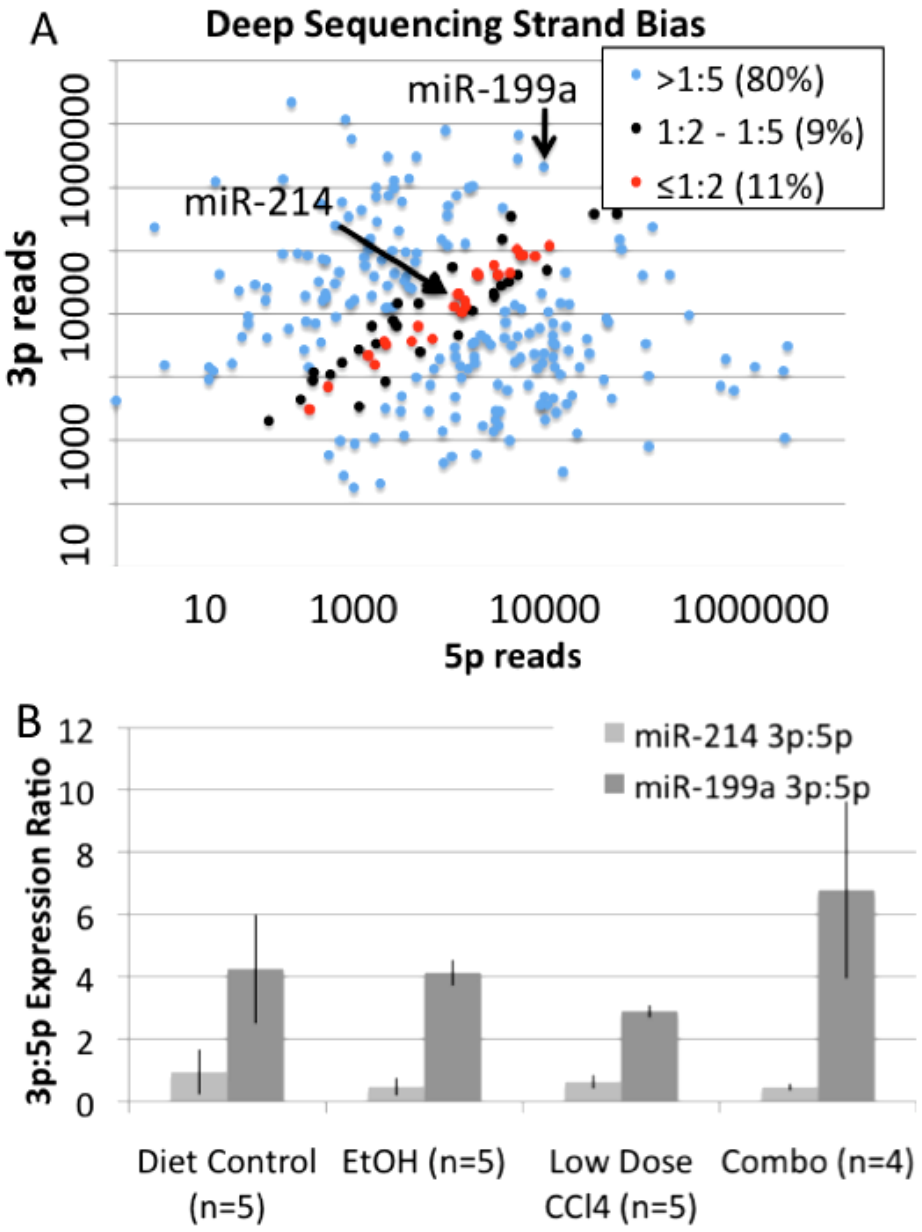

A) miRBase deep sequencing reads comparing 3p reads against 5p reads. miRNAs were classified as having 3p:5p read ratios of <1:2 (red), between 1:2 and 1:5 (black), and >1:5 (blue). miR-214 and miR-199a are indicated by arrows. B) 3p:5p read ratios of miR-214 and miR-199a of each group in the rat alcohol-induced liver fibrosis model. All

ratios were normalized to miR-214 3p:5p read ratio in the diet control group. Error bars represent one standard deviation of uncertainty.

Figure 2-4. All five unique mature sequences, transcribed from three loci, are upregulated during rodent fibrosis.

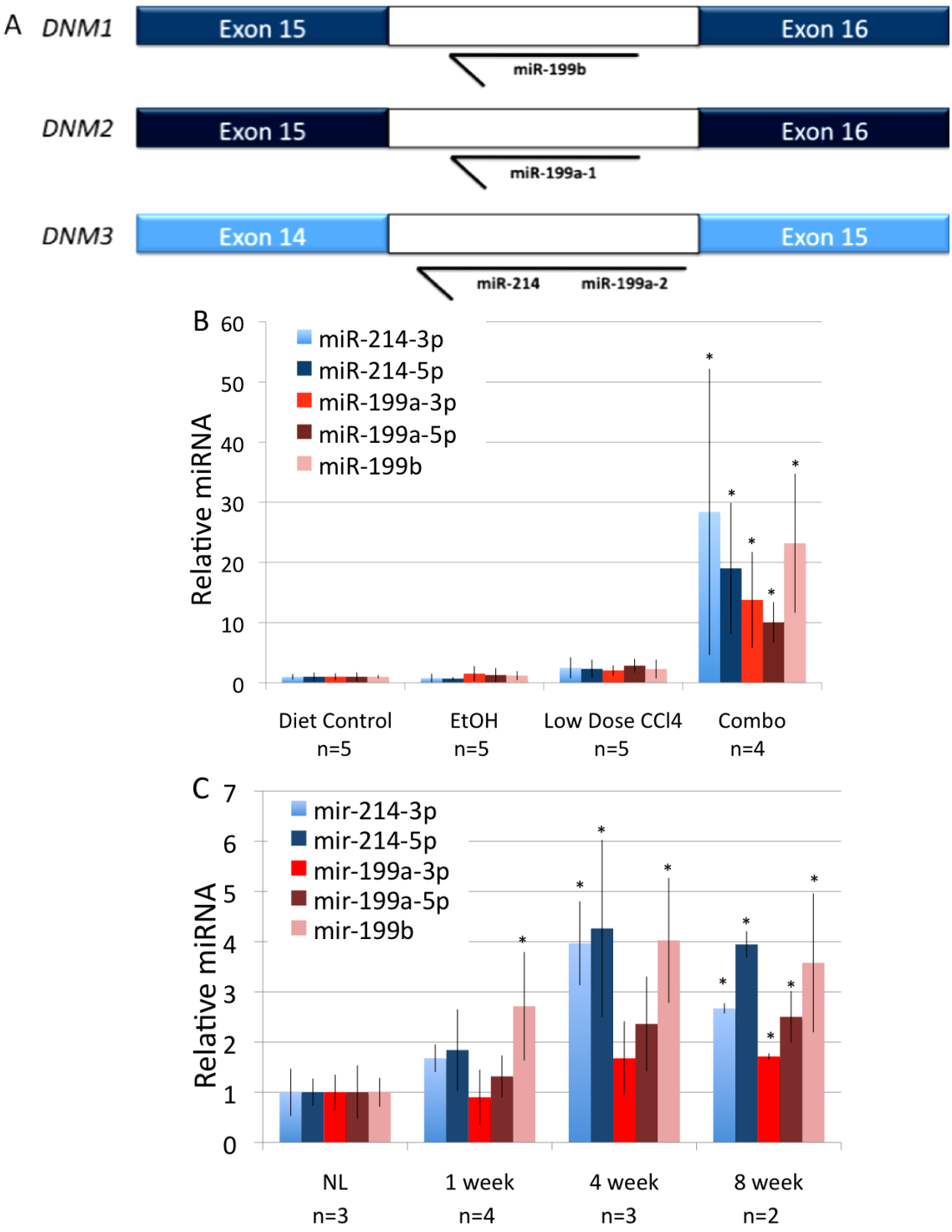

A) The miR-214/199 family is transcribed from the opposite strand of three dynamin genes at three different loci in the human genome. B) All five unique mature sequences are upregulated in the combination group of the rat alcohol-induced liver fibrosis model. C) All five unique mature sequences are upregulated after eight weeks of CCl_4 treatment in BL/6 mice. All groups were normalized to the Diet Control or No CCl_4 groups, respectively. All samples were normalized to 18s rRNA (* = p-value < 0.05). Error bars represent one standard deviation of uncertainty.

Figure 2-5. Rno-miR-214-5p, a third mature strand of miR-214, is expressed in human, mouse and rat.

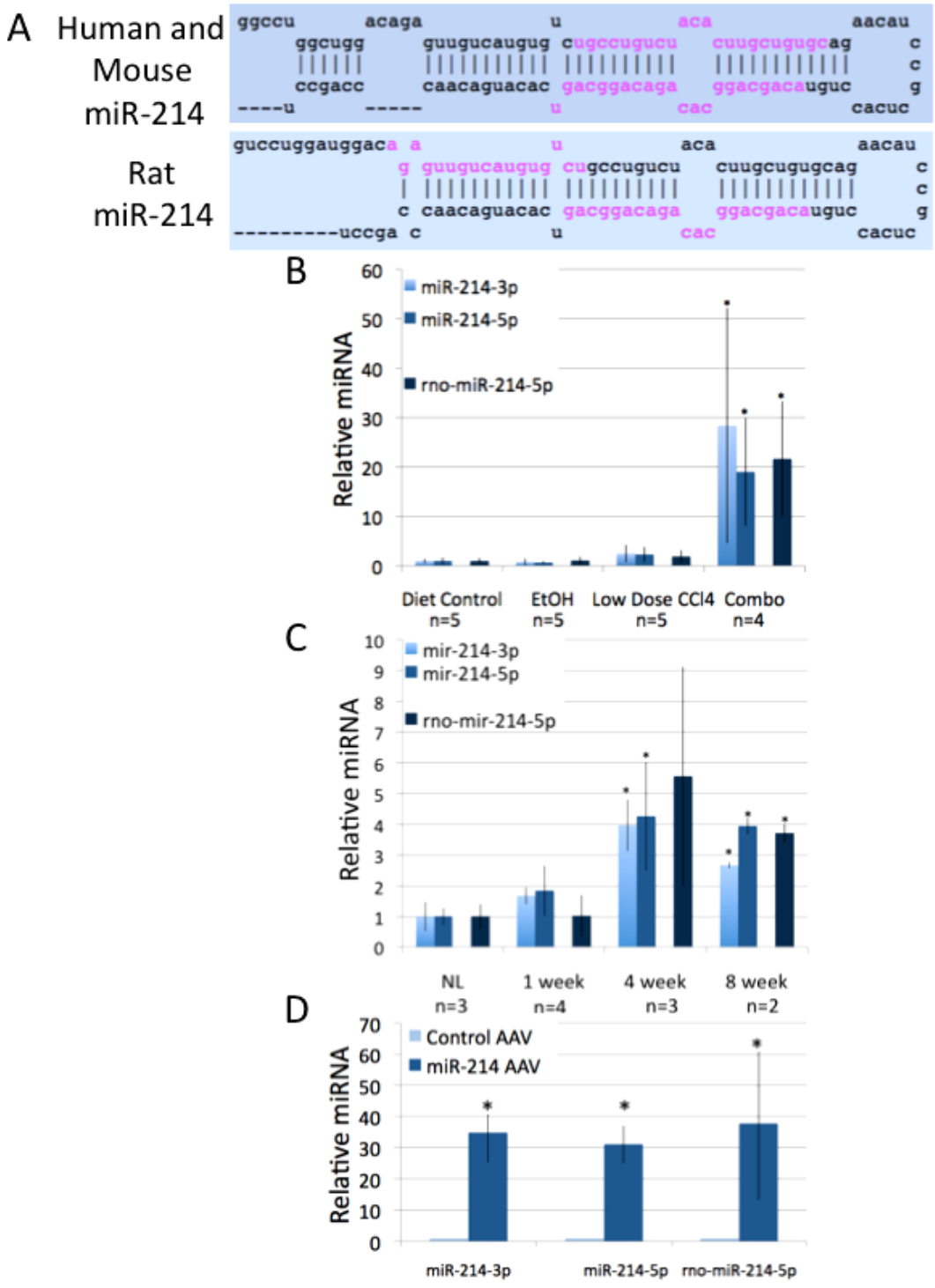

A) miRBase reports that hsa-miR-214-5p and mmu-miR-214-5p differ from rno-miR-214-5p (all in pink, top of hairpin). Note: the mature miR-214-5p sequences do not differ for each mature sequence among species. B-C) All three unique mature miR-214 sequences are significantly upregulated in the rat alcohol-induced and mouse CCl_4 fibrosis model. D) Transfection of the entire hairpin of miR-214 into HeLa cells using an AAV-vector leads to processing of all three miR-214 mature sequences. Rat and mouse cohorts were normalized to the Diet Control or No CCl_4 groups, respectively. HeLa cells transfected with miR-214 were normalized to transfection with control pAAV. All samples were normalized to 18s rRNA (* = p-value < 0.05). Error bars represent one standard deviation of uncertainty.

Figure 2-6. miR-214 is expressed predominantly in nonparenchyml cells.

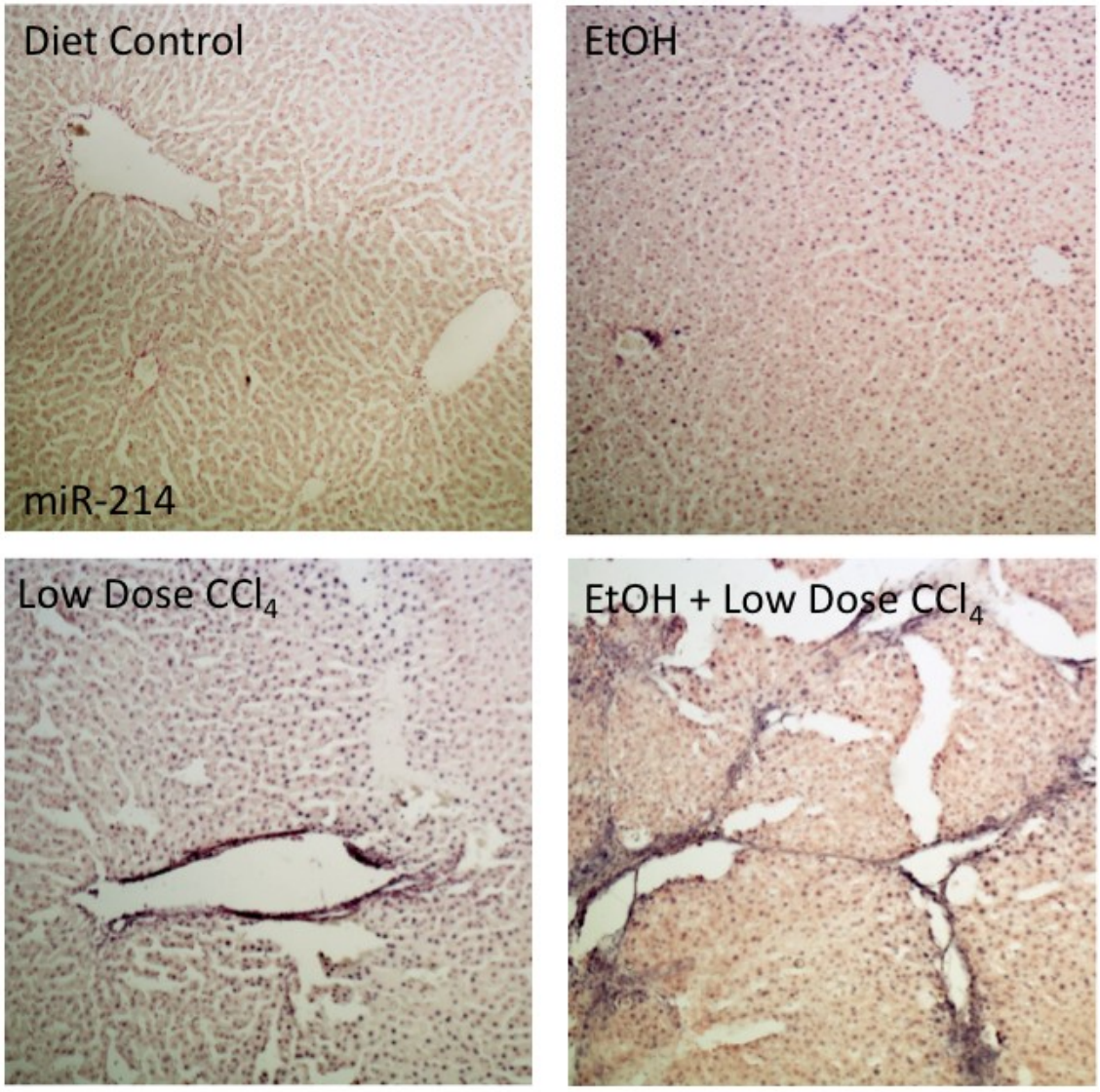

10x images of miR-214 expression (purple) in rat alcohol-induced liver fibrosis model.

All images were taken under identical conditions

Figure 2-7. The miR-214/199 family is highly expressed in stellate cells and is upregulated by TGF-beta.

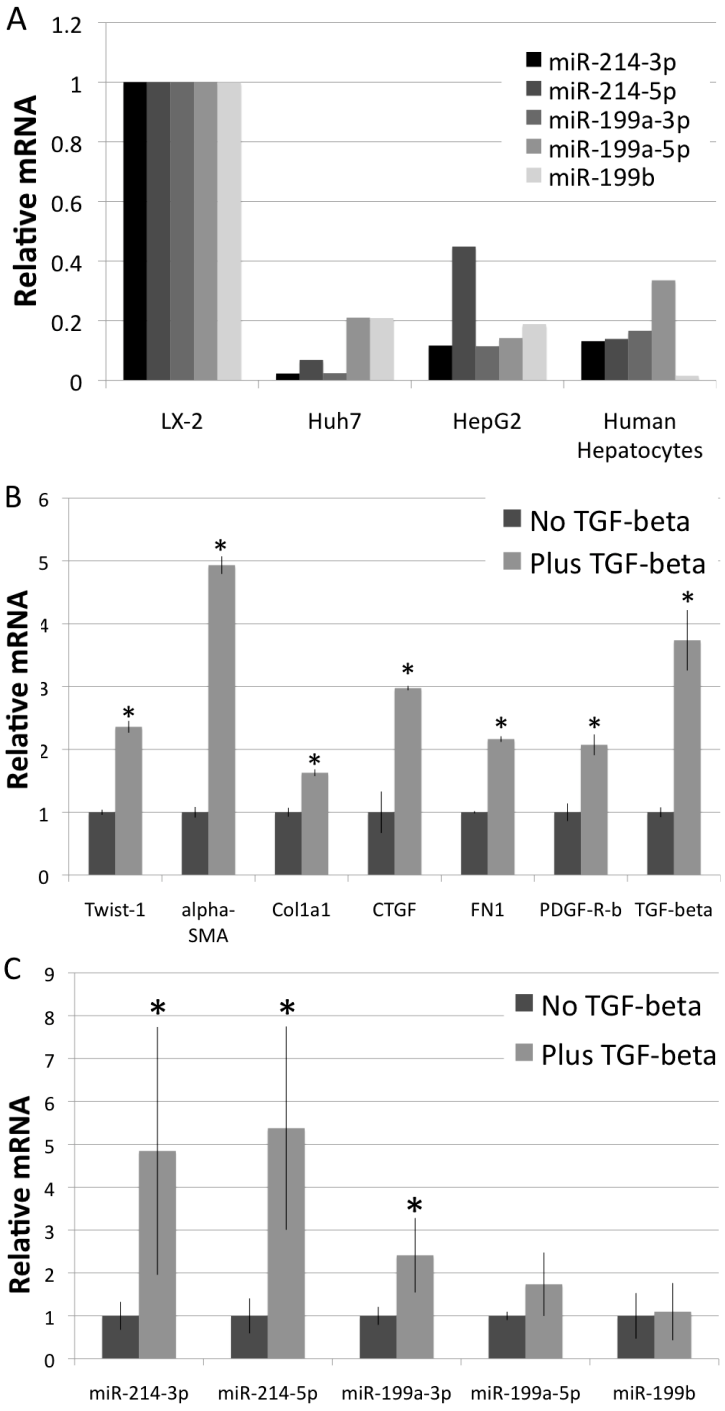

A) Relative expression of all five unique sequences in the miR-214/199 family, relative to LX-2 cell expression. B) Expression of pro-fibrotic genes in LX-2 cells after TGF-beta treatment. C) Expression of the miR-214/199 family in LX-2 cells after TGF-beta treatment. Pro-fibrotic genes were normalized to b-Actin, and the miR-214/199 family was normalized to 18s rRNA (* = p-value < 0.05). Error bars represent one standard deviation of uncertainty.

Figure 2-8. Twist1 is a conserved target of miR-214.

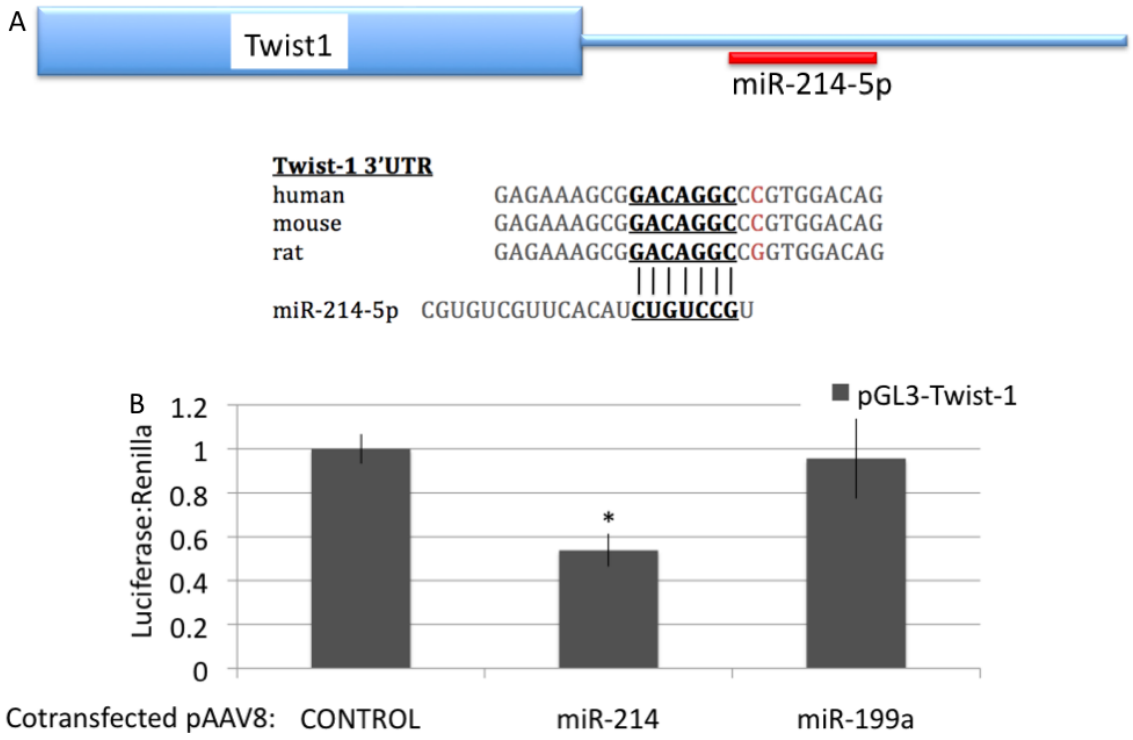

A) Twist1 has a conserved binding site for miR-214-5p B) HeLa cells were co-transfected with pGL3_Luc_Twist1-3'UTR and a AAV-vector with no miRNA, miR-214 or miR-199a. Expression of luciferase was normalized to renilla (* = p-value < 0.05). Error bars represent one standard deviation of uncertainty.

Figure 2-9. Twist1 and Twist2 are upregulated during liver fibrosis.

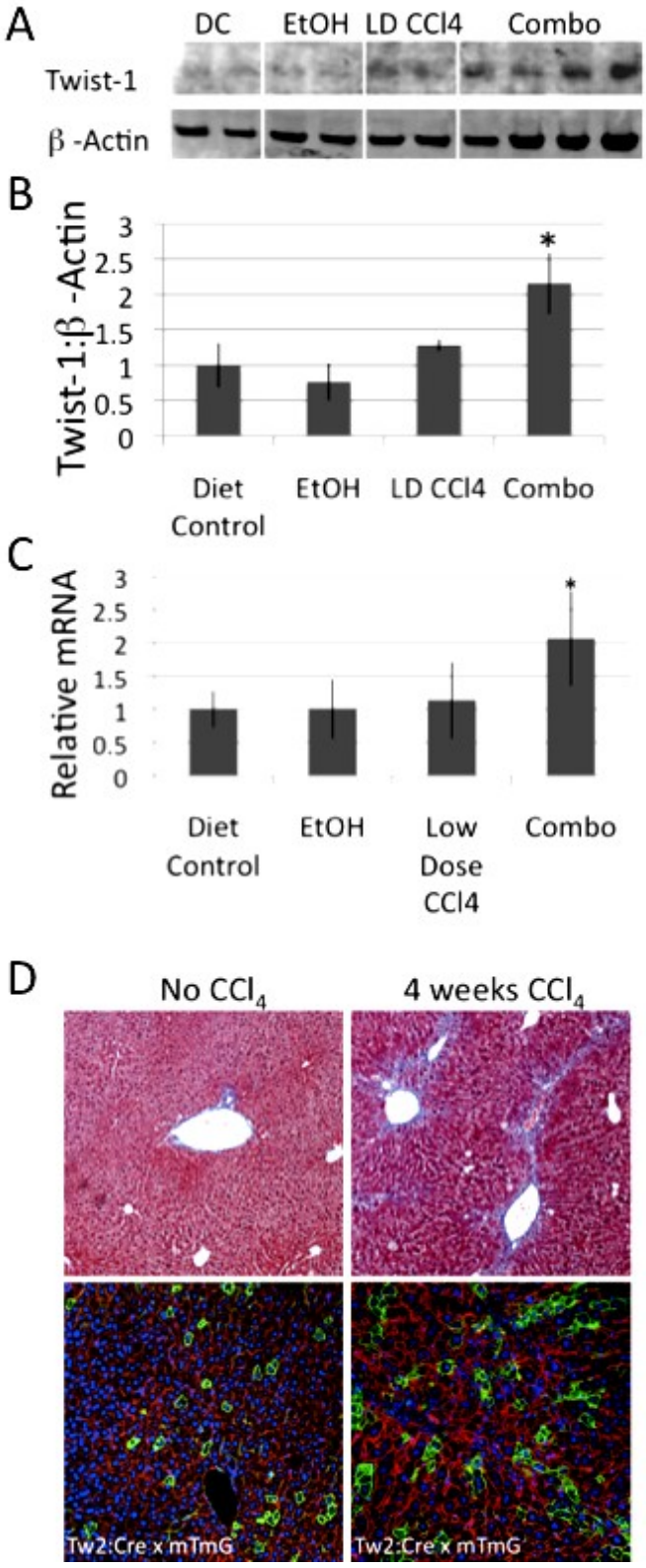

A) Twist1 Western blot in rat alcohol-induced fibrosis model. B) Quantification of Twist1 Western blot normalized to the diet control cohort. Individual lanes normalized to beta-Actin C) Twist1 mRNA expression in rat fibrosis model. All samples are relative to the diet control cohort. Relative expression was normalized to 18s rRNA D) Representative 10x images of Maisson trichrome-stained slides and epifluorescent membrane expression of mTomato (red) and eGFP (green) in Twist2:Cre/+; mTmG/+ mice after 4 weeks of CCl_4 treatment. Cells were counterstained with DAPI (blue). (* = p-value < 0.05). Error bars represent one standard deviation of uncertainty.

Figure 2-10. Inhibition of Twist1 in LX-2 cells limits stellate cell activation, migration and miR-214/199 expression.

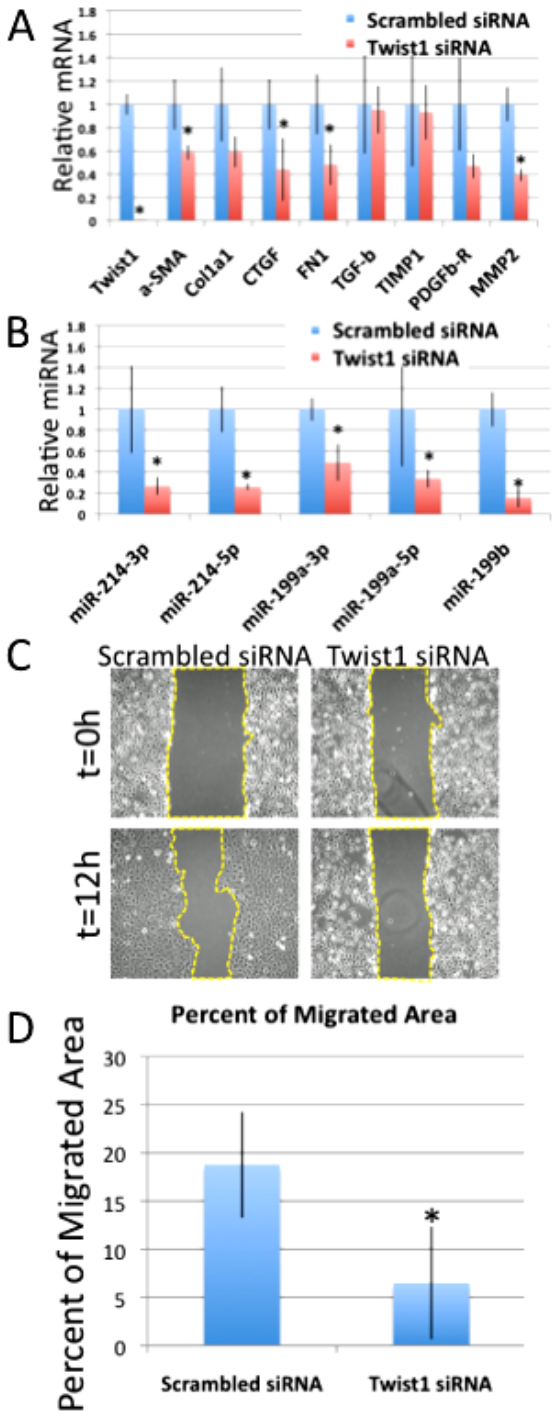

A) mRNA expression of pro-fibrotic genes in LX2 cells 24 hours after transfection of scrambled or Twist1 siRNA. All samples are relative to cells treated with scrambled siRNA. Relative expression was normalized to beta-Actin. B) Expression of the miR-214/199 family in LX2 cells 24 hours after transfection of scrambled or Twist1 siRNA. All samples are relative to cells treated with scrambled siRNA. Relative expression was normalized to 18s rRNA. C) 10x representative images of LX-2 cells treated with scrambled or Twist1 siRNA at t=0h and t=12h post-scratch. D) Quantified cell migration 12 hours after scratch. ImageJ was used to measure area devoid of cell migration (* = p-value < 0.05). Error bars represent one standard deviation of uncertainty.

Figure 2-11. Inhibition of miR-214-5p in LX-2 cells is associated with increase in alpha-SMA and Col1a1.

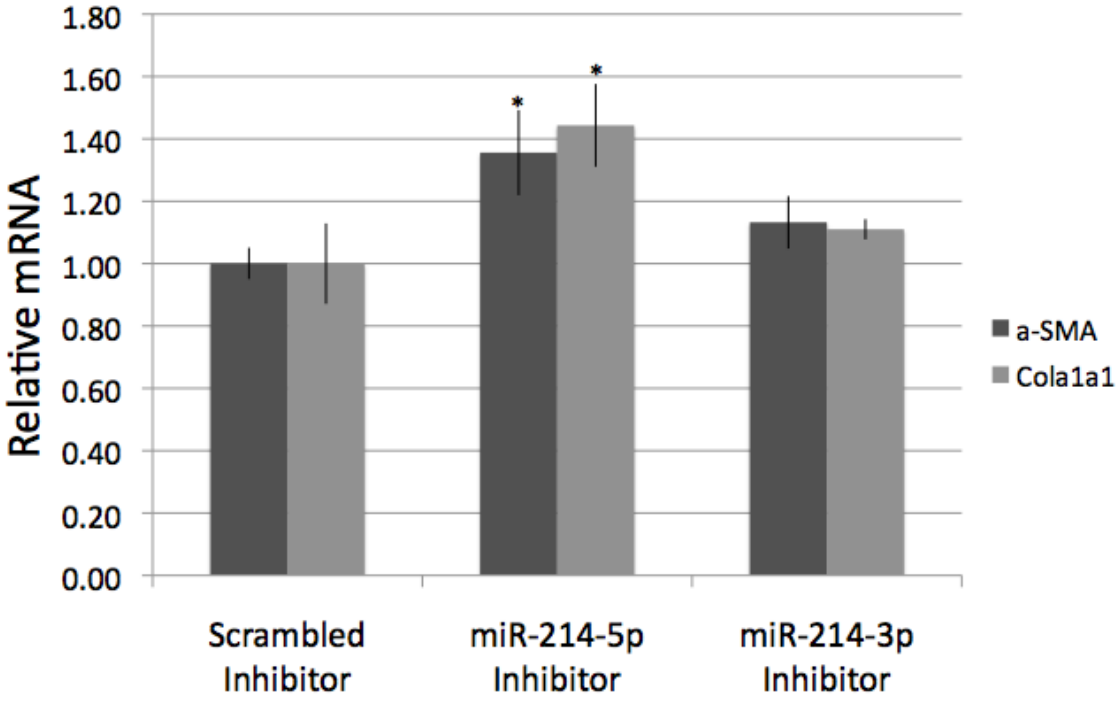

mRNA expression of alpha-SMA and Col1a1 in LX2 cells 24 hours after transfection with scrambled, miR-214-5p or mir-214-3p inhibitors. All samples are relative to cells treated with scrambled inhibitor. Relative expression was normalized to beta-Actin (* = p-value < 0.05). Error bars represent one standard deviation of uncertainty.

Figure 2-12. Inhibition of miR-214-5p in LX-2 cells causes upregulation of Twist1 and downstream Twist1 targets.

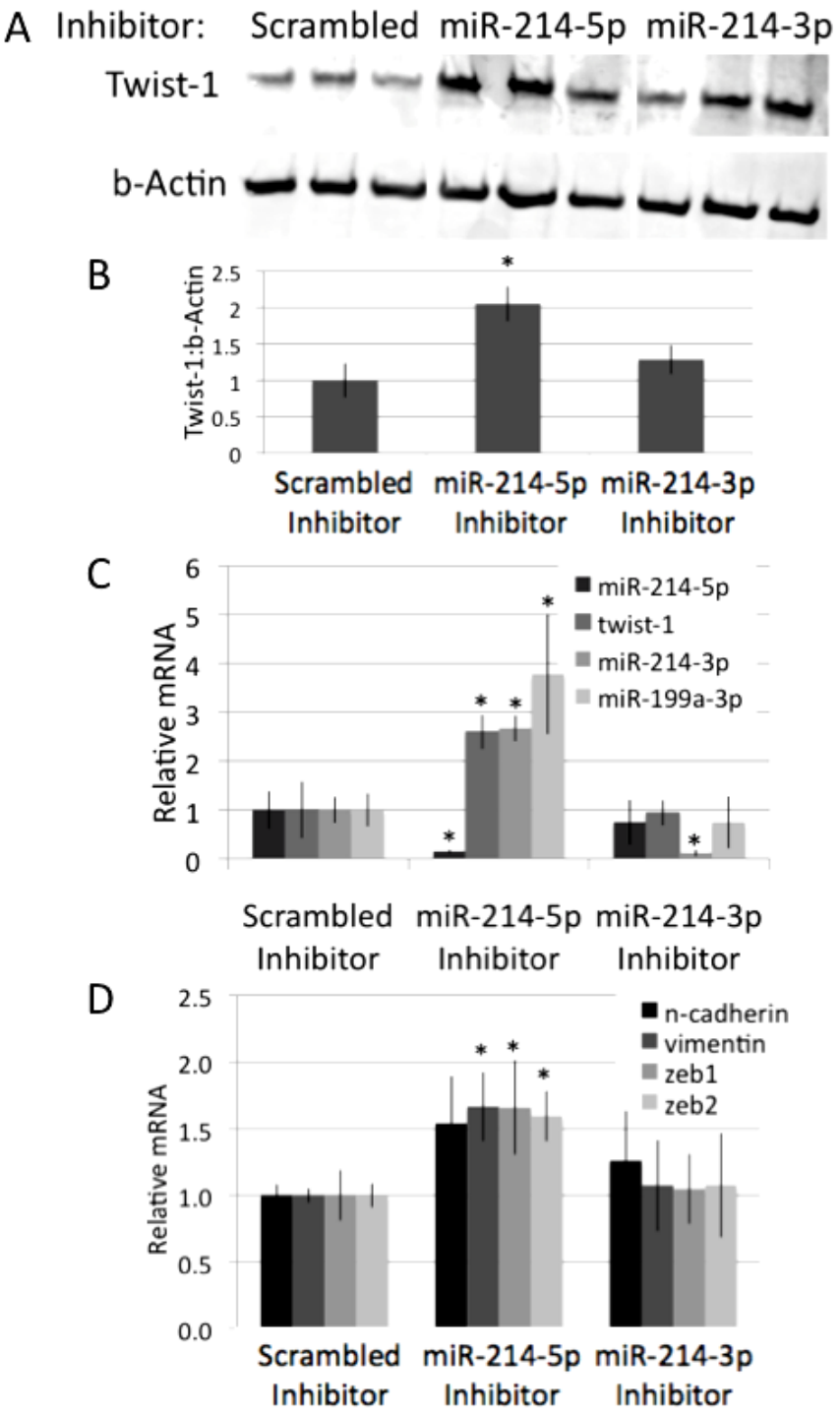

A) Twist1 Western blot in LX-2 cells transfected with miR-214 inhibitors. B) Quantification of Twist1 Western blot normalized to the group treated with scrambled inhibitor. Individual lanes normalized to beta-Actin. C) mRNA expression of Twist1 and the miR-214/199 family in LX2 cells 24 hours after transfection of scrambled, miR-214-5p or mir-214-3p inhibitors. All samples are relative to cells treated with scrambled inhibitor. miRNA Relative expression was normalized to 18s rRNA and Twist1 was normalized to beta-Actin. D) mRNA expression of mesenchymal genes in LX2 cells 24 hours after transfection of scrambled, miR-214-5p or mir-214-3p inhibitors. All samples are relative to cells treated with scrambled inhibitor. Relative expression was normalized to beta-Actin (* = p-value < 0.05). Error bars represent one standard deviation of uncertainty.

Figure 2-13. Inhibition of miR-214-5p is associated with an increase in stellate cell migration.

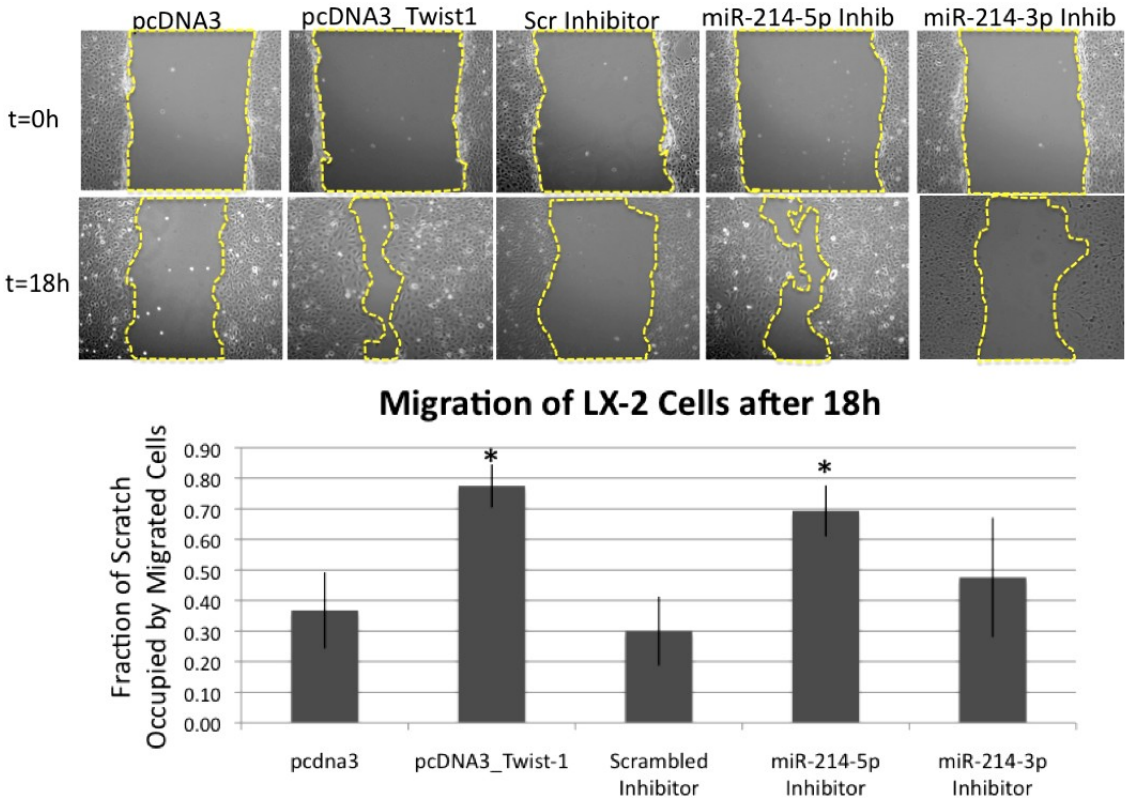

A) 10x representative images of LX-2 cells treated with Twist1 or miR-214 inhibitors at t=0h and t=18h post-scratch. B) Quantified cell migration 18 hours after scratch. ImageJ was used to measure area devoid of cell migration (* = p-value < 0.05). Error bars represent one standard deviation of uncertainty.

Figure 2-14. miR-214-5p targets Twist1 to limit expression of the miR-214/199 family and pro-fibrotic genes.

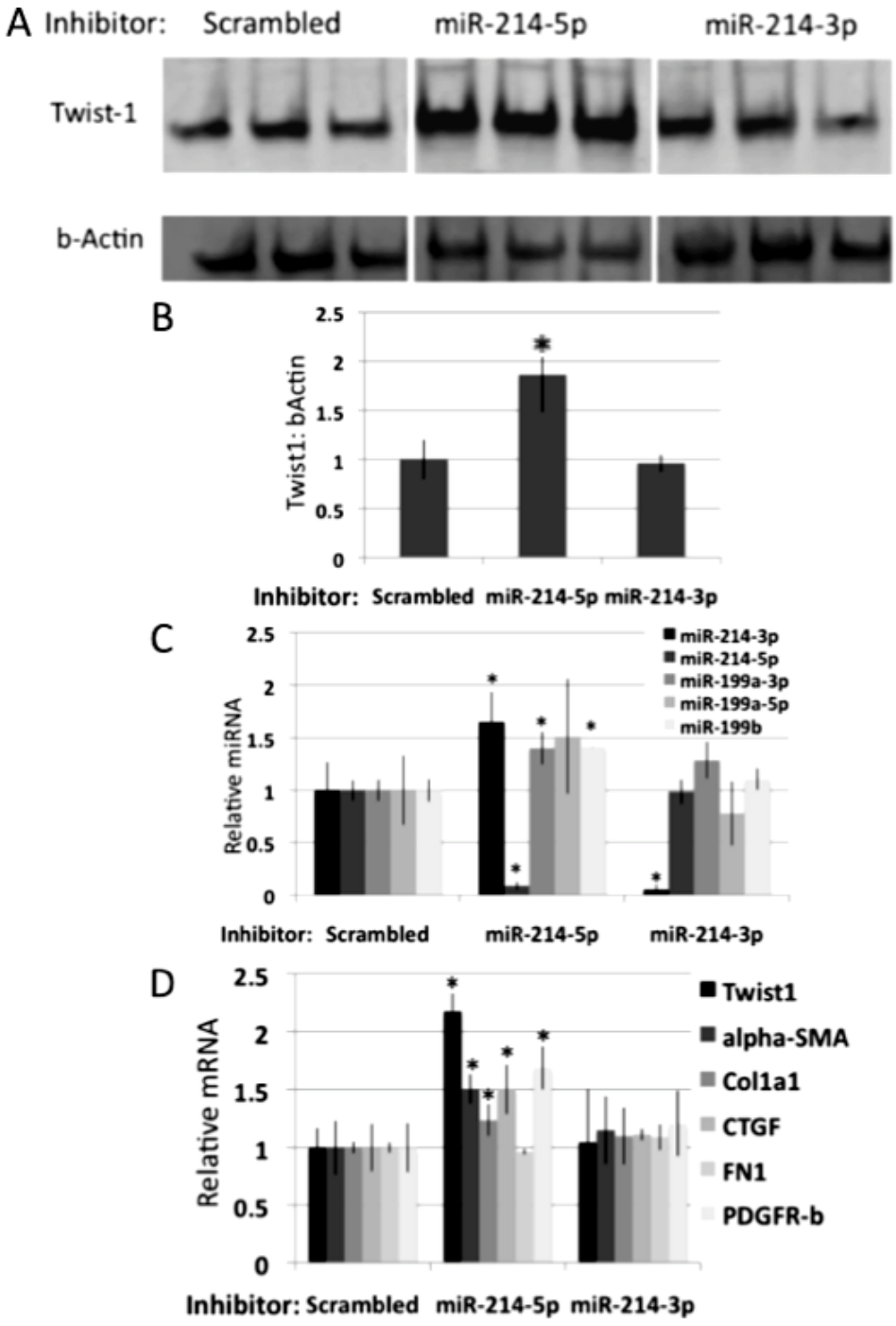

A) Twist1 Western blot in LX-2 cells transfected with Twist1 and miR-214 inhibitors.

B) Quantification of Twist1 Western blot normalized to the group treated with Twist1

and scrambled inhibitor. Individual lanes normalized to beta-Actin. C) mRNA expression of the miR-214/199 family in LX2 cells 24 hours after transfection of Twist1 and scrambled, miR-214-5p or mir-214-3p inhibitors. All samples are relative to cells treated with Twist1 and scrambled inhibitor. Relative expression was normalized to 18s rRNA. D) mRNA expression of pro-fibrotic genes in LX2 cells 24 hours after transfection of Twist1 and scrambled, miR-214-5p or mir-214-3p inhibitors. All samples are relative to cells treated with Twist1 and scrambled inhibitor. Relative expression was normalized to beta-Actin (* = p-value < 0.05). Error bars represent one standard deviation of uncertainty.

Figure 2-15. miR-214-5p targets Twist1 to limit stellate cell migration.

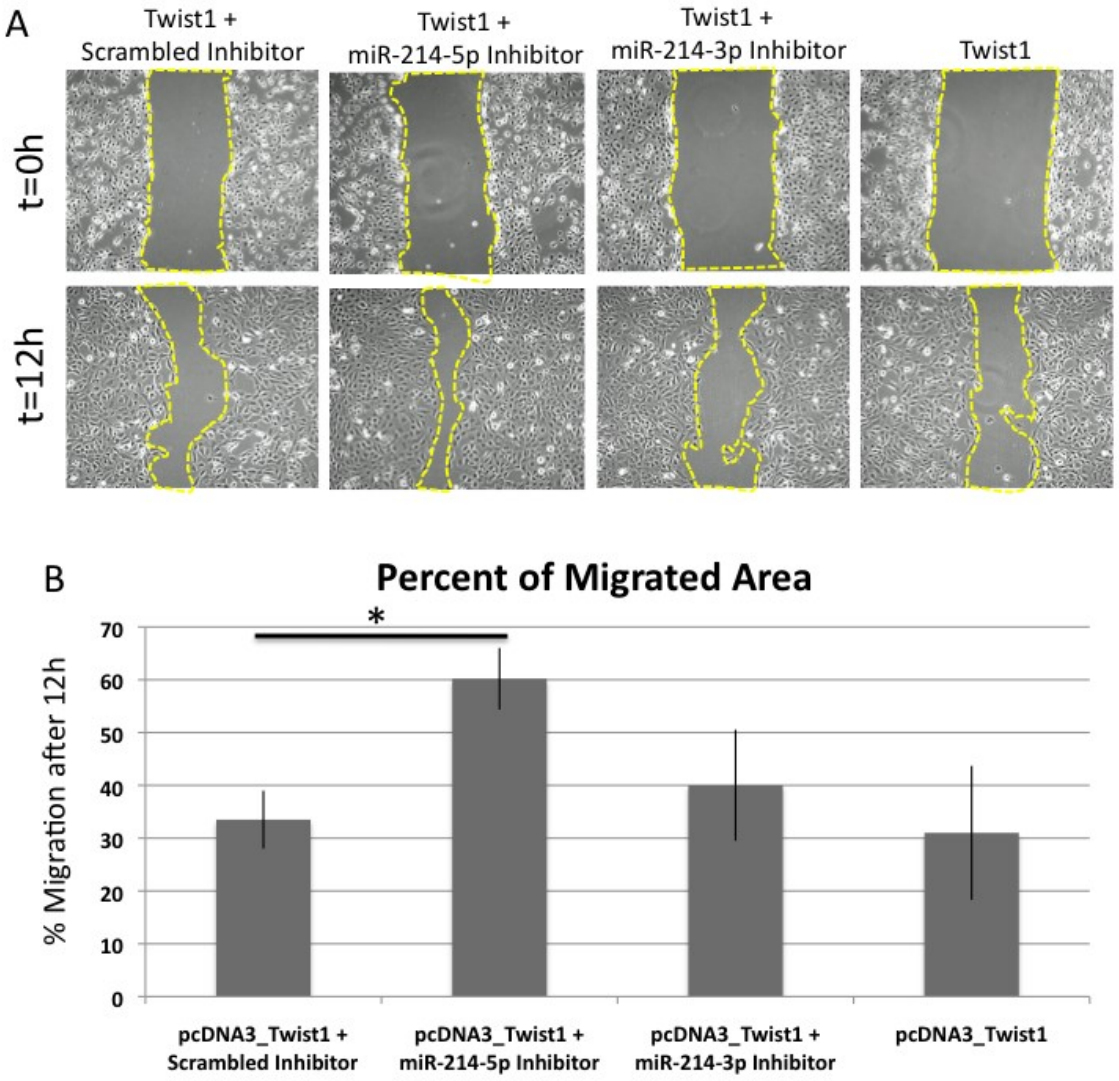

A) 10x representative images of LX-2 cells treated with Twist1 and miR-214 inhibitors at t=0h and t=12h post-scratch. B) Quantified cell migration 12 hours after scratch. ImageJ was used to measure area devoid of cell migration (* = p-value < 0.05). Error bars represent one standard deviation of uncertainty.

Figure 2-16. Proposed model of negative feedback loop between miR-214-5p and Twist1 in hepatic stellate cells.

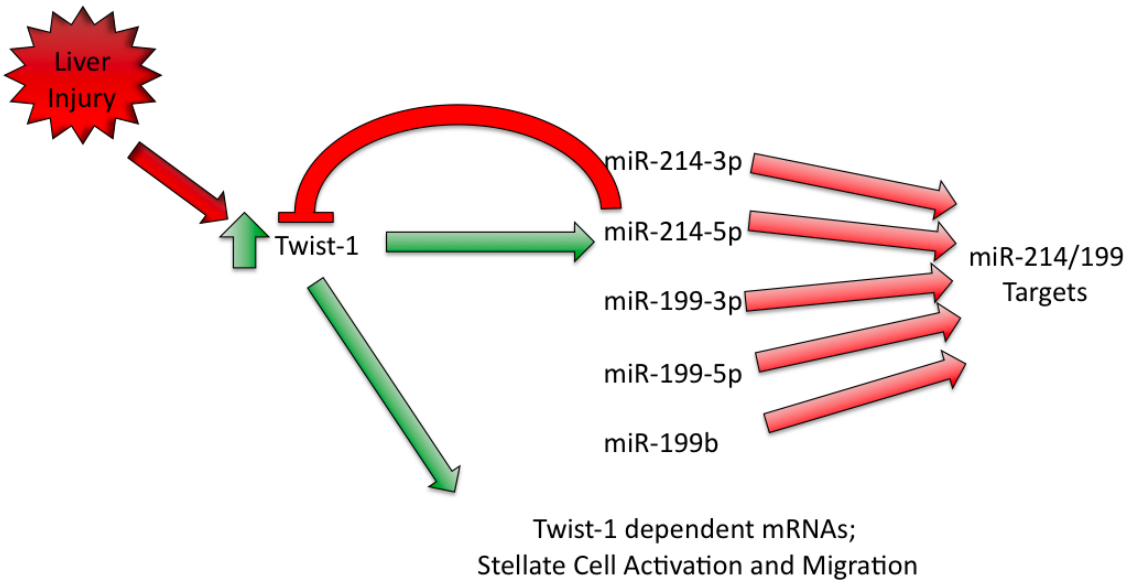

Liver injury upregulates Twist1, which transcriptionally upregulates the miR-214/199 family and Twist1 dependent mRNAs. miR-214-5p limits additional activation of Twist1, regulating stellate cell activation, migration and collagen deposition.

3. CHAPTER 3. HEPATIC MAINTENANCE OF MIR-29A PROVIDES NON-CELL AUTONOMOUS PROTECTION DURING LIVER FIBROSIS

3.1 Introduction

Using an approach similar to the model described in Chapter 2, we induced liver fibrosis in a cohort of wild type rodents and investigated changes in miRNA expression. This chapter will describe miRNA changes during carbon tetrachloride-induced liver fibrosis in C57BL/6 wild type female mice. Over an eight-week period, mice given biweekly injections of CCl_4 developed progressive fibrosis. Our goal was to identify miRNAs with differential patterns of expression, predict and test targets, and examine if expression could be manipulated to treat fibrosis.

Some miRNAs are processed as families and have conserved targets in the same pathways or gene networks (Zhang et al., 2009; Guo et al., 2012; Mendell, 2008). In our liver fibrosis model, the entire miR-29 family, which has three members transcribed from 2 loci, is downregulated. Downregulation of miR-29 has been implicated in organ fibrosis, including renal, lung and cardiac fibrosis (Wang et al., 2012; Cushing et al., 2011; van Rooij et al., 2008). During fibrosis, the organ undergoes homeostatic changes during which myofibroblasts produce extracellular matrix (ECM) proteins, including members of the collagen, elastin and fibrillin families. ECM proteins replace normal parenchyma, inhibit vascular development and disrupt cell-to-cell contact, all of which lead to impaired liver function. Many members of these ECM families have conserved predicted binding sites for miR-29a, suggesting that miR-29a may act as a negative regulator of matrix protein production.

Because miR-29 was downregulated in liver fibrosis, we postulated that modulation of miR-29a could ameliorate liver fibrosis and potentially restore normal liver histology and function. The liver possesses the ability to induce cell turnover and promote regression of fibrosis. Targeting cells in the liver to overexpress miR-29a could help to create a normal physiologic environment by inhibiting initial fibrosis development and even advanced scarring.

The liver metabolizes toxins and other foreign matter, making it a very appealing organ for foreign gene therapy delivery. In fact, others have had success delivering genes to the liver (Sands, 2010; Wang et al., 2008; Hu et al., 2013). Since systemic delivery of adeno-associate virus (AAV) serotype 8 predominantly infects hepatocytes, we administered miR-29a using a self-complementary AAV8 delivery system via a single tail vein injections and assessed collagen deposition in the organ after induced injury.

In this chapter, we present results from the low-density array qPCR at different stages of progressive fibrosis. We identify that miR-29a is downregulated, and we deliver miR-29a to the liver to restore expression. Our goal was to inhibit fibrosis development using a negative regulator or extracellular matrix proteins. Histologically, not only was fibrosis inhibited, it was reversed in a clinically relevant model. We examine cell specific expression, and determine viral delivery primarily infects hepatocytes. Finally, we investigate a non cell-autonomous mechanism based on identification of the virus in hepatocytes and collagen production in myofibroblasts, including stellate cells. Taken together, these data suggest that hepatocellular expression of miR-29a is an important regulator of liver fibrosis by limiting collagen expression in a non-cell autonomous manner.

3.2 Results

3.2.1 The miR-29 family is downregulated in carbon tetrachloride-induced hepatic fibrosis.

To understand miRNA dynamics under liver fibrotic conditions, we utilized a published approach to induce liver fibrosis using carbon tetrachloride (CCl_4). 2- and 3 month old C57BL/6 wild type female mice were given biweekly injections of CCl_4 for 0, 1, 4 and 8 weeks, and mice developed progressive fibrosis over the 8-week period (Figure 3-1A). Using a low-density array qPCR, we assessed expression of over 350 miRNAs at each time point. At 8 weeks of CCl_4 treatment, three members of the miR-29 family were among the 60 most downregulated miRNAs (Table 3-1, highlighted in yellow). Using individual assays, we confirmed that all three members of the miR-29 family are significantly downregulated at 4 and 8 weeks (Figure 3-1B). Interestingly, we did not detect a significant change in primary miR-29a, suggesting that downregulation of at least miR-29a could be due either to instability of the mature miRNA or decrease in miRNA processing.

Since about 80% of the mass of a normal liver consists of hepatocytes, we reasoned that downregulation of miR-29 could be specific to hepatocytes. To test this hypothesis, we treated primary human hepatocytes with a proinflammatory cytokine, TGF-beta. After 24 hours, all three mature sequences of miR-29 were significantly downregulated while other hepatocyte-specific miRNAs expressed remained constant (Figure 3-1C). Consistent with our *in vivo* observations, primary-miR-29a did not decrease, suggesting that downregulation of the miR-29 family in hepatocytes is due to changes during miRNA processing or stability of the mature miRNA.

3.2.2 Systemic injection of scAAV8.miR-29a.eGFP to hepatocytes is not toxic.

Among the predicted targets of the miR-29 family are extracellular matrix proteins, including members of the collagen, elastin and fibronectin families (Lewis et al., 2005). We hypothesized that augmenting expression of miR-29a using a non-integrating virus could ameliorate fibrosis development. We cloned the miR-29a hairpin downstream of a ubiquitous promoter, elongation factor 1 alpha (Figure 3-2A). During post-transcriptional processing of this vector, miR-29a is cleaved and processed while enhanced green fluorescent protein (eGFP) is translated. We transfected serial dilutions of the AAV vector into HEK-293 cells. Both miR-29a and eGFP expression steadily increased as we steadily increased the amount of transfected vector (Figure 3-2B and 3-2D).

We delivered $2x10^{11}$ AAV genomes to a cohort through one systemic tail vein injection (Figure 3-3A). After 4 weeks, there was no evidence of toxicity, as seen by histological examination (Figure 3-3B), bilirubin and liver function tests (unpublished data). eGFP was readily detectable in more than 50% of cells in the liver (Figure 3-3C). Surprisingly, there was no increase in primary or mature miR-29a (Figure 3-3D), suggesting either that the viral dosage was not sufficient to overexpress miR-29a, or that miR-29a expression in the liver is tightly regulated.

We stained liver sections with eGFP and markers for hepatocytes or stellate cells (Figure 3-4). We only detect overlap of eGFP expression when co-stained with albumin (Figure 3-4A), suggesting that AAV8 infection is limited primarily to hepatocytes. In

contrast, there was no evidence of coexpression of eGFP and either vimentin or desmin, both of which label stellate cells.

3.2.3 scAAV8.miR-29a.eGFP is protective against fibrosis and is associated with limited stellate cell activation.

To test efficacy of the miR-29a virus, we pretreated mice with $2x10^{11}$ AAV genomes, and induced hepatotoxic injury through biweekly injections of CCl_4 (Figure 3-5A). After 4 weeks of injury, miR-29a expression was significantly downregulated in our control group. However, the group treated with scAAV.miR-29a.eGFP maintained expression of miR-29a (Figure 3-5B). Downregulation of miR-29a in the cohort treated with scAAV.eGFP was associated with an increased histological and biochemical evidence of fibrosis (Figure 3-5C and 3-5E), and a pathologist blinded to the study determined that there was a significant increase in fibrosis between control- and miR-29a-treated mice (Figure 3-5D).

We wanted to test the efficacy of our treatment in the context of established disease. Therefore, we pretreated mice with CCl_4 for 4 weeks to induce injury before systemically delivering $2x10^{11}$ AAV genomes (Figure 3-6A). After 8 more weeks of CCl_4 treatment, we examined miR-29a expression and progression of fibrosis. Although maintenance of miR-29a was lost (Figure 3-6B), eGFP in the miR-29a group was detected (unpublished data). Importantly, fibrosis development was ameliorated in the miR-29a group both histologically and biochemically (Figure 3-6C and 3-6E). Interestingly, a blinded pathologist suggested that there was even regression of fibrosis at

12 weeks (Figure 3-6D), suggesting that mir-29a expression in hepatocytes is protective against CCl_4-induced liver fibrosis.

During liver fibrosis, stellate cells morphologically change and produce ECM proteins. Not only did hepatic miR-29a expression limit collagen deposition, but treatment of the miR-29a AAV also was associated with fewer alpha-SMA positive cells in our prevention and intervention model (Figure 3-7), suggesting that hepatocellular maintenance of miR-29a limits activation of stellate cells.

3.2.4 Hepatocytes export miR-29a via exosomes.

Both in our prevention model and in our intervention model, hepatocellular maintenance of miR-29a expression is protective against fibrosis development. There was limited expression of collagen, assessed by histology and protein expression. Since stellate cells and other myofibroblasts make extracellular matrix proteins, we postulated that one mechanism of protection could be through exosomal transfer of miR-29a from hepatocytes to myofibroblasts. Recent studies have provided evidence for packaging miRNAs into exosomes (Monteclavo et al., 2012; Record et al., 2011), suggesting one possible mechanism of non-cell autonomous function. We transfected pAAV.miR-29a.eGFP into HuH7 and HeLa cells, and isolated RNA from cells and exosomes. There was a significant increase in cellular and exosomal miR-29a in both cell lines treated with pAAV.miR-29a.eGFP (Figure 3-8AB). While miR-29a increased significantly, we did not detect a significant change in other microRNAs that are expressed in both compartments, suggesting that overexpression of miR-29a using the AAV vector leads to specific upregulation of miR-29a in hepatocyte exosomes.

3.2.5 Transfer of miR-29a from hepatocytes to stellate cells limits collagen production.

Since we determined that hepatocellular expression of miR-29a is protective, and that hepatic miR-29a is packaged and released from the cell via exosomes, we next asked if liver cells transfer miR-29a from one cell type to another. To test this, we utilized a co-culture system that mimicked what was seen under fibrotic conditions. Hepatocytes treated with either miR-29 inhibitor or pAAV8.miR-29a.eGFP were cultured with LX-2 cells co-transfected with miR-29 inhibitor and a luciferase vector containing either the wild type sequence or mutated sequence of human Col1a1. Others have confirmed that the Col1a1-3'UTR has 3 conserved binding sites for mir-29a (Mendell, unpublished data). After 24 hours, luciferase activity significantly increased when LX-2 cells were co-cultured with HuH7 cells treated with miR-29 inhibitor (Figure 3-9). Conversely, overexpressing miR-29a in HuH7 cells significantly decreased luciferase activity in LX-2 cells, suggesting that modulation of miR-29a in hepatocytes has profound effect on collagen production in hepatic stellate cells.

3.3 Discussion

Using a comprehensive approach to study miRNA changes, we identified that the miR-29 family is downregulated in fibrotic whole liver tissue. Because the miR-29 family targets many extracellular proteins, including Col1a1, Col3a1, Elastin and Fibrillin 1, we hypothesized that decreased miR-29 expression in whole liver could regulate fibrosis. Recent studies indicate that miR-29 is downregulated in hepatic stellate

cells during liver fibrosis (Roderburg et al., 2011), but its expression and function in hepatocytes remained unexplored. All three mature sequences of miR-29 are significantly downregulated after treatment with TGF-beta in primary human hepatocytes, suggesting that fibrosis is associated with downregulation of miR-29 in hepatocytes. While others have shown that TGF-beta transcriptionally downregulates miR-29a in other settings (Qin et al., 2011; Winbanks et al., 2011), primary miR-29a expression does not change during CCl_4 induced liver fibrosis, implying that the post-transcriptional mechanism is hepatocyte-specific. The actual mechanism of hepatocellular post-transcriptional downregulation of miR-29a, however, remains unknown but we postulate that it is either due to instability of the mature transcript or decrease in miRNA processing.

scAAV.miR-29a.eGFP did not induce overexpression *in vivo*, and we hypothesize two different possibilities to explain this observation. First, therapeutic delivery of $2x10^{11}$ AAV genomes may not be sufficient to observe overexpression of miR-29a. Others have reported detectable miRNA overexpression using the same approach but with a five-fold dose increase (Kota et al., 2009). Given that infection using the same control virus at a higher dose resulted in increased eGFP translation and more viral genomes, we conclude that this mode of delivery does not limit viral gene expression. Second, and more likely, expression of miR-29a in hepatocytes may be tightly regulated. Although serial transfections of pAAV.miR-29a.eGFP induce increased expression of miR-29a *in vitro*, uninjured animals treated with scAAV.miR-29a.eGFP have similar expression of miR-29a compared to baseline. Consistent with this hypothesis, we do not detect an increase in miR-29a in liver after systemic injection of a five-fold higher dose

of scAAV.miR-29a.eGFP (unpublished data). miR-29a may be tightly regulated such that overexpression in hepatocytes is not attainable.

In this study, we systemically delivered miR-29a using adeno-associated virus serotype 8, which has a high tropism for hepatocytes (Grimm et al, 2006; Sands, 2011). eGFP expression was only detected when co-staining with albumin, suggesting that transduction of AAV8 in the liver is limited predominantly to hepatocytes. Nonetheless, a single injection of $2x10^{11}$ AAV genomes, which led to about 50% liver cell transduction in our model, had a dramatic therapeutic benefit in miR-29a-treated livers when comparing histological sections and collagen expression. This observation was consistent not only when pretreating animals with scAAV.miR-29.eGFP but also when intervening with scAAV.miR29a.eGFP after induction of fibrosis. Surprisingly, miR-29a was associated with regression of fibrosis in animals that were pretreated with CCl_4.

Genetic deletion of miR-29a in hepatocytes has been associated with increased collagen deposition during CCl_4 treatment (Kogure et al., 2012). Consistent with these observations, we report for the first time therapeutic benefit through maintenance of miR-29a expression in hepatocytes. Systemic delivery of scAAV.miR-29a.eGFP was associated with fewer alpha-SMA positive cells. Because delivery was limited to hepatocytes, we hypothesize three potential mechanisms, and we acknowledge that a combination of any three are possible. First, hepatic expression of miR-29a could be limiting expression of pro-fibrogenic factors in hepatocytes. If miR-29a targets genes that promote release of proinflammatory cytokines and reactive oxygen species in hepatocytes, downstream activation of stellate cells and deposition of collagen would be limited. Second, the size of mature miRNAs allows for passage through direct cell-cell

gap junctions between hepatocytes and collagen-producing cells, and others have developed methods to follow transfer of miRNAs in this way (Greco et al., 2013; Katakowski et al., 2010). Finally, miRNAs have been reported to be packaged into exosomes, and transfer of functional miRNAs through exosomes has been explored in other settings (Mittelbrunn et al., 2011; Monteclavo et al., 2012; Valadi et al., 2007). Interestingly, both *in vivo* and *in vitro* models investigating a non-cell autonomous role between hepatocytes and stellate cells have led to the understanding that cross-talk between liver-specific cells has a functional benefit (Bhatia et al., 1999; Uyama et al., 2002; Coulouarn et al., 2012; Benten et al., 2005). In this study, we investigated if the latter possibility could contribute to miR-29a-associated protection in our AAV-treated mice.

We report for the first time that mature miR-29a is released from hepatocytes via exosomes. There is a significant increase in miR-29a in exosomes of hepatocytes (HuH7 cells) and a second line (HeLa cells) after transfection with pAAV8.miR-29.eGFP. Others have reported that members of the miR-29 family, including miR-29a, are released in exosomes from cells (Bellingham et al, 2012; Fabbri et al, 2012). miR-29a targets Col1a1 and other extracellular matrix proteins, made predominantly by stellate cells in a fibrotic liver. We confirmed uptake of miR-29a by stellate cells using a co-culture system transfecting a luciferase plasmid with the 3'UTR of Col1a1 into LX-2 cells. The luciferase plasmid is under independent transcriptional control so that expression of luciferase would be altered only through transfer of miR-29a from hepatocytes to stellate cells. Since expression of luciferase activity in LX-2 cells cultured with HuH7 cells was increased treated with miR-29 inhibitor and overexpression of miR-

29a in HuH7 cells was associated with decreased luciferase activity in LX-2 cells, we conclude that transfer of miR-29a by hepatocellular exosomes is one mechanism by which collagen production in stellate cells is controlled.

Until now, determining mode of delivery and targeting a specific cell population has limited efficacy of viral gene therapy. In the liver, others targeted collagen-producing cells using viral systems (Reetz et al., 2013). Hepatocytes play a central role in metabolism, making them a more straightforward target for viral treatment. Here we report a therapeutic benefit of hepatic transduction of miR-29a through one systemic injection of an adeno-associated virus. Our data indicate that this treatment is a powerful option to treat toxin-induced liver fibrosis. While we acknowledge other potential mechanisms that could limit collagen deposition, we conclude that one way the liver limits collagen production occurs via a non-cell autonomous transfer of miR-29a.

Although we report robust protection against fibrosis through delivery of miR-29a, utilization of this AAV system was limiting. We cannot detect both viral genomes and eGFP over the course of 12 weeks of CCl_4 treatment. In order to study the observations described in this chapter, we need more sustainable expression of miR-29a in the liver. Chapter 4 will introduce a miR-29a inducible transgenic mouse, which the lab will utilize to study these observations more systematically.

3.4 Materials and methods

3.4.1 Animal Models.

Animals were housed and experiments were performed with approval by the Johns Hopkins School of Medicine Animal Care and Use Committee. Two- and three-

month-old C57BL/6 female mice were given 1 mL/kg of CCl_4 (Sigma) intraperitoneally biweekly for zero, one, four or eight weeks. CCl_4 was diluted in corn oil at 1:7. AAV was administered at a dose of $2x10^{11}$ viral genomes per animal by tail vein injection. At the conclusion of the experiments, animals were sacrificed and their livers were perfused with cold PBS and harvested.

3.4.2 MicroRNA Array.

The microRNA array protocol was described in Chapter 2. Briefly, total mouse liver RNA was extracted using a mirVana miRNA Isolation Kit (Ambion, Inc.) according to the manufacturer's protocol. RNA was DNase treated (DNase I Amplification Grade; Invitrogen), and 500 ng RNA was reverse transcribed without pre-amplification using Megaplex RT Primers (Rodent Pool A v2.0; ABI) and TaqMan MicroRNA Reverse Transcription Kit (ABI), according to the manufacturer's protocol. The microarray was run on the 7900HT Fast Real-Time PCR System with TaqMan Array Rodent MicroRNA A Cards v2.0 (ABI), according to the manufacturer's protocol. The geometric mean of each plate was used for normalization.

3.4.3 Histology.

Histological slide preparation was described in Chapter 2. Briefly, whole liver tissue was fixed in 10% formalin (Sigma) overnight. The tissues then were transferred to 70% ethanol, embedded in paraffin, sectioned and stained with Masson's trichrome by the Johns Hopkins Reference Histology Lab (Baltimore, MD). A trained pathologist, who

was blinded to AAV and CCl_4 treatment details, scored the hepatic fibrosis of each animal on a scale of 0-4.

3.4.4 RNA Isolation and qPCR.

RNA isolation and qPCR were described in Chapter 2. Briefly, for animal and *in vitro* samples, total RNA was isolated from whole liver tissue using Trizol (Invitrogen) according to manufacturer's protocol. RNA was DNAse treated (Invitrogen), according to the manufacturer's protocol, and was reverse transcribed using TaqMan MicroRNA Reverse Transcription Kit (ABI) with primary or mature miRNA specific primers (ABI) and High Capacity Reverse Transcription Kit (ABI) for 18s rRNA and all other non-miRNAs, all according to the manufacturer's protocol. qPCR was performed using pre-designed TaqMan primers and probes (ABI), according to manufacturer's protocol. qPCR for alpha-SMA, Col1a1, FN1 and PDGF-R-b was performed using Fast SYBR Green Master Mix (ABI). Genes amplified using SYBR Green were normalized to beta-Actin. The 2(-delta delta C(T)) Method was used to analyze PCR reactions.

3.4.5 In vitro TGF-beta Treatment of Human Hepatocytes.

Human hepatocytes (CellzDirect, Durham, NC) were plated on plates coated with 5ug/ml collagen (Gibco, Grand Island, NY) in serum-rich media (DMEM, 10% FBS, 15mM Hepes, 10µg/ml gentamycin (Quality Biological, Gaithersburg, MD), 1x ITS (Sigma), 1mM dexamethasone (Sigma), and 2mM L-glutamine (Quality Biological)). 24h later, cells were washed and the same media minus FBS was added. After 24h of

serum starvation, cells were washed, and the same serum-free media plus 5ng/ml TGF-beta (Roche) was added for 24h, and RNA was collected.

3.4.6 Verification of pAAV8_miR-29a Amplification.

HEK-293 cells were grown in DMEM supplemented with 10%FBS, penicillin and streptomycin. Serial dilutions of pAAV8_Control_eGFP or pAAV_miR-29a_eGFP (cloned by Raghu Chivukula) were transfected with Lipofectamine 2000 (Invitrogen) according to the manufacturer's protocol. Cells were imaged and RNA was isolated 24 hours after transfection.

3.4.7 Immunostaining.

Formalin-fixed, paraffin-embedded tissues were sectioned. 5 μm sections were transferred to Superfrost/Plus Microscope Slides (Fisher Scientific) and melted onto the slide for 30' at 60°C. After washing in PBST, samples were blocked with PBS + 5% fetal bovine serum (Sigma) and 3% goat serum (Sigma). Slides were then incubated for 1 hour at room temperature with anti-albumin (Santa Cruz Biotechnologies, Inc), anti-vimentin (Millipore, Billerica, MA), anti-desmin (Sigma) anti-α-smooth muscle actin conjugated to Cy3 (Sigma), or anti-GFP antibody (Invitrogen). They were then washed 3 times in PBST and incubated for one hour at room temperature with one (or two) of the following secondary antibodies: Cy3 labeled goat anti-rabbit IgG (GE Healthcare, Niskayuna, NY), a Cy3 labeled anti mouse, Cy3 anti-chicken, (both Millipore), or Alexa Fluor 488 anti-rabbit (Cell Signaling Technology, Danvers, MA). Slides were washed three times in PBST and counterstained with Hoechst 33258 (Molecular Probes, Eugene,

OR), mounted using Prolong Gold Antifade Reagent (Invitrogen), and subsequently imaged under identical conditions.

3.4.8 Collagen Assay.

Collagen protein expression was determined by Sircol Soluble Collagen Assay (Biocolor, Carrickfergus, UK), which was performed according to the manufacturer's protocol.

3.4.9 Blood Chemistry Tests.

Blood was harvested and blood chemistry tests (LFTs, Albumin) were performed by the Department of Comparative Medicine at Johns Hopkins University (Baltimore, MD).

3.4.10 In vitro Co-culture Experiment.

HuH7 and LX-2 cells were grown in DMEM supplemented with 10%FBS, penicillin and streptomycin. Cells were transfected with plasmid DNA or miRIDIAN Hairpin Inhibitors (Thermo Fisher Scientific, Waltham, MA) using Lipofectamine 2000 (Invitrogen) according to the manufacturer's protocol. 24 hours after transfection, cells were lysed and cocultured using a 2:1 ratio of HuH7:LX-2 cells. Lysates were collected 24 hours after coculturing.

3.4.11 Luciferase Reporter Assays.

2.5×10^4 HeLa, HuH7 and LX-2 cells were plated in triplicate wells of a 24-well plate and transfected 24 hours later with 100 ng of the indicated pGL3 3' UTR reporter construct and 5 ng of phRL-SV40 (Promega) using Lipofectamine 2000 (Invitrogen) according to the manufacturer's protocol. 48 hours after transfection, cells were lysed and assayed for firefly and renilla luciferase activity using the Dual-Luciferase Reporter Assay System (Promega). Firefly luciferase activity was normalized to renilla luciferase activity for each transfected well.

3.4.12 Exosome Isolation.

Cells were transfected with Control or miR-29a pAAV as described above. Supernatant from five 10cm plates were collected and passed through a 0.22 μm filter. Cells were centrifuged at 20,000xg for 30' at 4 degrees Celsius to remove additional cellular debris. The supernatant was transferred to a new tube and spun by ultracentrifugation at 100,000xg for 60' at 4 degrees Celsius. From the remaining pellet, RNA was isolated using Trizol as previously described.

3.4.13 Statistics.

A student two-tailed t-test was used to determine significance for *in vitro* qPCR results, collagen assays and pathologist fibrosis scores. REST 2009 Software was used to determine significance for *in vivo* qPCR results.

3.5 Tables: Chapter 3

Table 3-1. 60 most downregulated miRNAs after 8 weeks of CCl_4 treatment in BL/6 mice.

Fold change of miRNA expression at 0, 1, 4 and 8 weeks of CCl_4 treatment.

miRNA	No CCl_4	1 week CCl_4	4 weeks CCl_4	8 weeks CCl_4
mmu-miR-383	1.00	0.05	0.21	0.06
mmu-miR-133a	1.00	13.62	0.19	0.22
mmu-miR-210	1.00	0.35	0.35	0.23
mmu-miR-802	1.00	0.24	0.09	0.24
mmu-miR-193	1.00	0.45	0.11	0.32
mmu-miR-465b-5p	1.00	1.68	0.50	0.36
mmu-miR-101a	1.00	0.53	0.21	0.38
rno-miR-345-3p	1.00	0.24	0.18	0.39
mmu-miR-491	1.00	0.32	0.31	0.41
mmu-miR-194	1.00	0.44	0.16	0.41
mmu-miR-107	1.00	0.29	0.14	0.42
mmu-miR-203	1.00	0.95	0.16	0.44
rno-miR-339-3p	1.00	1.98	0.61	0.44
mmu-miR-192	1.00	0.52	0.15	0.45
mmu-miR-30e	1.00	0.88	0.25	0.45
mmu-miR-429	1.00	1.33	0.47	0.46
mmu-miR-16	1.00	1.30	0.29	0.46
mmu-miR-337-5p	1.00	1.95	0.91	0.46
mmu-miR-200a	1.00	0.82	0.48	0.49
mmu-miR-7b	1.00	0.67	1.00	0.50
mmu-miR-29b	1.00	0.15	0.55	0.50
mmu-miR-218	1.00	1.72	0.77	0.52
mmu-miR-687	1.00	0.45	0.53	0.53
mmu-miR-126-3p	1.00	1.20	0.27	0.53
mmu-miR-15a	1.00	0.26	0.50	0.54
mmu-miR-30c	1.00	0.64	0.28	0.54
mmu-miR-365	1.00	0.35	0.32	0.55
mmu-miR-872	1.00	0.66	0.71	0.56
mmu-miR-187	1.00	0.74	0.24	0.56
mmu-miR-29c	1.00	0.35	0.24	0.57
mmu-miR-186	1.00	2.33	0.32	0.57
mmu-miR-30a	1.00	0.33	0.49	0.59
mmu-let-7g	1.00	0.43	0.33	0.59
mmu-miR-7a	1.00	0.20	1.02	0.59
mmu-miR-152	1.00	0.44	0.39	0.59
mmu-miR-106a	1.00	1.08	0.74	0.60

mmu-miR-139-5p	1.00	0.81	0.47	0.60
mmu-miR-27b	1.00	0.27	0.42	0.63
mmu-miR-126-5p	1.00	0.86	0.31	0.63
mmu-miR-17	1.00	1.03	0.79	0.64
mmu-miR-148a	1.00	0.46	0.31	0.64
mmu-miR-322	1.00	0.68	1.45	0.64
mmu-miR-200c	1.00	1.30	0.83	0.64
mmu-miR-30b	1.00	0.60	0.41	0.65
mmu-miR-24	1.00	1.18	0.50	0.65
mmu-miR-320	1.00	1.08	0.67	0.65
mmu-miR-30d	1.00	0.37	0.56	0.66
mmu-miR-26b	1.00	0.37	0.39	0.66
mmu-miR-361	1.00	0.46	0.88	0.66
mmu-miR-467d	1.00	0.34	3.72	0.66
mmu-miR-32	1.00	0.51	0.37	0.68
mmu-miR-191	1.00	2.10	0.50	0.68
mmu-miR-29a	1.00	0.50	0.38	0.69
mmu-miR-31	1.00	1.47	0.37	0.69
mmu-miR-542-5p	1.00	0.86	0.60	0.69
mmu-miR-103	1.00	0.44	0.51	0.71
mmu-miR-511	1.00	1.14	0.81	0.71
mmu-miR-338-3p	1.00	0.66	0.74	0.71
mmu-miR-185	1.00	0.52	0.28	0.71
mmu-miR-26a	1.00	0.38	0.44	0.72

N=2 in each group. All groups use geometric mean normalization method, using every miRNA as selected controls.

3.6 Figures: Chapter 3

Figure 3-1. The miR-29 family is downregulated in liver fibrosis.

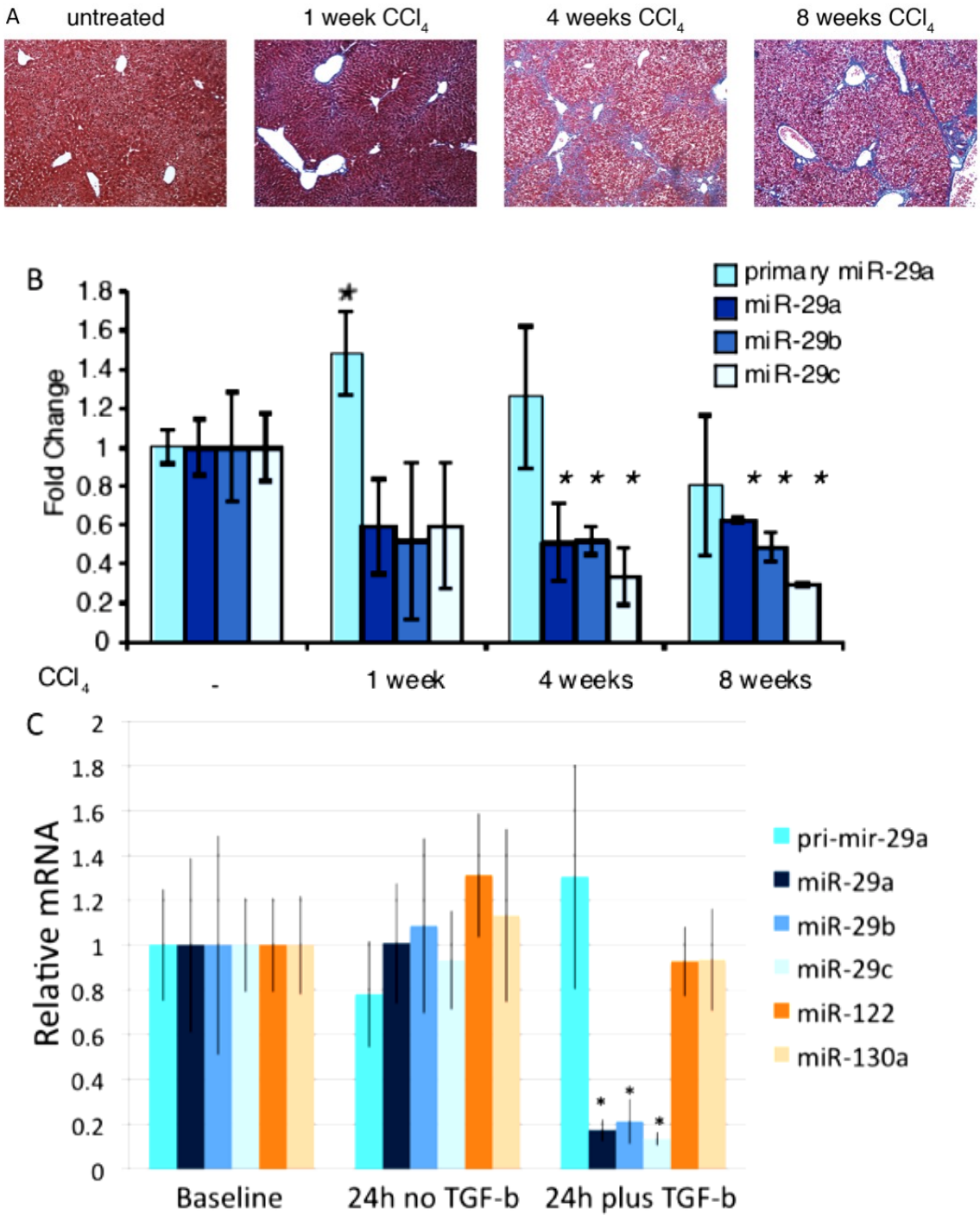

A) Representative 10x images of 5 μm liver sections with Maisson trichrome stain. B) Expression of primary miR-29a and miR-29a-c in mice treated with 1, 4 and 8 weeks of CCl_4. All samples are relative to no CCl_4. C) Expression of primary miR-29a, miR-29a-c, miR-122 and miR-130a in primary human hepatocytes treated with 5ng/ml TGF-beta for 24 hours. All samples are relative to baseline (t=0h TGF-beta treatment). Relative expression was normalized to 18s rRNA (* = p-value < 0.05).

Figure 3-2. Functional validation of scAAV8.miR-29a.eGFP.

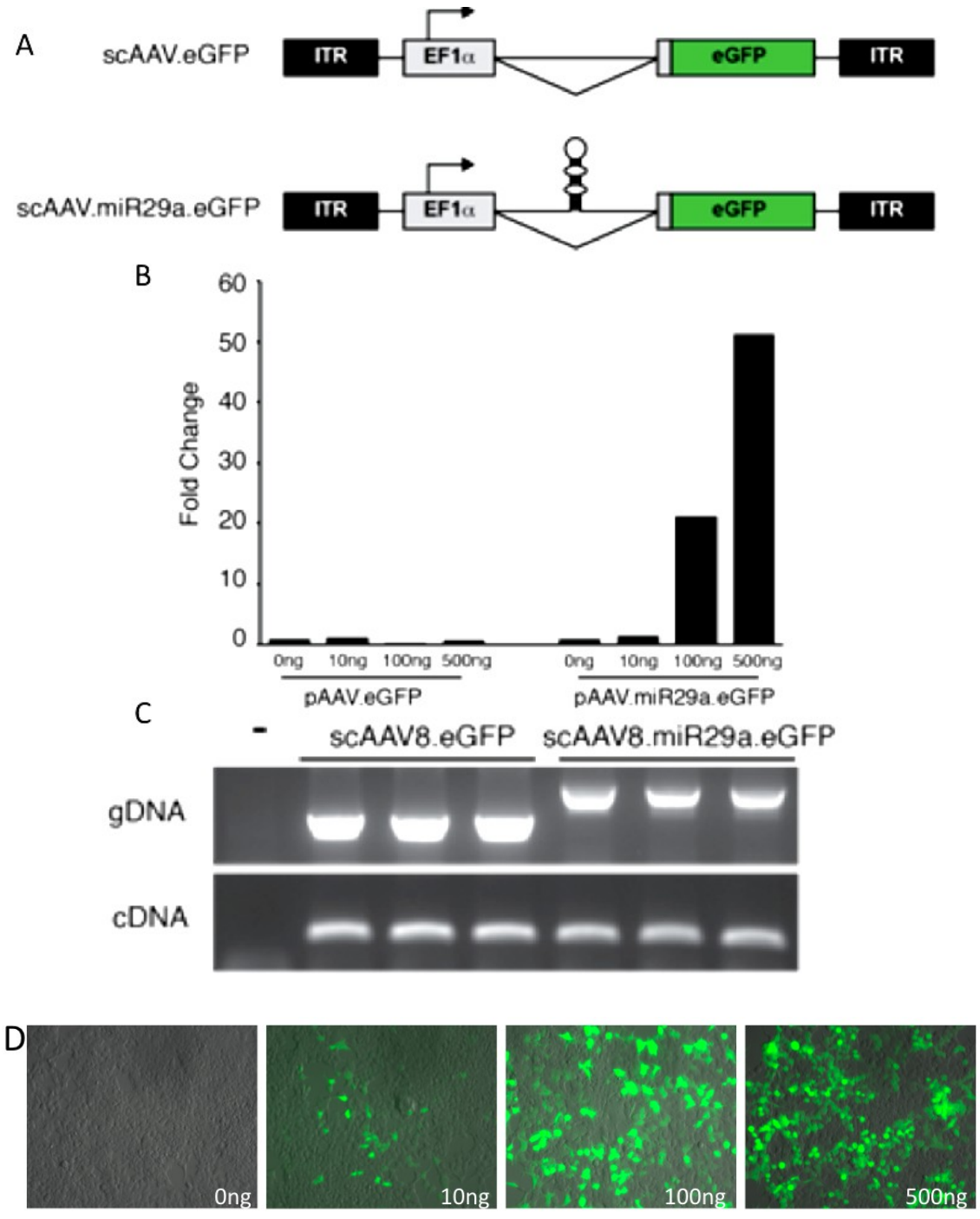

A) Schematic representation of scAAV vectors used in this study. Elongation factor 1 α promoter (EF1α), miRNA (shown in hairpin form) and enhanced green fluorescent protein (eGFP) are flanked by inverted terminal repeats (ITRs). B) miR-29a expression in scAAV.eGFP- or scAAV.miR29a.eGFP-transfected HEK-293 cells. Cells were transfected with 0 ng, 10 ng, 100 ng or 500 ng of respective vectors. All samples are relative to each 0 ng cohort. Relative expression was normalized to 18s rRNA. C) Endpoint PCR amplifying gDNA (top) or cDNA (bottom) from whole liver in animals injected either with scAAV.eGFP or with scAAV.miR29a.eGFP. Note the increased size in scAAV.miR29a.eGFP due to inclusion of the miR-29a hairpin. After excision, the primers amplify the same size band (bottom). D) Representative 20x images of HEK-293 cells treated with serial concentrations of scAAV.miR29a.eGFP for 24 hours.

Figure 3-3. Systemic delivery of scAAV8.miR-29a.eGFP is not toxic.

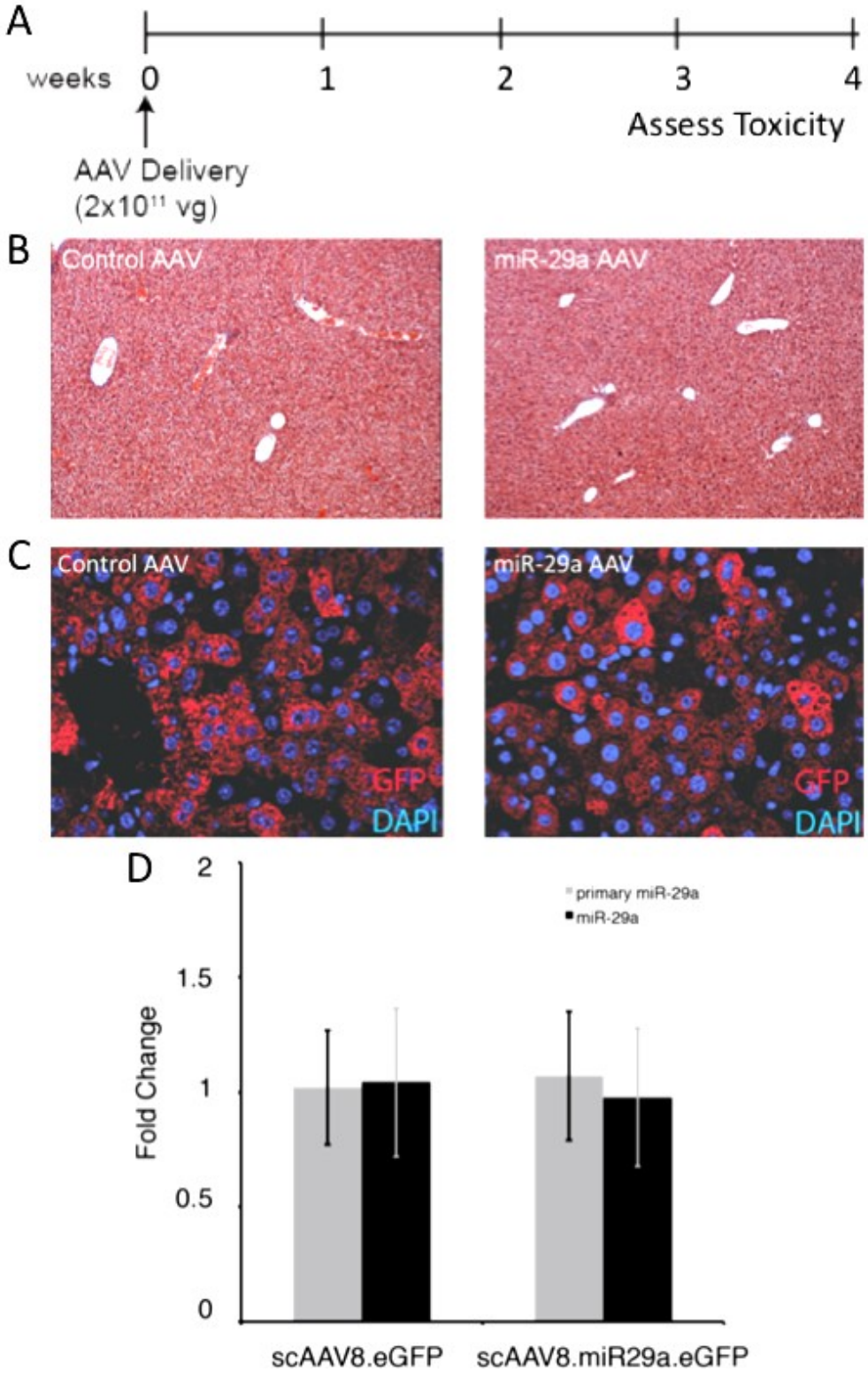

A) Timeline of miR-29a toxicity delivery experiment. B) Representative 20x Maisson trichrome images of 5 μm liver sections 4 weeks after systemic delivery of scAAV.eGFP- or scAAV.miR29a.eGFP. C) Representative 20x immunofluorescent images of 5 μm liver sections 4 weeks after systemic delivery of scAAV.eGFP- or scAAV.miR29a.eGFP detecting eGFP (red) counterstained with DAPI (blue). D) Expression of primary miR-29a and mature miR-29a in whole liver treated with systemic injection of scAAV. All samples are relative to scAAV.eGFP expression. Relative expression was normalized to 18s rRNA.

Figure 3-4. scAAV8.miR-29a.eGFP is predominantly expressed in hepatocytes.

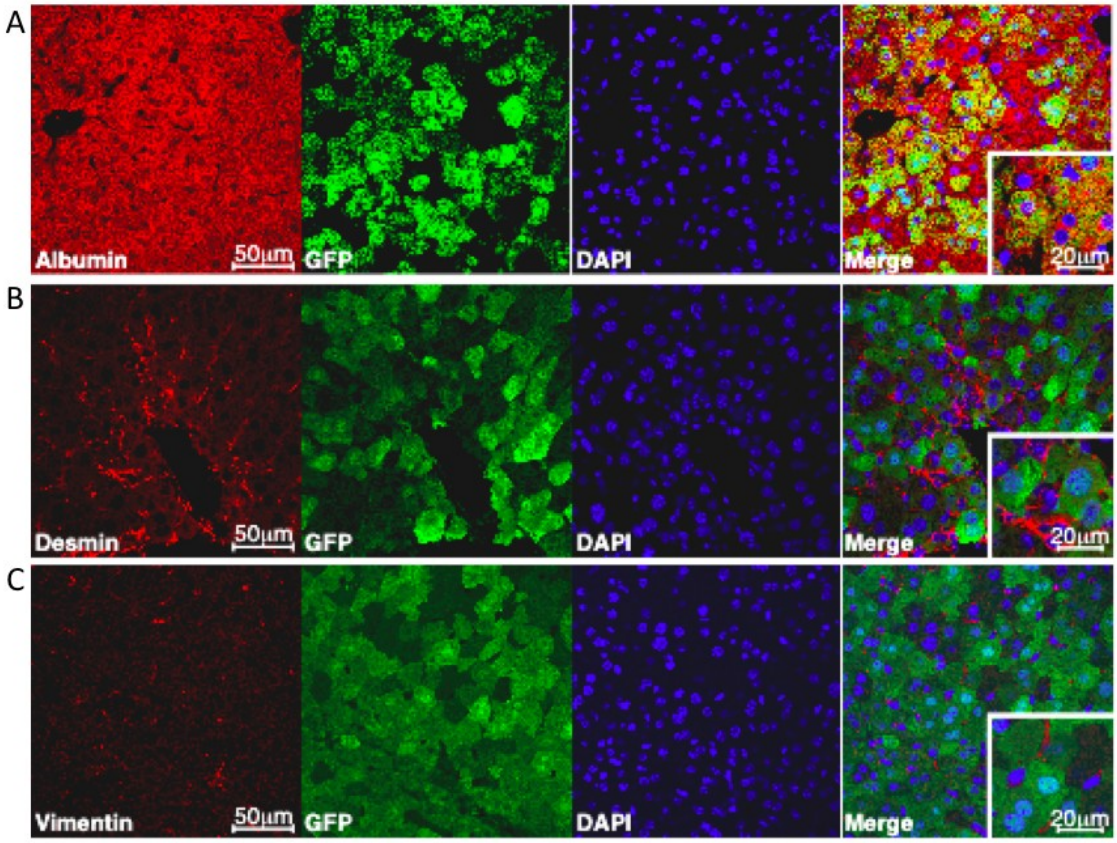

A) Representative 20x immunofluorescent images of 5 μm liver sections 4 weeks after systemic delivery of scAAV.eGFP- detecting Albumin (red) and eGFP (green) counterstained with DAPI (blue). B) Representative 20x immunofluorescent images detecting Desmin (red) and eGFP (green) counterstained with DAPI (blue). C) Representative 20x immunofluorescent images detecting Vimentin (red) and eGFP (green) counterstained with DAPI (blue).

Figure 3-5. scAAV8.miR-29a.eGFP pretreatment prevents fibrosis.

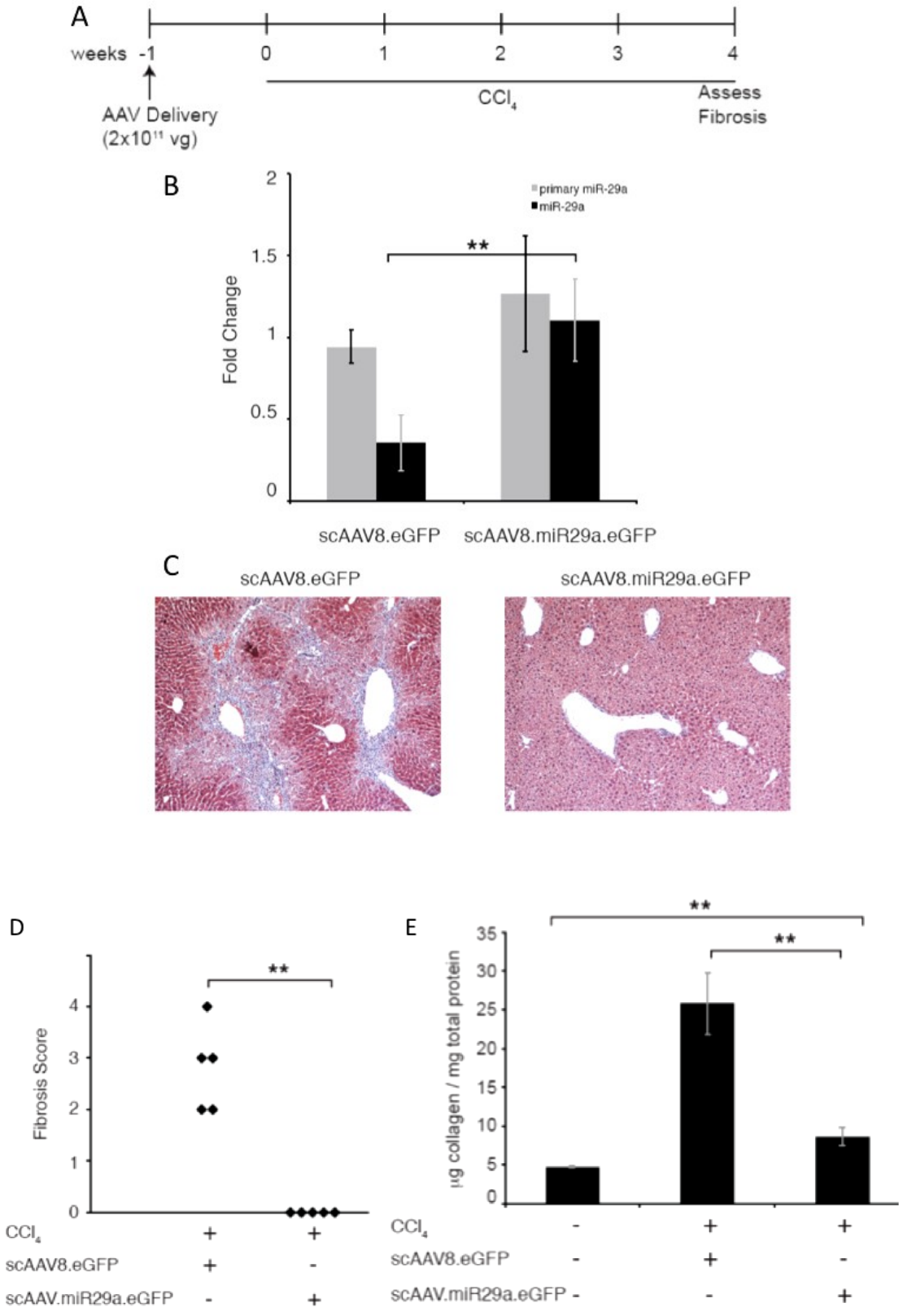

A) Timeline of miR-29a pretreatment experiment. B) Expression of primary miR-29a and mature miR-29a in whole liver treated with systemic injection of scAAV. All samples are relative to scAAV.eGFP expression. Relative expression was normalized to 18s rRNA. C) Representative 20x Maisson trichrome images of 5 μm liver sections in pretreatment group. D) Fibrosis scores of histological slides of livers from mice in the miR-29a pretreatment experiment. A blinded pathologist scored the histological slides. E) Collagen expression in livers from mice in the miR-29a pretreatment experiment. Collagen expression was normalized to livers from mice with no scAAV-treatment and no CCl_4. (** = p-value < 0.05)

Figure 3-6. Intervention with scAAV8.miR-29a.eGFP prevents and regresses fibrosis.

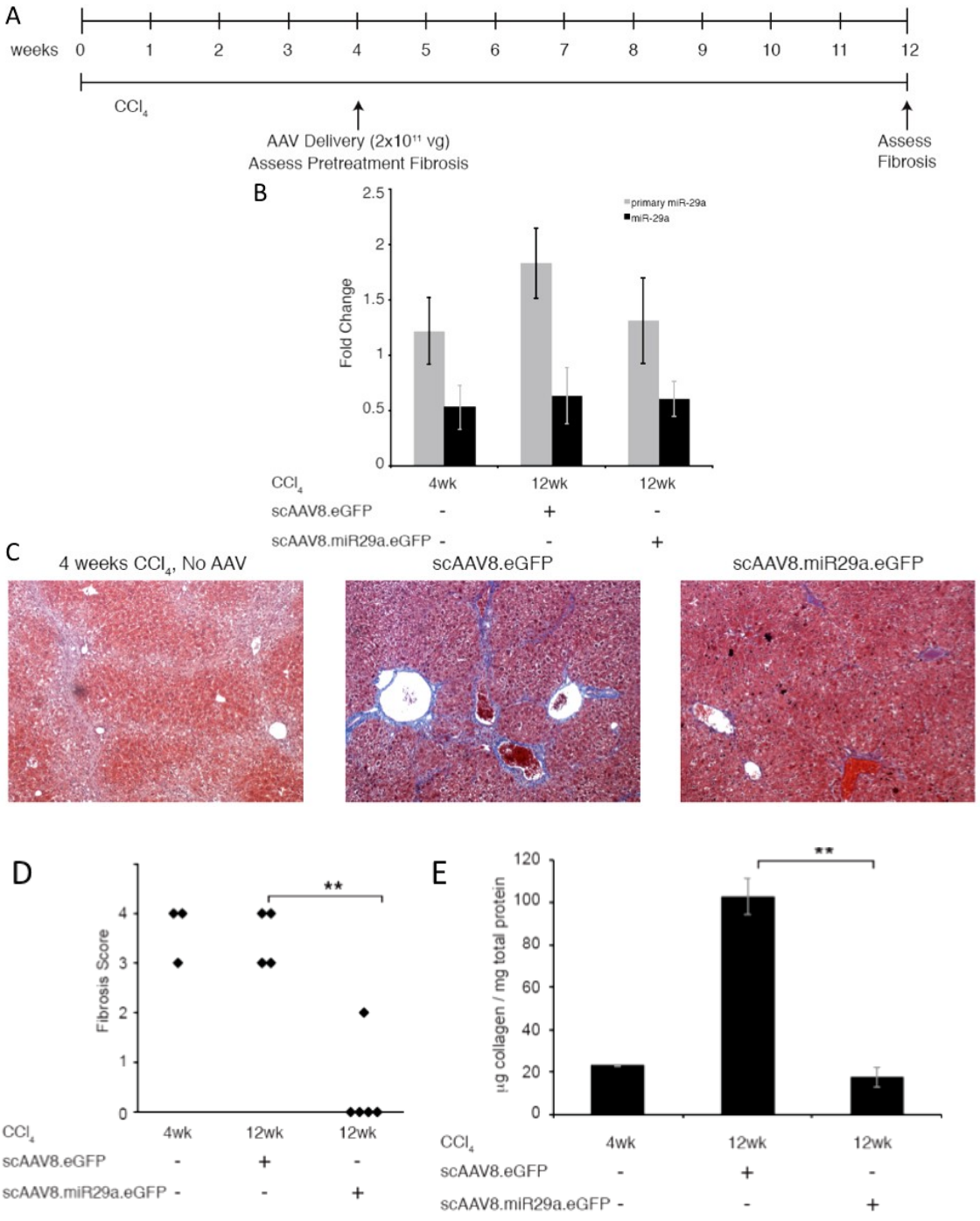

A) Timeline of miR-29a intervention experiment. B) Expression of primary miR-29a and mature miR-29a in whole liver treated with systemic injection of scAAV. All samples are relative to scAAV.eGFP expression with no CCl_4. Relative expression was normalized to 18s rRNA. C) Representative 20x Maisson trichrome images of 5 μm liver sections in intervention experiment. D) Fibrosis scores of histological slides of livers from mice in the miR-29a intervention experiment. A blinded pathologist scored the histological slides. E) Collagen expression in livers from mice in the miR-29a intervention experiment. Collagen expression was normalized to livers from mice with 4 weeks of CCl_4 treatment. (** = p-value < 0.05)

Figure 3-7. scAAV8.miR-29a.eGFP treatment and protection is associated with fewer alpha-SMA-positive cells.

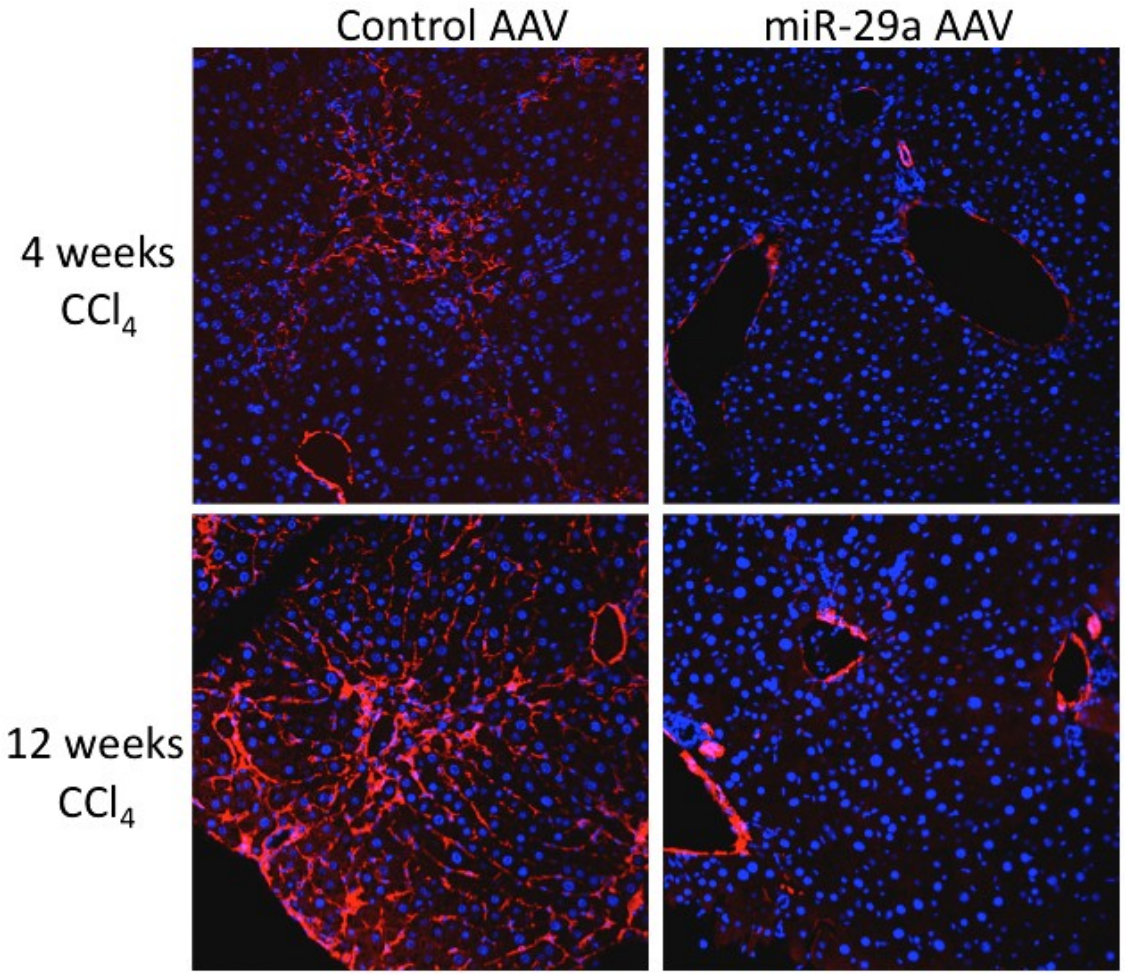

A) Representative 20x immunofluorescent images of 5 μm liver sections 4- and 12-weeks after systemic delivery of scAAV.eGFP- detecting alpha-SMA (red) counterstained with DAPI (blue).

Figure 3-8. miR-29a is expressed in exosomes from HuH7 and HeLa cells.

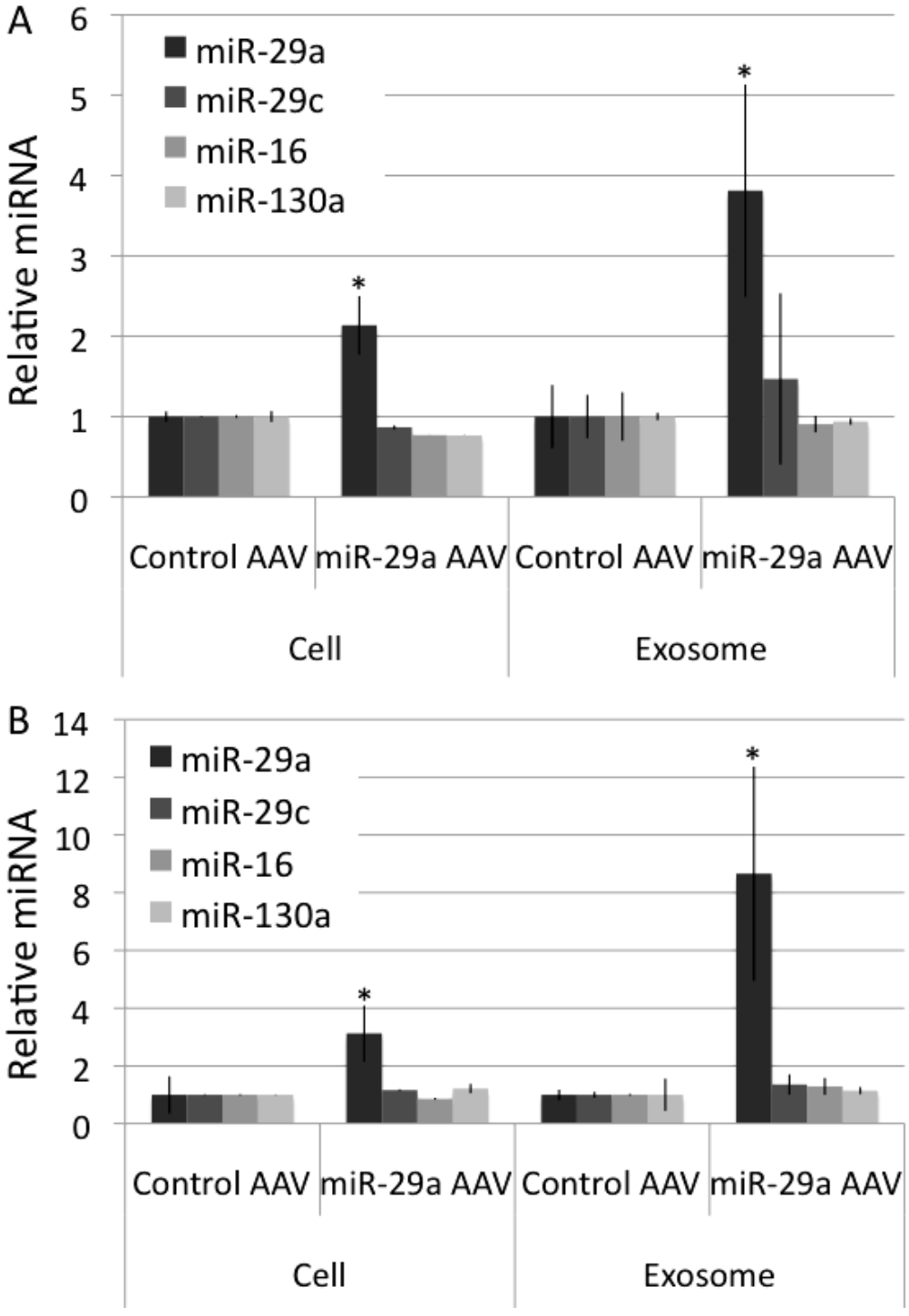

A) Expression of miR-29a, miR-29c, miR-16 and miR-130a in cells and exosomes of HuH7 cells transfected with control or miR-29a pAAV. B) Expression of miR-29a, miR-29c, miR-16 and miR-130a in cells and exosomes of HeLa cells transfected with control or miR-29a pAAV. All miRNA expression is relative to cells or exosomes treated with control pAAV. Relative expression was normalized to 18s rRNA (* = p-value < 0.05).

Figure 3-9. Inhibition or overexpression of miR-29a in hepatocytes affects collagen expression in co-cultured stellate cells.

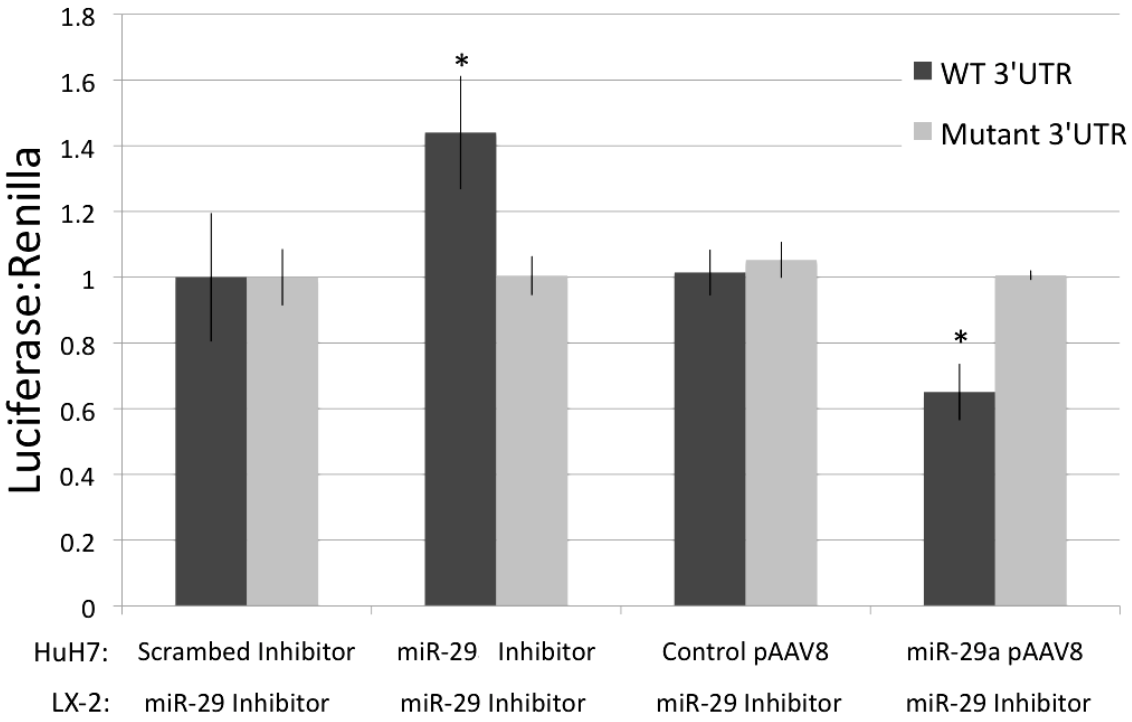

A) Luciferase expression of Luc_WT-Col1a1-3'UTR or Luc_Mutant-Col1a1-3'UTR in co-cultured HuH7 and LX-2 cells. All LX-2 cells were treated with 30 nM miR-29 cocktail inhibitor. HuH7 cells were transfected with 30 nM scrambled or miR29 cocktail inhibitor, or with control or miR-29a pAAV8 vector. Expression of luciferase was normalized to renilla (* = p-value < 0.05).

4. CHAPTER 4. GENERATION OF AN INDUCIBLE TRANSGENIC MIR-29A MOUSE

4.1 Introduction.

In Chapter 3, expression of miR-29a using an adeno-associated virus provided a dramatic therapeutic benefit to mice treated with carbon tetrachloride (CCl_4). However, miR-29a expression was not sustainable because repeated insults caused hepatic injury and loss of virus expression. After 12 weeks of CCl_4 treatment, mice treated with scAAV.miR-29a.eGFP lost most expression of eGFP and nearly all viral genomes. This chapter describes the creation of a miR-29a inducible transgenic mouse using a published approach (Beard et al., 2006). This mouse line will have consistent, cell-specific and inducible expression to study miR-29a using not only our CCl_4 model but also using other clinically relevant models. Importantly, we will use this transgenic mouse line to study the non-cell autonomous phenomenon presented in Chapter 3.

4.2 Construct of an inducible miR-29a transgenic mouse.

We inserted the miR-29a hairpin in the 3'UTR of eGFP. To test expression of this construct, we inserted this sequence, eGFP.miR-29a.polyA, into pcDNA3. GFP was readily detectable in HeLa cells after transfection (Figure 4-1A) and there was an increase in expression of miR-29a (Figure 4-1B). Having functional evidence that our construct expressed both eGFP and miR-29a, we inserted loxp-stop-loxp.eGFP.miR-29a.polyA into pBS31_tetO, and created a transgenic mouse line with expression of this inducible transgene downstream of Col1a1 (Figure 4-2). eGFP and miR-29a are downstream of a Tetracyclin-On promoter and a transcriptional inhibitor, loxp-stop-loxp

(LSL). Crossing our transgenic line to a Cre-specific driver line excises LSL and removes transcriptional inhibition downstream of the tetO promoter. Finally, from the ROSA26 locus, KH2* Cells express a tet-on transactivator, rtTA, which allows for controlled transcription of eGFP.miR-29a only when mice are treated with doxycycline. Using this method, miR-29a has cell-specific and temporal expression which will allow us to study cell-specific miR-29a targets.

4.3 Detection and expression of an inducible miR-29a transgenic mouse.

To examine miR-29a expression in our inducible transgenic mouse, we crossed miR-29a/+; rtTA/+ animals to Albumin:Cre/+ animals. After genotyping for each transgene (Figure 4-3A), animals were given doxycycline. While there was no increase in miR-29a after 7 days (Figure 4-3B), we saw hepatocellular expression of eGFP (Figure 4-3C). Importantly, samples positive for Albumin:Cre excised loxp-stop-loxp, and transgenic miR-29a was detected by endpoint PCR (Figure 4-3A).

4.4 Future directions

While we have functional evidence of expression of miR-29a, our transgenic mouse could be fine tuned to facilitate easier husbandry and increase expression. First, we have interbred miR-29/+; rtTA/+ mice to create double homozygous transgenic mice, allowing for more straightforward genotyping after crossing to different cre-driver lines. Second, we will utilize ubiquitous cre-driver lines that will ensure excision of LSL in every cell type. Finally, others have engineered a more potent tet-on transactivator (Das et al., 2004; Zuber et al., 2011), and we will investigate its potential in our mouse line.

After successful husbandry, we plan to utilize this mouse in different liver fibrosis studies, including a systematic investigation into the non-cell autonomous phenomenon that we observe in miR-29a AAV-treated mice. Sustained expression of miR-29a in hepatocytes and other liver cells would allow for miR-29a to be studied more systematically. Interestingly, miR-29a was not overexpressed in our Alb:cre triple transgenic baseline model, suggesting tight regulation of hepatocellular expression that is consistent with our AAV8 model. Our lab will pursue other liver specific studies, including isolation of miR-29a transgenic cells and identification of miR-29a targets using methods to isolate and sequence targets.

4.5 Materials and methods

4.5.1 Molecular cloning.

Loxp-stop-loxp.eGFP.miR-29a was inserted into pBS31_tetO at the EcoRI site (Thermo Scientific Open Biosystems, Pittsburgh, PA). eGFP.miR-29a was cloned into pcDNA3 at the XhoI site. Clones positive by digest were confirmed using Sanger sequencing (Sequencing Facility, Johns Hopkins University, Baltimore, MD). pDNA was transfected into HeLa cells using Lipofectamine 2000 using the manufacturer's protocol.

4.5.2 Generation of an inducible miR-29a transgenic mouse line.

Animals were housed and experiments were performed with approval by the Johns Hopkins School of Medicine Animal Care and Use Committee. pBS31_tetO.LSL.eGFP.miR-29a was transformed into KH2* mouse embryonic stem

cells using the manufacturer's protocol. Clones were sequenced, and positive clones were injected into WT C57BL/6 mice blastocysts. Founders were identified though outcrossing. Additional generations were outcrossed and genotyped for miR-29a and rtTA. Positively transgenic animals were given 2mg/ml doxycycline hyclate (Sigma-Aldrich) in water supplemented with 10mg/ml sucrose.

4.5.3 gDNA isolation, RNA isolation and PCR.

Mouse tails were excised in digested in Proteinase K (Invitrogen) overnight at 56ºC. The next day, gDNA was extracted using 5M NaCl, 100% EtOH and washed with 70% EtOH. gDNA was resuspended in H2O and used as template. DreamTaq 2x Master Mix (Fermentas) was used for endpoint PCR reactions using the manufacturer's protocol.

RNA was isolated from HeLa cells or whole liver tissue, and qPCR was performed as described in Chapters 2 and 3. RNA isolation and qPCR were described in Chapter 2. Briefly, total RNA was isolated using Trizol (Invitrogen) according to manufacturer's protocol. RNA was DNAse treated (Invitrogen), according to the manufacturer's protocol, and was reverse transcribed using TaqMan MicroRNA Reverse Transcription Kit (ABI) with primary or mature miRNA specific primers (ABI) and High Capacity Reverse Transcription Kit (ABI) for 18s rRNA and all other non-miRNAs, all according to the manufacturer's protocol. qPCR was performed using pre-designed TaqMan primers and probes (ABI), according to manufacturer's protocol. miR-29a was normalized to 18s rRNA. The 2(-delta delta C(T)) Method was used to analyze PCR reactions.

4.5.4 Immunofluorescence.

Liver was excised, rinsed in cold PBS and fixed in 4% paraformaldehyde (Electron Microscopy Sciences, Hatfield, PA) overnight. The next day, tissue was embedded in OCT and snap-frozen in liquid nitrogen. 5 μm sections were cut and stained for eGFP using the same protocol described in Chapter 3. Briefly, samples were blocked with PBS + 5% fetal bovine serum (Sigma) and 3% goat serum (Sigma). Slides were then incubated for 1 hour at room temperature with anti-GFP antibody (Invitrogen). They were then washed 3 times in PBST and incubated for one hour at room temperature with Cy3 labeled goat anti-rabbit IgG (GE Healthcare, Niskayuna, NY). Slides were washed three times in PBST and counterstained with Hoechst 33258 (Molecular Probes, Eugene, OR), mounted using Prolong Gold Antifade Reagent (Invitrogen), and subsequently imaged under identical conditions.

4.6 Figures: Chapter 4

Figure 4-1. eGFP and miR-29a expression in HeLa cells transfected with eGFP-miR29.

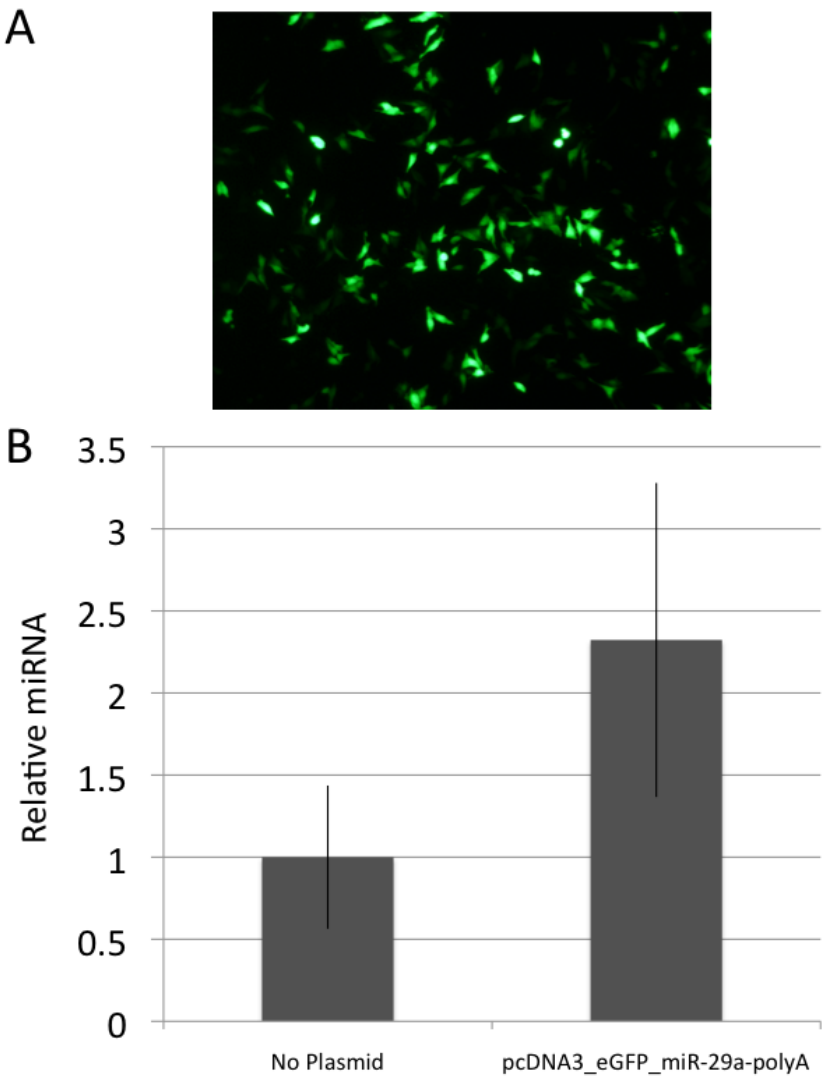

A) Representative 20x fluorescent image detecting eGFP (green) expression. B) Expression of miR-29a in HeLa cells transfected with pcDNA3_eGFP_miR-29a-polyA. miRNA expression is relative to no plasmid mock transfection. Relative expression was normalized to 18s rRNA.

Figure 4-2. Inducible miR-29a construct.

The miR-29a transgene was inserted 1.6kb downstream of Col1a1 on chromosome 11 using FRT (Flp Recognition Target) Sites. The constuct consisted of a Tet-regulatable element (TRE), loxp-stop-loxp (LSL), enhanced green fluorescent protein (eGFP), and the miR-29a hairpin.

Figure 4-3. Detection of transgenic miR-29a and eGFP in miR-29a animal using an albumin specific cre driver line.

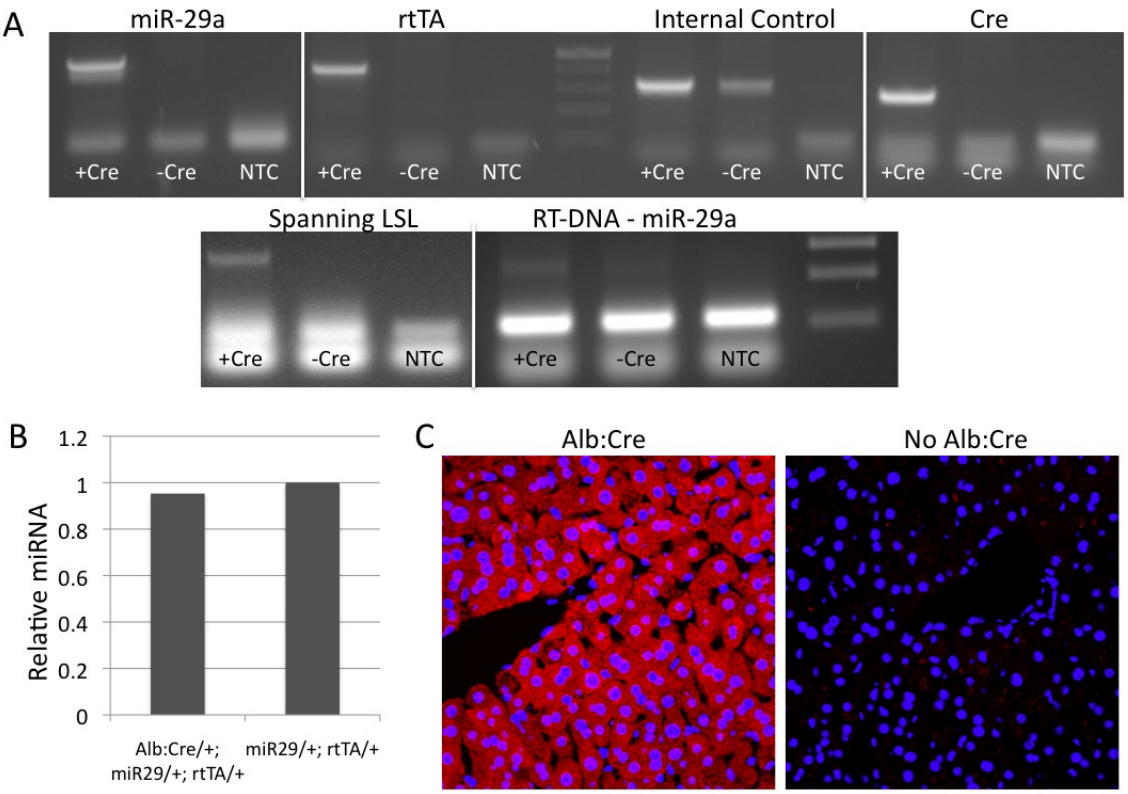

A) Endpoint PCR detecting miR-29a, rtTA, IL2 (an internal control to test gDNA quality), Cre, and deletion of loxp-stop-loxp using gDNA as template. The last PCR uses RT-DNA as template and amplifies miR-29a. B) Expression of miR-29a from whole liver in animals with and without Albumin:Cre. miRNA expression is relative to no albumin:cre. Relative expression was normalized to 18s rRNA. C) Representative 40x immunofluorescent images of 5 µm liver sections detecting eGFP (red) counterstained with DAPI (blue) after 7 days of doxycycline treatment. Animals were given 2mg/ml doxycycline hyclate in water supplemented with 10mg/ml sucrose.

5. CHAPTER 5. CONCLUDING REMARKS

5.1 Importance of studying cell-specific microRNA expression

We set out to survey miRNA dysregulation during liver fibrosis in order to identify unknown targets and novel mechanisms. As members not only of the Human Genetics Program but also of the Department of Surgery, our interest predominantly focuses on understanding changes in gene expression during solid organ dysfunction. By studying gene expression dysregulation during liver fibrosis, we hypothesized that we could identify novel markers to predict fibrosis progression and even develop individualized treatment options for patients who either have spent time on a wait list or have received an organ.

We identified two families of miRNAs that are dysregulated during organ fibrosis. The miR-214/199 family is upregulated during liver fibrosis, and the miR-29 family is downregulated. Nevertheless, through identification of targets using *in silico* predictions and *in vitro* validation, we discovered that both of these families have members whose expression is protective during fibrosis.

We focused our efforts on globally examining microRNA changes during progression of liver fibrosis. By examining whole tissue using a low density array, we successfully surveyed expression of over 350 miRNAs as fibrosis developed. However, it became increasingly evident that studying miRNA changes in a complex organ with a heterogeneous cell population could cause identification of false positives and omission of cell-specific miRNA changes. During fibrosis, immune cells infiltrate and myofibroblasts proliferate in the organ, causing a dramatic change in cell composition.

When examining miRNA expression in fibrotic liver tissue, an increase, for example in stellate cells, could cause an increase in miRNA expression if that miRNA is stellate cell-specific. Single cell isolation, promoter-specific transgenic lines, co-immunohistochemistry and/or *in vitro* investigation of miRNA dynamics need to be utilized when observing changes in expression of whole tissue. The projects described in this thesis elucidate expression and function of miR-214-5p and miR-29a in different liver cell populations and should serve as examples of how to examine miRNA expression systematically in complex tissue. miR-214-5p expression predominates parenchymal cells, including stellate cells. While miR-29a is highly expressed in a variety of cell types, it functions differently in each cell type. By identifying cell-specific expression, researchers can pinpoint and test targets more efficiently.

In Chapter 3, we deliver miR-29a to hepatocytes and report functional prevention and reversal of fibrosis, which was associated with a decrease in stellate cell activation. miRNAs target and regulate genes often times in the same networks and pathways. This study has suggested that modulation of a single miRNA can have profound implications on solid organ gene expression non-cell autonomously. Future studies indentifying miRNA changes and elucidating functional targets in a pathophysiological setting would lead to development of specific biomarkers and therapies.

5.2 The miR-214/199 family in liver fibrosis: additional opportunities on the horizon

In Chapter 2, I report overexpression of the miR-214/199 family during liver fibrosis. Twist1, which is also upregulated in this pathophysiological setting, regulates

this miRNA family. We identified a negative feedback loop between miR-214-5p and Twist1, and provided evidence that this feedback loop limits proliferation, migration and ECM production in hepatic stellate cells.

miR-214-5p is one of five unique sequences in the miR-214/199 family, and all five mature sequences are processed in hepatic stellate cells. Other members of this family have been implicated in different settings of fibrosis, and evolutionarily conserved families that are upregulated in the same setting could target similar networks and pathways. For example, miR-214-3p has been reported to target Plexin-B1 to limit proliferation of cervical cancer cells, and miR-199a overexpression in hepatocellular carcinoma is associated with limited HIF1A and phospho-AKT, which promotes growth and migration (Qiang et al., 2011; Jia et al., 2012). Future studies to identify targets of these miRNAs specifically in stellate cells would uncover if other members of the miR-214/199 family target similar myofibroblast-specific gene networks or pathways as miR-214-5p and Twist1.

While there are five reports mature sequences in this microRNA family, our studies have identified a second mature strand for miR-214-5p. Given the potential for the impact of discovering a microRNA hairpin that processes more than two mature strands, elucidation of rno-miR-214-5p and any potential targets represents an extremely interesting project. Consistent with other mature sequences in this hairpin, rno-miR-214-5p is significantly upregulated in during liver fibrosis. Since all miRNAs in DNM3os are under the same transcriptional control, one would hypothesize that there are functional rno-miR-214-5p targets that promote stellate cell activation and migration.

Our *in vitro* studies suggest that miR-214-5p is a potent regulator of stellate cell activation. Given these observations, an *in vivo* model knocking out miR-214 in the liver would assess its protective function in liver fibrosis. Alternatively, *in vivo* mimics or viral vectors overexpressing miR-214 could be protective against fibrosis by limiting Twist1 and other pro-fibrotic genes.

In this study, we systematically examined expression and function of miR-214 in activated nonparenchymal cells. One of the most interesting observations we encountered is that miR-214-3p and miR-199a-3p increase mildly over recurrence of HCV of a newly transplanted graft. Although samples like these are difficult to obtain, we should slowly grow our database of human samples to correlate our observed rodent and *in vitro* phenotypes with the human condition. Additionally, examining cell specific expression of the miR-214/199 family in human samples using *in situ* hybridization techniques would confirm upregulation of this miRNA family in nonparenchymal cells.

5.3 The miR-29 family: additional opportunities on the horizon

In Chapter 3, I described a project in which we systemically delivered miR-29a to the liver and ameliorated a fibrotic phenotype. miR-29a targets many ECM proteins, including Co1la1. While we only transduce hepatocytes, we see dramatic therapeutic benefit that includes decrease in collagen accumulation. We elucidate a possible non cell-autonomous mechanism in which miR-29a is packaged into exosomes and received by stellate cells, where collagen translation is inhibited.

We created an inducible miR-29a transgenic mouse to address a few problems. First, miR-29a expression using an AAV virus was limited after repeated insults of CCl_4.

This non-integrating vector is lost during repeated hepatocellular divisions. Second, we could timely and spatially regulate expression of miR-29a in this system through the use of Cre-specific driver lines and treatment with doxycycline. Finally, isolation of miR-29a-positive cells lend insight into cell autonomous targets that could limit release of proinflammatory factors that activate stellate cell activation and collagen production.

The use of AAV serotype 8 to deliver miR-29a revealed the possibility for new mechanisms of protection. Hepatocellular miR-29a could limit release of pro-fibrotic cytokines and other signals that activate myofibroblasts. However, this mechanism remains unclear. To address this possibility, our lab is utilizing a protocol in which we treat hepatocytes and stellate cells with a biotin-tagged miR-29a oligo. By fixing transfected cells and isolating miR-29a bound 3'UTR targets using an avidin antibody, we can identify targets that would limit non-cell autonomous activation of stellate cells.

Our ultimate goal in this project is to identify novel targets and develop a sustainable therapy for protection against liver fibrosis. miR-29a is a potent regulator of ECM protein, and determining a way to deliver miR-29a to any solid organ, especially the liver, would limit development of fibrosis. Identification and testing of sustainable packaging systems which deliver miR-29a to specific cell populations would allow for enhanced protection against developing liver fibrosis.

5.4 Concluding remarks

The work in this thesis has identified two novel pathways in which microRNAs are protective against liver fibrosis. Both miR-214-5p and miR-29a are differentially

expressed in this pathologic setting. Using both *in vitro* and *in vivo* models, we suggest that these two miRNA families are important negative regulators of organ fibrosis.

In both studies, we provide evidence of cell specific expression of miR-214-5p and miR-29a, and we identify two mechanisms by which liver fibrosis is ameliorated. Future directions in this field should focus on identifying cell specific expression of miRNAs using *in vitro* gene expression manipulation, *in situ* hybridization techniques and transgenic models. Using these approaches, the field will more rapidly identify and validate mRNA targets in order to develop diagnostic markers and gene therapies to treat this disease.

References

Aurora, A.B., et al. "MicroRNA-214 protects the mouse heart from ischemic injury by controlling Ca^{2+} overload and cell death." J Clin Invest (2012) 122(4):1222-32.

Bala, S., Szabo, G. "MicroRNA Signature in Alcoholic Liver Disease." Int J Hepatol (2012) 2012:498232.

Bartel, D.P. "MicroRNAs: genomics, biogenesis, mechanism, and function." Cell (2004) 116(2):281-97.

Beard, C., et al. "Efficient method to generate single-copy transgenic mice by site-specific integration in embryonic stem cells." Genesis (2006) 44(1):23-8.

Bellingham, S.A., et al. "Small RNA deep sequencing reveals a distinct miRNA signature released in exosomes from prion-infected neuronal cells." Nucl Acids Res (2012) 40(21):10937-49.

Benton, D., et al. "Hepatocyte transplantation activates hepatic stellate cells with beneficial modulation of cell engraftment in the rat." Hepatology. (2005) 42(5):1072-81.

Bhatia, S.N., et al. "Effect of cell–cell interactions in preservation of cellular phenotype: cocultivation of hepatocytes and nonparenchymal cells." FASEB J (1999) 13(14):1883-900.

Chakraborty, J.B., et al. "Mechanisms and Biomarkers of Apoptosis in Liver Disease and Fibrosis." International Journal of Hepatology (2012):648915.

Coulouarn, C., et al. "Hepatocyte-stellate cell cross-talk in the liver engenders a permissive inflammatory microenvironment that drives progression in hepatocellular carcinoma." Cancer Res. (2012) 15;72(10):2533-42.

Cushing, L., et al. "miR-29 is a major regulator of genes associated with

pulmonary fibrosis." Am J Respir Cell Mol Biol (2011) 45(2):287-94.

Das, A.T., et al. "Viral evolution as a tool to improve the tetracycline-regulated gene expression system." J Biol Chem (2004) 279(18):18776-82.

Denby, L., et al. "miR-21 and miR-214 are consistently modulated during renal injury in rodent models." Am J Pathol (2011) 179(2):661-72.

Derfoul, A., et al. "Decreased microRNA-214 levels in breast cancer cells coincides with increased cell proliferation, invasion and accumulation of the Polycomb Ezh2 methyltransferase." Carcinogenesis. (2011) 32(11):1607-14.

Deuffic, S., et al. "Trends in primary live cancer." Lancet (1998) 351:214–215.

El-Serag, H., Mason, A.C. "Rising incidence of hepatocellular carcinoma in the United States." N Engl J Med (1999) 340:745–750.

Fabbri, M., et al. "MicroRNAs bind to Toll-like receptors to induce prometastatic inflammatory response." Proc Natl Acad Sci USA (2012) 109(31):E2110-6.

Greco, S.J., Rameshwar, P. "Analysis of the transfer of circulating microRNA between cells mediated by gap junction." Methods Mol Biol (2013) 1024:87-96.

Grimm, D., et al. "Liver Transduction with Recombinant Adeno-Associated Virus Is Primarily Restricted by Capsid Serotype Not Vector Genotype." J Virol (2006) 80(1):426.

Grimson, A., et al. "MicroRNA Targeting Specificity in Mammals: Determinants beyond Seed Pairing." Molecular Cell (2007) 27:91-105.

Guo, L., et al. "Dynamic evolution of mir-17-92 gene cluster and related miRNA gene families in vertebrates." Mol Biol Rep (2012) 2012 Dec 28.

Haybaeck, J., et al. "The parallel universe: microRNAs and their role in chronic hepatitis, liver tissue damage and hepatocarcinogenesis." Swiss Med Wkly (2011) 141:w13287.

He, Y., et al. "The potential of microRNAs in liver fibrosis." Cell Signal (2012) (12):2268-72.

Hinz, B., et al. "Recent developments in myofibroblast biology: paradigms for connective tissue remodeling." Am J Pathol (2012) 180(4):1340-55.

Hoyert, D.L., Xu, J. "Deaths, preliminary data for 2011." Natl Vital Stat Rep (2012) 61(6):1-65.

Hu, Y., et al. "A highly efficient synthetic vector: nonhydrodynamic delivery of DNA to hepatocyte nuclei in vivo." ACS Nano (2013) 7(6):5376-84.

Iizuka, M., et al. "Induction of microRNA-214-5p in human and rodent liver fibrosis." Fibrogenesis Tissue Repair (2012) 5(1):12.

Jia, X.Q., et al. "Lentivirus-mediated overexpression of microRNA-199a inhibits cell proliferation of human hepatocellular carcinoma." Cell Biochem Biophys (2012) 62(1):237-44.

Jiao, J., et al. "Hepatic fibrosis." Curr Opin Gastroenterol (2009) 25(3):223-9.

Jopling, C.L., et al. "Modulation of Hepatitis C Virus RNA Abundance by a Liver-Specific MicroRNA." Science (2005) 309(5740):1577-81.

Katakowski, M., et al. "Functional microRNA is transferred between glioma cells." Cancer Cell (2010) 70(21): 8259-8263.

Kisseleva, T., et al. "Myofibroblasts revert to an inactive phenotype during regression of liver fibrosis." PNAS (2012) 109:24 9448-9453.

Kogure, T., et al. “Hepatic miR-29ab1 expression modulates chronic hepatic injury.” J Cell Mol Med (2012) 16(11):2647-54.

Kota, J., et al. “Therapeutic microRNA delivery suppresses tumorigenesis in a murine liver cancer model.” Cell (2009) 137(6):1005-17.

Kuchenbauer, F., et al. “Comprehensive analysis of mammalian miRNA* species and their role in myeloid cells.” Blood (2011) 118(12):3350-8.

Kwiecinski, M., et al. “Expression of platelet-derived growth factor-C and insulin-like growth factor I in hepatic stellate cells is inhibited by miR-29.” Lab Invest (2012) 92(7):978-87.

La Vecchia, C., et al. “Trends in mortality from primary liver cancer in Europe.” Eur J Cancer (2000) 36:909 –915.

Lakner, A.M., et al. “Inhibitory effects of microRNA 19b in hepatic stellate cell-mediated fibrogenesis.” Hepatology (2012) 56(1):300-10.

Liang, C.C., et al. “In vitro scratch assay: a convenient and inexpensive method for analysis of cell migration in vitro.” Nature Protocols (2007) 2, 329–333.

Lieber, C.S., DeCarli, L.M. “The feeding of alcohol in liquid diets: two decades of application and 1982 update.” Alcoholism: Clinical and Experimental Research (1982) 6, 523-531.

Lee, C.C., et al. “Prediction of personalized microRNA activity.” Gene (2012) S0378-1119 (12) 01517-X.

Lee, U.E., Friedman, S.L. “Mechanisms of hepatic fibrogenesis.” Best Pract Res Clin Gastroenterol (2011) 25(2):195-206.

Lee, Y., et al. “The nuclear RNase III Drosha initiates microRNA processing.” (2003) Nature 425, 415–419.

Lee, Y.B., et al. “Twist1 regulates the miR-199a/214 cluster during development.” Nucleic Acids Res (2009) 37(1):123-8.

Lewis, B., et al. “Conserved Seed Pairing, Often Flanked by Adenosines, Indicates that Thousands of Human Genes are MicroRNA Targets.” Cell (2005) 120:15-20.

Li, B., et al. “Down-regulation of miR-214 contributes to intrahepatic cholangiocarcinoma metastasis by targeting Twist.” FEBS J (2012) 279(13):2393-8.

Li, J., et al. “miR-122 regulates collagen production via targeting hepatic stellate cells and suppressing P4HA1 expression.” J Hepatol (2012) S0168-8278(12)00879-3.

Llovet, J.M., et al. “Hepatocellular carcinoma.” Lancet (2003); 362 (9399):1907–1917.

Loebel, D.A., et al. “A conserved noncoding intronic transcript at the mouse Dnm3 locus.” Genomics (2005) 85(6):782-9.

Lorenzen, J.M., et al. “MicroRNAs as mediators and therapeutic targets in chronic kidney disease.” Nat Rev Nephrol (2011) 7(5):286-94.

Lund, E., et al. “Nuclear export of microRNA precursors.” (2004) Science 303, 95–98.

Maubach G., et al. “miRNA studies in *in vitro* and *in vivo* activated hepatic stellate cells.” World J Gastroenterol (2011) 17(22):2748-73.

Mendell, J.T. “miRiad roles for the miR-17-92 cluster in development and disease.” Cell (2008) 133(2):217-22.

Milic, S., Stimac, D. “Nonalcoholic fatty liver disease/steatohepatitis: epidemiology, pathogenesis, clinical presentation and treatment.” Dig Dis (2012) 30(2):158-62.

Mittelbrunn, M., et al. “Unidirectional transfer of microRNA-loaded exosomes from T cells to antigen-presenting cells.” Nat Commun (2011) 2:282.

Montecalvo, A., et al. “Mechanism of transfer of functional microRNAs between mouse dendritic cells via exosomes.” Blood (2012)119(3):756-766.

Murakami, Y., et al. “The progression of liver fibrosis is related with overexpression of the miR-199 and 200 families.” PLoS One (2011) 6(1):e16081.

Ogawa, T., et al. “MicroRNA-221/222 upregulation indicates the activation of stellate cells and the progression of liver fibrosis.” Gut (2012) 61(11):1600-9.

Parlakgumus, A., et al. “Two drugs with paradoxical effects on liver regeneration through antiangiogenesis and antifibrosis: Losartan and Spironolactone: a pharmacologic dilemma on hepatocyte proliferation.” J Surg Res. (2013)179(1):60-5.

Pai, H.C., et al. “Moscatilin inhibits migration and metastasis of human breast cancer MDA-MB-231 cells through inhibition of Akt and Twist signaling pathway.” J Mol Med (Berl) (2013) 91(3):347-56.

Peng, W.J., et al. “MicroRNA-29: a potential therapeutic target for systemic sclerosis.” Expert Opin Ther Targets (2012) 16(9):875-9.

Pollack, A. “European agency backs approval of a gene therapy.” New York Times (2012) B1.

Prickett, M., Jain, M. “Gene therapy in cystic fibrosis”: Transl Res (2012) S1931-5244(12)00407-0.

Reetz, J., et al. “Development of Adenoviral Delivery Systems to Target Hepatic Stellate Cells In Vivo.” PLoS One (2013) 8(6):e67091.

Qiang, R., et al. “Plexin-B1 is a target of miR-214 in cervical cancer and promotes the growth and invasion of HeLa cells.” Int J Biochem Cell Biol (2011) 43(4):632-41.

Qin, Q., et al. “Normal and disease-related biological functions of Twist1 and underlying molecular mechanisms.” Cell Res (2011) 22(1):90-106.

Qin, W., et al. “TGF-B/Smad3 signaling promotes renal fibrosis by inhibiting miR-29.” J Am Soc Nephrol (2011) 22(8):1462-74.

Rawat, D., et al. “Phenotypic variation and long-term outcome in children with congenital hepatic fibrosis.” J Pediatr Gasteroenterol Nutr (2013) 57(2):161-6.

Record, M., et al. “Exosomes as intercellular signalosomes and pharmacological effectors.” Biochem Pharmacol (2011) 81, 1171-1182.

Roberts, E.A., Schilsky, M.L. “Diagnosis and Treatment of Wilson Disease: An Update.” Hepatology (2008) 47(6):2089-111.

Roderburg, C., et al. “Micro-RNA profiling reveals a role for miR-29 in human and murine liver fibrosis.” Hepatology (2011) 53(1):209-18.

Roderburg, C., et al. “miR-133a mediates TGF-β-dependent de-repression of collagen-synthesis in hepatic stellate cells during liver fibrosis.” J Hepatol (2012) S0168-8278(12)00891-4.

Sands, M.S. “AAV-mediated liver-directed gene therapy.” Methods Mol Biol (2011) 807:141-57.

Santoro, M.M., Nicoli, S. “miRNAs in endothelial cell signaling: The endomiRNAs.” Exp Cell Res (2013) S0014-4827 (12) 00486-7.

Sood, P., et al. “Cell-type-specific signatures of microRNAs on target mRNA expression.” Proc Natl Acad Sci USA (2006) 103(8):2746-51.

Starega-Roslan, J., et al. “Structural basis of microRNA length.: Nucleic Acids Res (2011); 39(1):257–268.

Taddei, T., et al. “Inherited metabolic diseases of the liver.” Curr Opin Gasteroenterol (2008) 24(3):278-86.

Topic, A., et al. “Alpha-1-antitrypsin in pathogenesis of hepatocellular carcinoma.” Hepat Mon. (2012) 12(10 HCC):e7042.

Uyama, N., et al. “Regulation of cultured rat hepatocyte proliferation by stellate cells.” J Hepatol (2002) 36(5):590-9.

Valadi, H., et al. “Exosome-mediated transfer of mRNAs and microRNAs is a novel mechanism of genetic exchange between cells.” Nat Cell Biol (2007) 9(6):654-659.

van Rooij, E., et al. “Dysregulation of microRNAs after myocardial infarction reveals a role of miR-29 in cardiac fibrosis.” Proc Natl Acad Sci USA (2008) 105(35):13027-32.

Vettori, S., et al. “Role of MicroRNAs in Fibrosis.” Open Rheumatol J (2012) 6:130-9.

Wang, B., et al. “Suppression of microRNA-29 expression by TGF-β1 promotes collagen expression and renal fibrosis.” J Am Soc Nephrol (2012) 23(2):252-65.

Wang, Z., et al. “Gene delivery into hepatocytes with the preS/liposome/DNA system.” Biotechnol J (2008) 3(9-10):1286-95.

Watanabe, T., et al. "Dnm3os, a non-coding RNA, is required for normal growth and skeletal development in mice." Dev Dyn (2008) 237(12):3738-48.

Winbanks, C.E., et al. "TGF-beta regulates miR-206 and miR-29 to control myogenic differentiation through regulation of HDAC4." J Biol Chem (2011) 286(16):13805-14.

Yang, J., et al. "Exploring a New Twist on Tumor Metastasis." Cancer Res (2006) *66;*4549.

Yang, J.S., et al. "Widespread regulatory activity of vertebrate microRNA* species." RNA (2011) 17(2):312–326.

Yi, R., et al. "Exportin-5 mediates the nuclear export of pre-microRNAs and short hairpin RNAs." Genes Dev (2003) 17*,* 3011–3016.

Yin, G., et al. "TWISTing stemness, inflammation and proliferation of epithelial ovarian cancer cells through MIR199A2/214." Oncogene (2010) 29(24):3545-53.

Zhang, Y., et al. "Functional screening for miRNAs targeting Smad4 identified miR-199a as a negative regulator of TGF-β signalling pathway." Nucleic Acids Res (2012) 40(18):9286-97.

Zhang, Y., et al. "Diversity and evolution of MicroRNA gene clusters." Sci China C Life Sci (2009) 52(3):261-6.

Zincarelli, C., et al. "Analysis of AAV serotypes 1-9 mediated gene expression and tropism in mice after systemic injection." Mol Ther (2008) 16(6):1073-80.

Zuber, J., et al. "Toolkit for evaluating genes required for proliferation and survival using tetracycline-regulated RNAi." Nat Biotechnol (2011) 29(1):79-83.

Appendix 1. Cloning and qPCR Primers.

Cloning Primers	**Primer Sequence**
Hsa-miR-214 Fw	5’ GCC GGG CCG GCC TCG AGG ATC CTG TA 3’
Hsa-miR-214 Rev	5’ CGG CGG CCG GCC TCG AGC TAG CAT T 3’
Hsa-miR-199a Fw	5’ GCC GGG CCG GCC TCG AGG ATC CAG T 3’
Hsa-miR-199a Rev	5’ CGG CGG CCG GCC TCG AGC TAG CGC G 3’
Hsa-Twist1 3’UTR Fw	5’ CGC CTC TAG AGC TGG ATA ACT AAA AAT 3’
Hsa-Twist1 3’UTR Rev	5’GGC GTC TAG ACA CAA ACA ACT GTT C 3’
Hsa-Twist1 Fw	5’ GCG CGG AAT TCA TGA TGC AGG ACG TGT CCA GC 3’
Hsa-Twist1 Rev	5’ CGC GCG AAT TCC TAG TGG GAC GCG GAC ATG G 3’
BsrGI miR-29a Tg Mus Fw	5’ GCG GTG TAC AAG TAA GAG CCC AAT GTA TGC TGG 3’
MluI miR-29a Tg Mus Rev	5’ CGG CAC GCG TTG CAT TAT TGC TTT GCA TTT G 3’
XhoI eGFP_mir29 Fw	5’ GCG CGG GAT CCA TGG TGA GCA AGG 3’
XhoI eGFP_mir29 Rev	5’ CGG CCC TCG AGA AAT TCC AAC ACA CTA TTG C 3’

qPCR Primer	**Primer Sequence**
Hsa-Alpha-SMA Fw	5’ CTG TTC CAG CCA TCC TTC AT 3’
Hsa-Alpha-SMA Rev	5’ CCG TGA TCT CCT TCT GCA TT 3’
Hsa-Col1a1 Fw	5’ CAA GAG GAA GGC CAA GTC GAG G 3’
Hsa-Col1a1 Rev	5’ CGT TGT CGC AGA CGC AGA T 3’
Hsa-CTGF Fw	5’ CCT GGT CCA GAC CAC AGA GT 3’
Hsa-CTGF Rev	5’ TGG AGA TTT TGG GAG TAC GG 3’
Hsa-FN1 Fw	5’ GAA CTA TGA TGC CGA CCA GAA 3’
Hsa-FN1 Rev	5’ GGT TGT GCA GAT TTC CTC GT 3’
Hsa-PDGF-R-beta Fw	5’ CGC AGC AGT GAG AAG CAA GC 3’
Hsa-PDGF-R-beta Rev	5’ TAG TCC ACC AGG TCT CCG TAG C 3’
Hsa-TGF-beta Fw	5’ AGC GAC TCG CCA GAG TGG TTA 3’
Hsa-TGF-beta Rev	5’ GCA GTG TGT TAT CCC TGC TGT CA 3’
Hsa-MMP9 Fw	5' TCG AAC TTT GAC AGC GAC AAG AA 3’
Hsa-MMP9 Rev	5’ TCA GTG AAG CGG TAC ATA GGG TAC A 3’
Hsa-MMP2 Fw	5’ TGA CAT CAA GGG CAT TCA GGA G 3’
Hsa-MMP2 Rev	5’ TCT GAG CGA TGC CAT CAA ATA CA 3’
Hsa-TIMP1 Fw	5’ GGA TAC TTC CAC AGG TCC CAC AA 3’
Hsa-TIMP1 Rev	5’ CTG CAG GTA GTG ATG TGC AAG AGT C 3’
Hsa-Twist1 Fw	5’ CAT CGA CTT CCT CTA CCA GGT C 3’
Hsa-Twist1 Rev	5’ TGT CCA TTT TCT CCT TCT CTG GA 3’
Hsa-E-cadherin Fw	5’ GGA TGT GCT GGA TGT GAA TG 3’
Hsa-E-cadherin Rev	5’ CAC ATC AGA CAG GAT CAG CAG AA 3’
Hsa-N-cadherin Fw	5’ TGT TTG ACT ATG AAG GCA GTG G 3’

Hsa-N-cadherin Rev	5’ TCA GTC ATC ACC TCC ACC AT 3’
Hsa-Vimentin Fw	5’ GAG AAC TTT GCC GTT GAA GC 3’
Hsa-Vimentin Rev	5’ TCC AGC AGC TTC CTG TAG GT 3’
Hsa-Zeb1 Fw	5’ GC ACCT GAA GAG GAC CAG AG 3’
Hsa-Zeb1 Rev	5’ TGC ATC TGG TGT TCC ATT TT 3’
Hsa-Zeb2 Fw	5’ CAA GAG GCG CAA ACA AGC 3’
Hsa-Zeb2 Rev	5’ GGT TGG CAA TAC CGT CAT 3’
Rno-DNM1 Fw	5’ CCG CCG CAA CCA TGG GCA AC 3’
Rno-DNM1 Rev	5’ GGC AAG AAG TCC CTG CCC ACG AA 3’
Rno-DNM2 Fw	5’ GAG GCG GGC ACC ATG GGC ACC 3’
Rno-DNM2 Rev	5’ GGA AGG AAG TCC CGG CCC ACG 3’
Rno-DMN3 Fw	5’ GGA AGA ACT GAT CCC TCT GGT G 3’
Rno-DNM3 Rev	5’ CAC GAA GTT CTC GAG CAC TGA GC 3’
Hsa-Beta-Actin Fw	5’ ACC TTC TAC AAT GAG CTG CG 3’
Hsa-Beta-Actin Rev	5’ CCT GGA TAG CCA CGT ACA TGG 3’
Rno-Beta-Actin	5’ CCC ATT GAA CAC GGC ATT 3’
Rno-Beta-Actin	5’ TTG GCC TTA GGG TTC AGA 3’

Curriculum vitae

Matthew K. Knabel

515 South Milton Avenue
Baltimore, MD 21224
(570) 479-2954
mknabel1@jhu.edu

Education

Johns Hopkins University School of Medicine, Baltimore, MD 2008-2013
Graduate Student, Lab of Dr. Daniel Warren

Ph. D. in Human Genetics & Molecular Biology (expected defense: October 2013)
Thesis: *Understanding the cellular mechanisms and therapeutic potential of microRNAs in liver fibrosis*

- Techniques utilized: nucleic acid and protein isolation; PCR; Western blot; Northern blot; immunohistochemistry; confocal, fluorescent and brightfield microscropy; managing animal colonies; harvesting small animal organs; cloning; cell culture; radioactivity.
- Identified and characterized cell-specific dynamic expression of miRNAs during liver fibrosis
- Prepared and reviewed technical manuscripts submitted to peer-reviewed journals
- Developed and utilized rodent models of liver fibrosis
- Processed and analyzed nucleic acid and protein expression from mammalian tissue and cell culture samples

Johns Hopkins University, Baltimore, MD 2002-2006

- B.A. Biology
- Dean's List
- National Society of Collegiate Scholars
- 4-year Varsity Letter, Football

Work Experience

Johns Hopkins University School of Medicine, Baltimore, MD 2006-2008
Lab Technician – Labs of Dr. Steven Leach and Dr. Michael Parsons

- Managed an aquatic room that included collaborations with eight different labs
- Created transgenic zebrafish lines to study pancreatic cell lineage differentiation
- Trained to perform molecular biology techniques involving nucleic acids, protein, cell culture and organism biology with attention to outcome analysis
- Encouraged to pursue a Ph.D. in molecular biology because of excellent performance as a lab technician

Registrations and Publications

USPTO – Admitted to Practice (Registration Number: 71762)

Knabel MK, et al (In preparation). miR-214 and Twist1: a protective negative feedback loop in nonparenchymal cells during liver fibrosis.

Knabel MK, et al (Submitted). Hepatic maintenance of miR-29a is protective during liver fibrosis.

Lonze,BE, Holzer HT, **Knabel MK**, Locke JE, DiCamillo GA, Karhadkar SS, Montgomery RA, Sun Z, Warren DS, Cameron AM. In vitro and ex vivo delivery of short hairpin RNAs for control of hepatitis C viral transcript expression. *Arch Surg*. 2012 Apr;147(4):384-7.

Luo W, Hu H, Chang R, Zhong J, **Knabel M,** O'Meally R, Cole RN, Pandey A, Semenza GL. Pyruvate kinase M2 is a PHD3-stimulated coactivator for hypoxia-inducible factor 1. Cell. 2011 May 27;145(5):732-44.

Mark AL, Sun Z, Warren DS, Lonze BE, **Knabel MK**, Melville Williams GM, Locke JE, Montgomery RA, Cameron AM. Stem cell mobilization is life saving in an animal model of acute liver failure. Ann Surg. 2010 Oct;252(4):591-6.

Awards and Teaching Experience

First place, 2012 Poster Session. 6th Annual Department of Surgery Research Poster Session. "mir-214 and mir-199a are Upregulated in Liver Fibrosis."

Teaching Assistant, "Molecular Biology & Genomics." Fall Semester, 2011